

NOVEL DONOR-ACCEPTOR TYPE POLYMERS TOWARDS EXCELLENT
NEUTRAL STATE GREEN POLYMERIC MATERIALS FOR REALIZATION OF
RGB BASED ELECTROCHROMIC DEVICE APPLICATIONS

A THESIS SUBMITTED TO
THE GRADUATE SCHOOL OF NATURAL AND APPLIED SCIENCES
OF
MIDDLE EAST TECHNICAL UNIVERSITY

BY

GÖRKEM E. GÜNBAŞ

IN PARTIAL FULFILLMENT OF THE REQUIREMENTS
FOR
THE DEGREE OF MASTER OF SCIENCE
IN
CHEMISTRY

NOVEMBER 2007

**NOVEL DONOR-ACCEPTOR TYPE POLYMERS TOWARDS EXCELLENT
NEUTRAL STATE GREEN POLYMERIC MATERIALS FOR
REALIZATION OF RGB BASED ELECTROCHROMIC DEVICE
APPLICATIONS**

Submitted by **GÖRKEM E. GÜNBAŞ** in partial fulfillment of the requirements for
the degree of **Master of Sciences in Department of Chemistry, Middle East
Technical University** by,

Prof. Dr. Canan Özgen
Dean, Graduate School of **Natural and Applied Sciences** _____

Prof. Dr. Ahmet M. Önal
Head of Department, **Department of Chemistry** _____

Prof. Dr. Levent Toppare
Supervisor, **Department of Chemistry, METU** _____

Examining Committee Members:

Prof. Dr. Leyla Aras
Department of Chemistry, METU _____

Prof. Dr. Levent Toppare
Department of Chemistry, METU _____

Prof. Dr. Cihangir Tanyeli
Department of Chemistry, METU _____

Prof. Dr. Raşit Turan
Department of Physics, METU _____

Prof. Dr. Kadir Pekmez
Department of Chemistry, Hacettepe University _____

I hereby declare that all information in this document has been obtained and presented in accordance with academic rules and ethical conduct. I also declare that, as required by these rules and conduct, I have fully cited and referenced all material and results that are not original to this work.

Name, Last name: GÜNBAŞ E. Görkem

Signature:

ABSTRACT

NOVEL DONOR-ACCEPTOR TYPE POLYMERS TOWARDS EXCELLENT NEUTRAL STATE GREEN POLYMERIC MATERIALS FOR REALIZATION OF RGB BASED ELECTROCHROMIC DEVICE APPLICATIONS

Görkem E. Günbaş
M.S., Department of Chemistry
Supervisor: Prof. Dr. Levent Toppare

November 2007, 84 pages

Polymers having one of the three complementary colors (red, green, and blue) in the reduced state and high transmissivity in the oxidized state are key materials towards use in electrochromic devices and displays. Although many neutral state red and blue polymers were reported up to date, neutral state green polymeric materials appear to be limited. For potential application of electrochromic materials in display technologies, one should have to create the entire color spectrum and this can be only achieved by having materials with additive or subtractive primary colors in their neutral states. To obtain a green color there should be at least two simultaneous absorption bands. Although the neutral state color is of great importance, the transmittance in the oxidized state is crucial too. The materials having one of the three primary colors should also possess highly transmissive oxidized states in order to be used in commercial electrochromic device applications. Donor-acceptor molecules lead to lower band gap due to resonances that enable a stronger double bond character between the donor and acceptor units. The materials with low band-gaps produce cathodically coloring polymers due to the lower energy transition in the doped state. Moreover, donor-acceptor type materials commonly show two absorption maxima. Since donor-acceptor approach seems to be the key to the complex nature of producing these materials, novel donor-acceptor type polymers were synthesized, and electrochromic properties were investigated in detail. Additionally a solution-processable donor-acceptor type polymer was realized using method of introducing alkyl side chains in the polymer structures.

Keywords: Electrochromism, Donor-Acceptor Polymers, Green Polymers, High Optical Contrast

ÖZ

RGB TEMELLİ ELEKTROKROMİK CİHAZ UYGULAMALARINI GERÇEKLEŞTİRMEK İÇİN İNDİRGENMİŞ HALİNDE YEŞİL ÖZGÜN DONÖR AKSEPTÖR TİPİ POLİMERİK MALZEMELER

Görkem E. Günbaş
Yüksek Lisans, Kimya Bölümü
Tez Yöneticisi: Prof. Dr. Levent Toppare

Ekim 2007, 84 sayfa

İndirgenmiş halinde üç tamamlayıcı renkten (kırmızı, yeşil ve mavi) birine sahip, yükseltildiğinde yüksek geçirgenlik gösteren polimerler, elektrokromik ve görüntü cihazları uygulamaları için anahtar malzemelerdir. Şimdiye kadar indirgenmiş halinde kırmızı ve mavi olan birçok polimer rapor edilmiş olmasına rağmen, indirgenmiş halinde yeşil olan polimerik malzemeler sınırlıdır. Elektrokromik malzemelerin görüntü teknolojilerindeki potansiyel uygulamaları için, tüm renk spektrumu oluşturulmalıdır ve bu ancak indirgenmiş halinde birincil renklere sahip malzemelerle gerçekleştirilebilir. Yeşil renk elde etmek için en az iki soğurma bandı olmalıdır. İndirgenmiş haldeki rengin önem taşımaya başlamasına rağmen, yükseltildiğinde haldeki rengin geçirgenliğinde büyük önem taşımaktadır. Ticari elektrokromik cihaz uygulamaları için, indirgenmiş halinde üç ana renkten birine sahip malzemelerin aynı zamanda yükseltildiğinde yüksek geçirgenliğe sahip olmaları gerekir. Donör-akseptör moleküller, bu birimler arasında yüksek çift bağ karakterinin yarattığı rezonans dolaylı bant aralığını düşürürler. Düşük bant aralığına sahip malzemeler, katılanmış haldeki düşük enerji geçişinden dolayı indirgenmiş halde renklenmiş polimerler üretir. Ayrıca donör akseptör tipi malzemeler çoğunlukla iki soğurma maksimumu gösterirler. Bu tip malzemelerin üretiminin karmaşık doğasında donör akseptör yaklaşım kilit nokta olduğu için, özgün donör akseptör tipi malzemeler sentezlenmiş ve elektrokromik özellikleri detaylı incelenmiştir. Buna ek olarak, polimerin yapısına alkil zincirleri ekleme metoduyla, çözünebilir ve işlenebilir bir polimer sentezi de gerçekleştirilmiştir.

Anahtar Sözcükler: elektrokromizm, donör-akseptör polimerler, yeşil polimerler, yüksek optik kontrast

TO HALE AND EŞREF,

For every single thing...

ACKNOWLEDGEMENT

Many Thanks;

To Levent Toppare, for giving me the opportunity to find the capacity inside me and turning my future dream plans into reality. Words can not express my gratitude.

To Asuman Durmus, for filling the huge my internal emptiness and giving me the most beautiful reason to wake up in the mornings. Thanks are extended for the electrochemistry work which makes this thesis got completed.

To Gursel Sonmez, for the spark he initiated the idea behind my research and helped realization of every single thing in this thesis. I'm deeply sorry since you did not get to see that we turned your dreams into reality.

To Senem Kıralp, for taking me from the darkness and showing me the way to the brightest road, a road that I could not imagine in the first place.

To Nazmiye Akca for always being there for me and for the endless support even sometimes I do not deserve it.

To Selen Akilli for always believing in me and making me feel strong enough to achieve everything.

To Semih Seyyidođlu, for finding a way to cheer me up or otherwise beats me to death when I am deeply stressed out at all.

To Ilker Kutuk, for always being a brother to me and for the great help throughout the experiments that last until the first lights of the new day.

To Bora Bilgic, my brother, for valuable discussions and showing me the other side of the medallion.

To Abidin Balan, for always making me feel like that I am not the single child.

To Buđra Epik, for the great friendship, for endless laughs, for the great help and discussions in many reactions run in this thesis and increasing the content since we worked 24 hours a day.

To Kadir Kaleli for completing the square and being a great support as a friend during my studies.

To Funda Ozyurt, for being a sister to me, for always forcing me to stand still and never giving me the chance to break down into pieces.

To Tugba Ozdemir, for very valuable advices for the experiments and for the ones that she can understand very well when she is reading these sentences. Thanks are also for cheering me up when I need to smile very much.

To Uygur Kayahan, for being he is and having faith in me.

To Simge Tarkuc , Basak Yigitsoy, Serhat Varis for sharing the first and most exciting times of this research with me and for the great contribution to everything present in this thesis.

To Asli Taskin, for the great friendship and for being such a handy and frank person.

To Pinar Camurlu, for the guidance in every endless road, and turning me into a perfectionist.

To Cihangir Tanyeli and İdris Mecidoğlu, for their invaluable guidance at the initial stages of organic synthesis.

To Ayşegül Yıldırım, for her help throughout my studies, kindness, for the great friendship and lovely songs in the laboratory.

To Ersin Yıldız, for columns, work-ups, TLCs, stirrers, glassware and for his great friendship.

To Metin Ak for many valuable discussions on the synthesis and electrochemistry studies.

To Yasemin Udum, for covering all the jokes I made and being such a sweet person.

To Tolga Yapıcı, for the great help during preparation of this thesis and for the great friendship.

To Emre Yazıcıoğlu, for his great helps when we first started with organic synthesis.

To Ali Coşkun, for being an inspiration for me and showing me that one can accomplish everything by having enough faith and determination.

To Serdar Atılğan, for the help, guidance, support, and for being himself whenever you need him.

To Yusuf Nur, for running the mass analyses and friendship.

To TUBITAK, for the financial support.

TABLE OF CONTENTS

ABSTRACT.....	iv
ÖZ	v
ACKNOWLEDGEMENT	vii
TABLE OF CONTENTS	ix
LIST OF FIGURES	xii
CHAPTERS	
1. INTRODUCTION	1
1.1 Brief History	1
1.2 Band Theory.....	2
1.3 Conducting Polymer Redox Processes	5
1.4 Electrochromism	5
1.5 Electrochromism in Conducting Polymers	7
1.6 Factors Affecting the Color of a Conducting Polymer	9
1.7 Polarons, Bipolarons and π -Dimers	11
1.8 Polymerization Methods	13
1.9. Donor-Acceptor Theory and Low Band Gap Systems	14
1.10 Pendant Group Effects	23
1.11 Alkyl Solubilizing Groups	23
1.12 Donor-Acceptor Approach for the Synthesis of n-Dopable Conjugated Systems	23
1.13 Importance of Neutral State Green Polymeric Materials.....	25
1.14 Donor-Acceptor Methods towards Green Polymeric Materials.....	29
1.15 Aim of this Work	30

2. EXPERIMENTAL	31
2.1. Materials.....	31
2.2. Equipments.....	31
2.3. Monomer Syntheses	32
2.3.1. 2,3-Diphenyl-5,7-bis(3,4-ethylenedioxy-2-thienyl)thieno[3,4-b]pyrazine (GS).....	32
2.3.2. 2,3-Bis(4-tert-butylphenyl)-5,8-(2,3-dihydrothieno[3,4-b][1,4]dioxin-7-yl)quinoxaline (TBPEQ)	33
2.3.3 2,3-Diphenyl-5,8-(2,3-dihydrothieno[3,4-b][1,4]dioxin-7-yl)quinoxaline (DPEQ).....	34
2.3.4 2,3-Bis(3,4-bis(decyloxy)phenyl)-5,8-bis(2,3-dihydrothieno[3,4-b][1,4] dioxin-5yl)quinoxaline (DOPEQ).....	36
2.4. Polymer Syntheses	36
2.4.1. Homopolymerization of GS	36
2.4.2. Copolymerization of GS with BiEDOT	37
2.4.3. Polymerization of TBPEQ and DPEQ	38
2.4.4. Polymerization of DOPEQ.....	38
2.4.5. Chemical Polymerization of DOPEQ	39
2.5. Characterization of Polymer Films:	39
2.5.1. Cyclic Voltammetry	39
2.5.2 Spectroelectrochemistry	42
2.5.3. Switching Properties	42
2.5.4 Colorimetry	43
3. RESULTS AND DISCUSSION	44
3.1. Characterization of the D-A-D Molecules.	44
3.1.1. 2,3-Diphenyl-5,7-bis(3,4-ethylenedioxy-2-thienyl)thieno[3,4-b]pyrazine.....	44
3.1.2. 2,3-bis(4-tert-butylphenyl)-5,8-(2,3-dihydrothieno[3,4-b][1,4dioxin-7-yl)quinoxaline (TBPEQ)	45

3.1.3.	2,3-diphenyl-5,8-(2,3-dihydrothieno[3,4-b][1,4]dioxin-7-yl)quinoxaline (DPEQ)	47
3.1.4.	2,3-bis(3,4-bis(decyloxy)phenyl)-5,8-bis(2,3-dihydrothieno[3,4-b][1,4]dioxin-5yl)quinoxaline(DOPEQ).....	48
3.2.	Electrochemical and Electrochromic Properties of Donor-Acceptor-Donor Type Polymers	49
3.2.1	Electrochemical and Electrochromic Properties of Poly(2,3-Diphenyl-5,7-bis(3,4-ethylenedioxy-2-thienyl)thieno[3,4-b]pyrazine) (PGS).....	49
3.2.2.	Electrochemical and Electrochromic Properties of Poly(2,3-Diphenyl-5,7-bis(3,4-ethylenedioxy-2-thienyl)thieno[3,4-b]pyrazine-co-bi-etylenedioxy thiophene) P(GS-co-Biedot)	57
3.2.3.	Electrochemical and Electrochromic Properties of 2,3-bis(4-tert-butylphenyl)-5,8-(2,3-dihydrothieno[3,4-b][1,4]dioxin-7-yl)quinoxaline(TBPEQ) and 2,3-diphenyl-5,8-(2,3-dihydrothieno[3,4-b][1,4]dioxin-7-yl)quinoxaline (DPEQ).	61
3.2.4	Electrochemical and Electrochromic Properties of 2,3-bis(3,4-bis(decyloxy)phenyl)-5,8-bis(2,3-dihydrothieno[3,4-b][1,4]dioxin-5yl) quinoxaline (DOPEQ):	69
4.	CONCLUSION	76
	REFERENCES.....	77

LIST OF FIGURES

FIGURES

Figure 1.1. Common conjugated polymers.	1
Figure 1.2 Formation of band structure from monomer to polymer. A. Poly(acetylene) hypothetical orbital and band structure. B. PA orbital and band structure after the system undergoes a Peierls distortion.[10]	3
Figure 1.3 Evolution of the band structure of PPy from monomer to hexamer and polymer as determined by density functional theory. [13b]	4
Figure 1.4 The three common viologen redox states, dication, radical cation, neutral species.	6
Figure 1.5 Polaron and bipolaron band diagrams in non-degenerate ground state polymers: (a) neutral, (b) slightly doped and (c) heavily doped polymer.....	8
Figure 1.6 Schematic representation of parameters that play a determining role on the band gap [26].....	9
Figure 1.7 Charge carriers in conjugated polymers. (A) Solitons are the primary method of charge transport in doped PA. (B) Polarons and bipolarons are the charge carriers for doped poly(heterocycles) with non-degenerate ground states although π -dimers (C) are proposed as an alternative to polarons, especially in oligomeric materials. [10]	14
Figure 1.8 Electrochemical polymerization mechanism of EDOT.[40]	15
Figure 1.9. Possibilities for positioning of band edges in both high and low band gap polymers.....	16
Figure 1.10 Stability of CPs in their oxidized or reduced forms depends on where the formal oxidation potential (E°) lies (a direct consequence of the VB (p-type) or CB (n-type). A p-type polymer with a low E° is stable in its neutral state. Adapted from [10]......	18

Figure 1.11 Planarity effects on band gap and the electrical and optical properties of	20
conjugated polymers. Adapted from [40].	20
Figure 1.12 Overview of methods for the modification of band gap. [10]	21
Figure 1.13 The Donor-Acceptor approach, alternating donor and acceptor moieties results in a polymer that has the combined optical properties of the parent donor or acceptor monomers. [10].....	22
Figure 1.14. Reduction potentials (vs SCE) of common nitrogen containing heterocyclics. Structures highlighted in purple are either commercially available or their dihalo derivatives can easily be synthesized. Structures highlighted in green have easily protonated sites. [40]	24
Figure 1.15. Poly(3-methylthiophene) (P3MT), poly(2,3-di(thien-2-yl)thieno[3,4- b]pyrazine) (PDDTP) and poly(3,4-ethylenedioxythiophene) (PEDOT) were the red, green and blue colored polymers respectively. Adapted from [72].	27
Figure 1.16. Combined spectroelectrochemistry of P3MT, PDDTP and PEDOT in the neutral state. Adapted from [72].	27
Figure 1.17. Combined spectroelectrochemistry of P3MT, PDDTP and PEDOT in the oxidized state. Adapted from [72].....	28
Figure 2.1 Synthetic route to monomer GS.....	33
Figure 2.2 Synthetic route to monomers DPEQ and TBPEQ.	35
Figure 2.3 Synthetic route to monomer DOPEQ.	37
Figure 2.4. Schematic representation of copolymerization of BiEDOT and GS.	38
Figure 2.5 Cyclic Voltammogram of a representative type of electroactive monomer. [22].	41
Figure 2.6 CIELAB color space.	43
Figure 3.1 ¹ H-NMR spectrum of GS.....	44
Figure 3.2 ¹³ C-NMR spectrum of GS.....	45

Figure 3.3 ^1H -NMR spectrum of TBPB.....	45
Figure 3.4 ^{13}C -NMR spectrum of TBPB.....	46
Figure 3.5 ^1H -NMR spectrum of TBPEQ.....	46
Figure 3.6 ^{13}C -NMR spectrum of TBPEQ.....	47
Figure 3.7 ^1H -NMR spectrum of DPEQ.....	47
Figure 3.8 ^1H -NMR spectrum of DOPEQ.....	48
Figure 3.9 ^{13}C -NMR spectrum of DOPEQ.....	48
Figure 3.10. Repeated potential scan electropolymerization of GS at 100 mV/s in 0.1 M TBAPF ₆ /Dichloromethane (DCM).....	49
Figure 3.11. Scan rate dependence of PGS in TBAPF ₆ /ACN (a) 25, (b) 50, (c) 100, (d) 200, (e) 300 mV/s.....	51
Figure 3.12 Spectroelectrochemistry of PGS film on an ITO coated glass slide in monomer-free 0.1 M TBAPF ₆ /ACN electrolyte solution. A) p-type doping at applied potentials; (a) -0.8, (b) -0.6, (c) -0.5, (d) -0.4, (e) -0.3, (f) -0.1 (g) +0.2, (h) +0.5, (i) +0.8. vs Ag/Ag ⁺ . B) n-type doping at applied potentials (a) -1.7, (b) -2.0, (c) -2.2 V vs Ag/Ag ⁺	52
Figure 3.13 ESR and UV-Vis Spectra of PGS film at various oxidation states on Pt and ITO electrodes respectively. a-b) after oxidation at +1.2 V (fully oxidized state), c-d) after addition of certain amount of hydrazine (polaronic state), e-f) in pure hydrazine (neutral state).....	54
Figure 3.14 Electrochromic switching, optical absorbance change of PGS deposited on ITO electrode monitored at 522 and 1750 nm in 0.1 M TBAPF ₆ /ACN.....	56
Figure 3.15. Cyclic voltammetry of the copolymer in 0.1M TBAPF ₆ /ACN at scan rate of 100 mV/s.....	58
Figure 3.16 Spectroelectrochemistry of copolymer as a function of applied potential between -1 and 0.6 V in 0.1 M TBAPF ₆ /ACN: (a) -1.0, (b) -0.8, (c) -0.6, (d) -0.4, (e) -0.2, (f) 0.0, (g) +0.4, (h) 0.6 V vs Ag wire.....	59

Figure 3.17. Electrochromic switching, optical absorbance change monitored at 538 nm and 1750 nm for copolymer in 0.1 M TBAPF ₆ /ACN.....	60
Figure 3.18 Repeated potential scan electropolymerization of TBPEQ at 100 mV/s in 0.1 M TBAPF ₆ /DCM on ITO electrode.....	61
Figure 3.19 Repeated potential scan electropolymerization of PDPEQ at 100 mV/s in 0.1 M TBAPF ₆ /DCM on ITO electrode.....	62
Figure 3.20 Scan rate dependence of PTBPEQ film in TBAPF ₆ /ACN (a) 100, (b) 150, (c) 200, (d) 250, (e) 300 mV/s.	62
Figure 3.21 Repeated potential scan electropolymerization of PDPEQ at 100 mV/s in 0.1 M TBAPF ₆ /DCM on ITO electrode.....	63
Figure 3.22. a. p-doping. Spectroelectrochemistry of PTBPEQ film on an ITO coated glass slide in monomer-free, 0.1 M TBAPF ₆ /ACN electrolyte-solvent couple at applied potentials(V); (a) -1.0, (b) -0.8, (c) -0.6, (d) -0.4, (e) -0.3, (f) -0.2 (g) -0.1, (h) -0.05, (i) 0, (j) 0.05, (k) 0.1, (l) 0.15, (m) 0.2, (n) 0.25, (o) 0.3, (p) 0.35, (q) 0.4, (r) 0.45, (s) 0.5, (t) 0.55, (u) 0.6, (v) 0.65, (w) 0.7, (x) 0.75, (y) 0.8 b. n-doping Spectroelectrochemistry of PTBPEQ at 0.8, -1.0 and -1.7 V.	65
Figure 3.23 a. p-doping. Spectroelectrochemistry of PDPEQ film on an ITO coated glass slide in monomer-free, 0.1 M TBAPF ₆ /ACN electrolyte-solvent couple at applied potentials between -1.0 to 1.0 V b. n-doping Spectroelectrochemistry of PDPEQ at 0.8, -1.0 and -1.7 V.....	66
Figure 3.24 Electrochromic switching, optical absorbance change monitored at 452 and 711 nm and 2000 nm for PTBPEQ in 0.1 M TBAPF ₆ /ACN.	68
Figure 3.25 Electrochromic switching, optical absorbance change monitored at 448 and 732 nm and 1800 nm for PDPEQ in 0.1 M TBAPF ₆ /ACN.....	69
Figure 3.26. Repeated potential scan electropolymerization of DOPEQ at 100 mV/s in 0.1 M TBAPF ₆ /DCM/ACN on ITO electrode	70
Figure 3.27. Single scan cyclic voltammetry of chemically synthesized PDOPEQ at 100 mV/s in 0.1 M TBAPF ₆ /ACN on ITO electrode	71

Figure 3.28. Scan rate dependence of PDOPEQ (electrochemically synthesized) film in TBAPF ₆ /ACN (a) 100, (b) 150, (c) 200, (d) 250, (e) 300 mV/s.....	71
Figure 3.29. Scan rate dependence of PDOPEQ (chemically synthesized) film, spray-coated on ITO, in TBAPF ₆ /ACN (a) 100, (b) 150, (c) 200, (d) 250, (e) 300 mV/s.....	72
Figure 3.30. Colors of PDOPEQ film on an ITO coated glass slide at neutral and oxidized states and spectroelectrochemistry of PDOPEQ film on an ITO coated glass slide in monomer-free, 0.1 M TBAPF ₆ /ACN electrolyte-solvent couple at applied potentials; (a) -0.6, (b) -0.15, (c) 0 (d) 0.05, (e) 0.075, (f) 0.1 (g) 0.15, (h) 0.175, (i) 0.2, (j) 0.225, (k) 0.25, (l) 0.275, (m) 0.3, (n) 0.35, (o) 0.4, (p) 0.45, (q)0.5, (r) 0.55, (s) 0.6, (t) 0.65, (u) 0.7, (v) 0.8 V	73
Figure 3.31 Colors of chemically synthesized PDOPEQ that spray-coated on an ITO coated glass slide at neutral and oxidized states and spectroelectrochemistry of PDOPEQ film on an ITO coated glass slide in monomer-free, 0.1 M TBAPF ₆ /ACN electrolyte-solvent couple at applied potentials; (a) -0.5, (b) 0.25, (c) 0.3, (d) 0.35, (e) 0.4, (f) 0.45, (g) 0.5, (h) 0.55, (i) 0.65, (j) 0.75, (k) 0.85, (l)0.95, (m) 1.1, (n) 1.2 V	74
Figure 3.32. Electrochromic switching, optical absorbance change monitored at 415 and 690 nm and 1800 nm for PDOPEQ in 0.1 M TBAPF ₆ /ACN.....	75

CHAPTER I

INTRODUCTION

1.1 Brief History

The major interest on conjugated polymer was driven by the ground breaking work of Shirakawa et. al. where polyacetylene achieved high electrical conductivity upon doping [1].

Further research in the field has led to other conjugated polymers, like polythiophenes, polypyrroles and many others [2] (figure 1.1.)

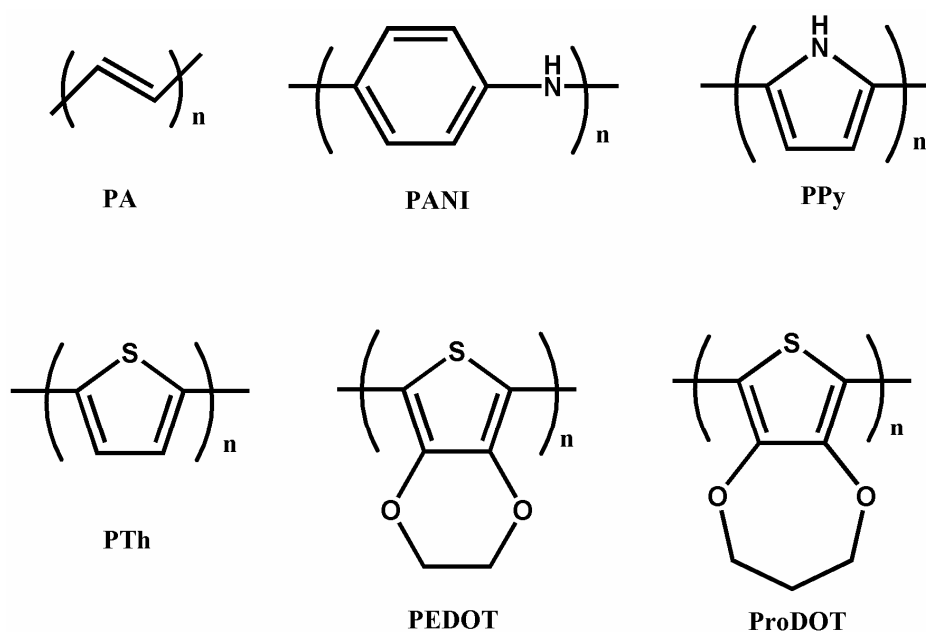


Figure 1.1. Common conjugated polymers.

These promising works increased the hope for usage of these materials as highly conducting metals for electrical transport and batteries. However, because of the instability of these conducting polymers in the doped state, other more realistic applications have been utilized like electrochromic rearview mirrors[3], polymer light-emitting diodes[4], organic solar cells [5], gas sensors [6], thin-film transistors[7] and electrochromic devices [8]. As a result of this breakthrough work the 2000 Nobel Prize in Chemistry went to Alan J. Heeger, Alan G. MacDiarmid and Hideki Shirakawa “for the discovery and development of conductive polymers” which reflects both research and practical importance of conducting polymers and their applications in modern science and daily life.

1.2 Band Theory

Band theory has been used to describe the characteristic properties of insulators, metals, and semiconductors. Metals possess partially filled bands, which lead to free movement of charge carriers resulted in conduction. In a semiconductor, there is a filled valence band and an empty conduction band separated by a band gap (E_g) where no energy levels are present. The conduction band can be populated by electrons across the band gap either thermally or photochemically. Semiconductors can be doped to increase the conductivity of the material. Charge carriers can be holes (p-type) or electrons (n-type) [9].

Although polyacetylene (PA) is fundamentally obsolete material compared to today's research interest, its structural simplicity offers a simple way for understanding the band theory of conducting polymers. PA is a simple chain of sp^2 hybridized carbon atoms with alternating single and double bonds. The theoretical study was performed long before than the synthesis of the material and it was found that there is an extensive delocalization which causes all the bond lengths to be equal (figure 1.2 A.).

According to the electron added orbital diagram, there is no energy difference between VB and CB. This approach seems to be reasonable since high conductivity demands partially filled bands.

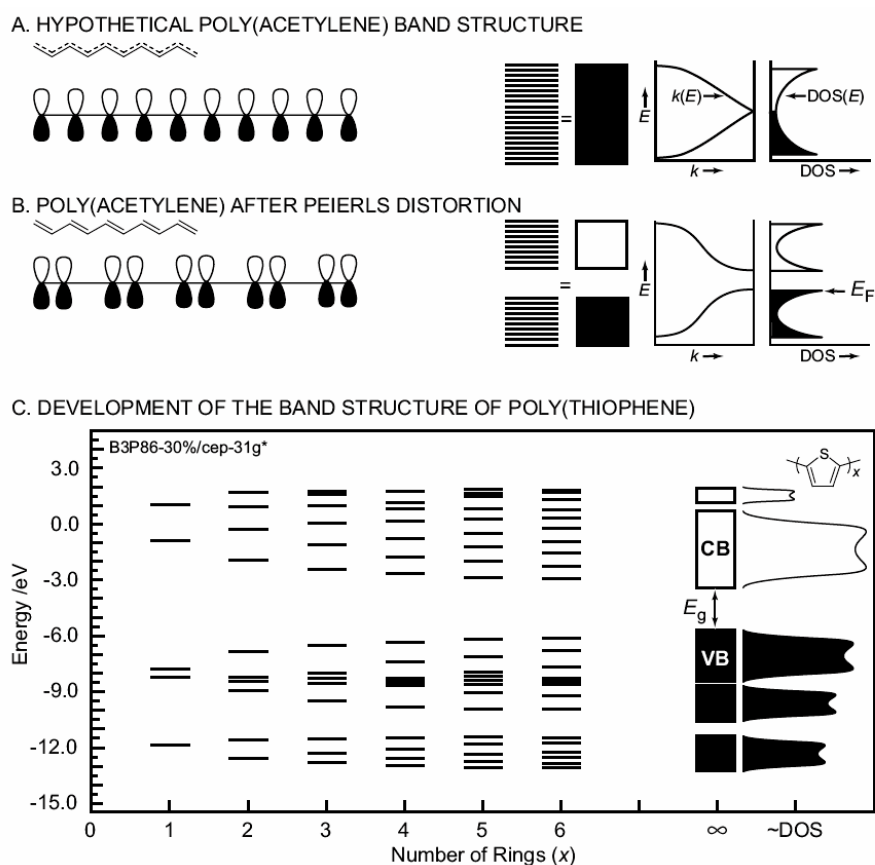


Figure 1.2 Formation of band structure from monomer to polymer. A. Poly(acetylene) hypothetical orbital and band structure. B. PA orbital and band structure after the system undergoes a Peierls distortion.[10]

PA(cis) it was found to be an insulating material with a very low conductivity of ca. 10^{-13} S cm^{-1} (trans-PA has a neutral conductivity of 10^{-5} - 10^{-6} S cm^{-1} .) Although isomerization occurs incompletely by heating, it can be achieved effectively upon doping (n-type) and charge compensation with AsF_5 [11]. Trans-PA

effectively dimerizes via Peierls distortion, [12] opening up a band gap at the Fermi level and drastically reducing the conductivity since electrons have to be thermally excited across the band gap to delocalize in the partially filled CB (figure 1.2 B). Hence, PA must be doped to either partially fill the CB by adding electrons (n-type doping) or partially vacate the VB by oxidation (p-type doping). Even though this doping process is possible and quite effective at improving the conductivity to a maximum of $2 \times 10^4 \text{ S cm}^{-1}$, it was resulted in an air unstable material and led synthetic chemists to work on other polymers that could be doped more efficiently. In the early 1980's it was discovered that electron rich poly(heterocycles) could be chemically or electrochemically oxidized to form CPs with relatively high conductivities. The evolution of the band structure of PTh is shown in Figure 1.2 C for its monomer, hexamer and polymer. Figure 1.3 shows the same formation of bands from overlapping molecular orbitals for polypyrrole (PPy) as determined by Density Functional Theory (DFT) calculations. These calculations are becoming widely used in CP research due to their accounting of electron correlation, accuracy in band gap prediction and relatively light computational requirements. (13)

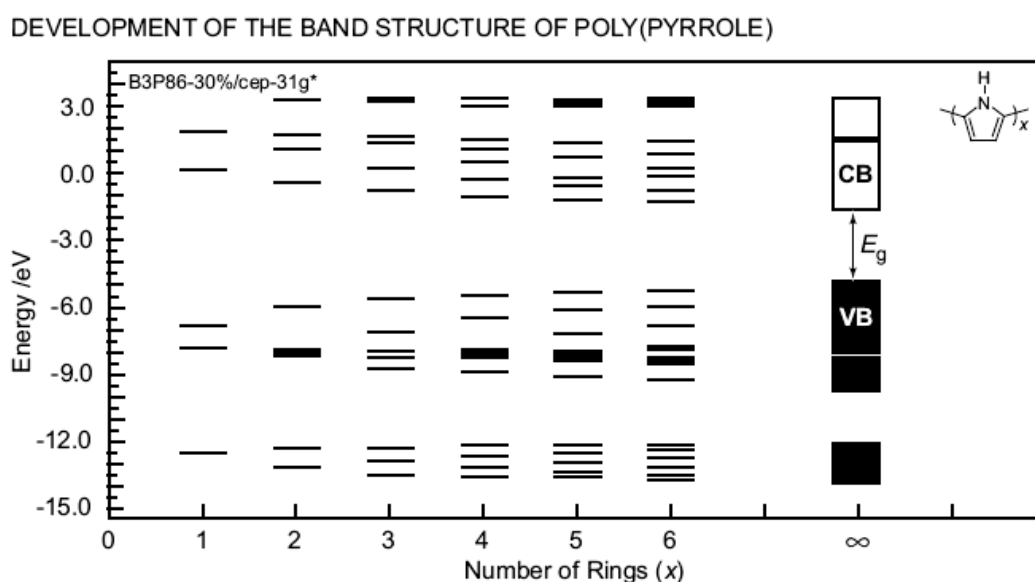


Figure 1.3 Evolution of the band structure of PPy from monomer to hexamer and polymer as determined by density functional theory. [13b]

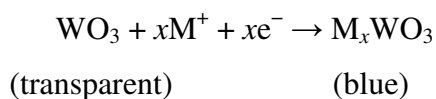
1.3 Conducting Polymer Redox Processes

Perhaps the most significant discovery in the entire field of conducting polymers was that the conductivity of PA could be increased by eleven orders of magnitude by chemical exposure to iodine or arsenic pentafluoride [1] and by electrochemical methods [14]. This phenomenal effect was realized by a doping process induced by the oxidation or reduction of PA, and is analogous to the doping of semiconducting inorganic materials. The electronic structure of many conducting polymers can be altered through oxidation or reduction. The oxidation of a neutral polymer by removing an electron from its valence band is referred to *p*-doping and the reduction of a polymer by adding an electron to its conduction band is referred to *n*-doping. Doping of conducting polymers is perhaps their most attractive property since this can not only make them highly conducting, but it can also completely change their optical, magnetic, and mechanical properties. The *p*-doping process has been explored to a much greater extent than *n*-doping due to the requirement of stringently dry and oxygen-free conditions [15]. However, there exist vast amount of publications on the *n*-doping process [15-18].

1.4 Electrochromism

Electrochromism is mainly defined as the reversible and visible change in transmittance and/or reflectance that is associated with an electrochemically induced oxidation–reduction reaction. It results from the generation of different electronic absorption bands in visible region upon switching between the states. The color change is commonly between a transparent state and a colored state, or between the two colored states. The electrochromic materials may exhibit several colors and termed as multichromic and the process is called as multicolor electrochromism. [19]. Basically, three classes of electrochromic materials are known; metal oxide films, molecular dyes and conducting polymers. A typical and most widely studied example of metal oxides is definitely the tungsten trioxide (WO_3). Tungsten oxide has almost a cubic structure which may be simply described as an “empty-

perovskite” formed by WO_6 octahedral that share corners. The empty space inside the cubes is considerable and this provides the availability of a large number of interstitial sites where the guest ions can be inserted. Tungsten trioxide (with all tungsten sites with an oxidation state W_{VI}) is a transparent thin film. Upon electrochemical reduction, W_{V} sites are generated to yield electrochromism (blue coloration to the film). Although, there is still controversy about the coloration mechanism, it is generally accepted that the injection and extraction of electrons and metal cations (Li^+ , H^+ , etc.) are responsible [20]. WO_3 is a cathodically ion insertion material. The blue coloration in the thin film of WO_3 can be erased by the electrochemical oxidation. The generalized equation can be written as follows:



Diquaternization of 4,4'-bipyridyl produces 1,1'-disubstituted-4,4'-bipyridilium salts, commonly known as “viologens” [21] which are also an important class of materials that reveals electrochromism. Of the three common viologen redox states (Figure 1.4), the dication is the most stable one and it is colorless. Reductive electron transfer to viologen dications forms radical cations. Generally the viologen radical cations are intensely colored, with high molar absorption coefficients, owing to optical charge transfer between the (formally) +1 and zero valent nitrogens. A suitable choice of nitrogen substituents in viologens to attain the appropriate molecular orbital energy levels can, in principle, allow color choice of the radical cation.

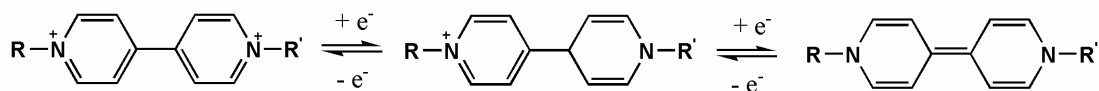


Figure 1.4 The three common viologen redox states, dication, radical cation, neutral species.

1.5 Electrochromism in Conducting Polymers

Electrochromism can be exploited in several optical devices with potential use in various applications, such as in information display and data storage, rear-view mirrors and visors in the automotive industry and smart windows in architecture (to control luminosity and save energy through the control of sunlight transmission) [22]. Among organic molecules, conducting polymers have attracted significant interest in the field of electrochromism, since they offer additional advantages such as low processing cost, enhanced mechanical properties, good UV stability, high coloration efficiency, fast switching ability and fine-tuning of the band gap through the modification of polymer's chemical structure. By adjusting the electronic character of the π system along the neutral polymer backbone, the π - π^* transition can be varied across the electromagnetic spectrum from UV to near-infrared region [23]. The redox switching of conjugated polymers is accompanied by changes in electronic transitions. Figure 1.5 shows the expected transitions in a conjugated polymer [24]. In the neutral state the polymer exhibits single broad transition from the valence band to the conduction band. The energy difference between these two levels is the band gap (E_g), is measured from the onset of the π to π^* absorption in the neutral state of the polymer. Upon oxidation, an electron removed from the valence band, and polarons form. This results in a state where an unpaired electron with energy state higher than the valence band. Accordingly, there occurs the lowering of the corresponding antibonding level in the conduction band; leading to formation of new two intragap states. This should lead to possible four new transitions.

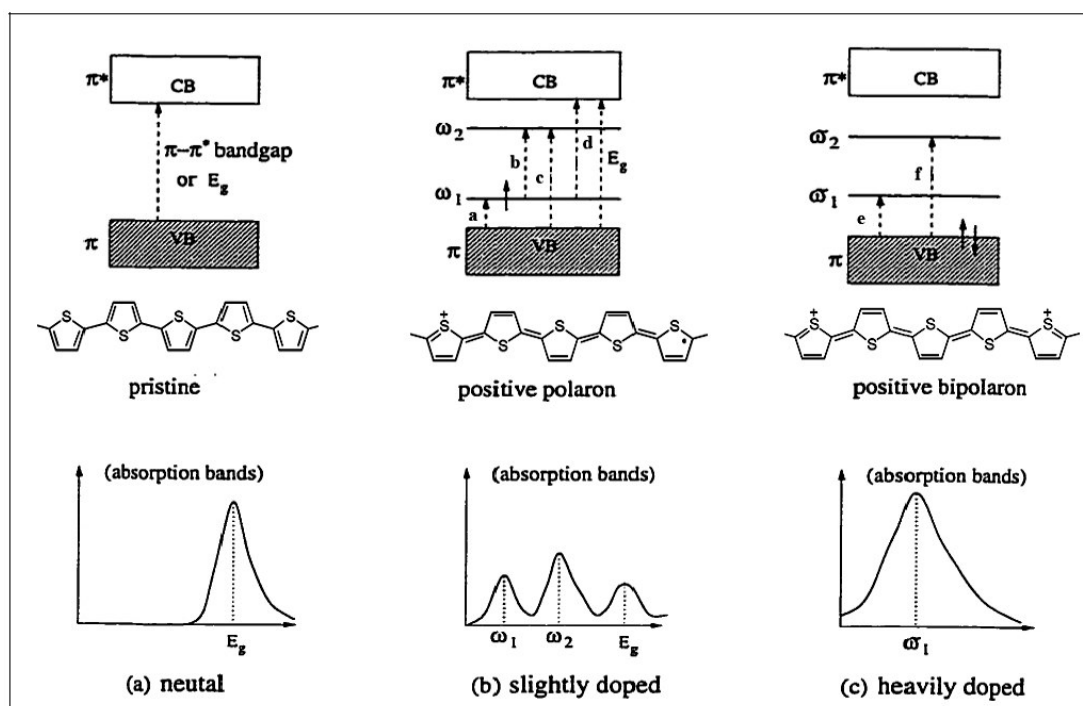


Figure 1.5 Polaron and bipolaron band diagrams in non-degenerate ground state polymers: (a) neutral, (b) slightly doped and (c) heavily doped polymer.

Among the conducting polymers polypyrrole is the one of the first to be investigated both in terms of its electropolymerization mechanism and optical properties. Doped (oxidized) polypyrrole film is blue-violet ($\lambda_{\max} = 670$ nm). Electrochemical reduction yields the yellow-green ($\lambda_{\max} = 420$ nm) “undoped” form. Removal of all dopant anions from polypyrrole yields a pale-yellow film. However, complete dedoping is only achieved if the PPy films are extremely thin. This means that thick films of polypyrrole (this is necessary to achieve high optical contrast) can not be used in device construction. This material is also highly susceptible to degradation upon repetitive color switching. Color changes involve the movement of counter ions into and out of the matrix. The charged species enter the polymer matrix and migrate slowly through the film. The speed of the color change depends on the speed at which the dopant ions can migrate in and out of the polymer matrix. Since the response time depends on the movement of charge compensating counter ions,

open polymer morphology often results in a reduced response time [25]. The ideal electrochromic polymer should have a high contrast between its extreme states with a having short switching time. Stability and maintenance of color after switching the current off are also among the expected features to be fulfilled.

1.6 Factors Affecting the Color of a Conducting Polymer

In the neutral state of the polymer, the color depends on the energy gap between the valence and conduction bands. The energy gap between bipolaron band and conduction band determines the color in oxidized state. These characteristics are all related to the conjugation of polymer, the electrochemical nature of side groups and their effects on the polymer backbone. Energy is related to the bond alternation ($E_{\Delta r}$), the mean deviation from planarity (E_{θ}), the aromatic resonance energy (E_{Res}), the inductive and mesomeric electronic effects of substituents (E_{Sub}) and interchain interactions (E_{Int}) (Figure 1.6).

$$E_g = E_{\Delta r} + E_{\theta} + E_{Res} + E_{Sub} + E_{Int}$$

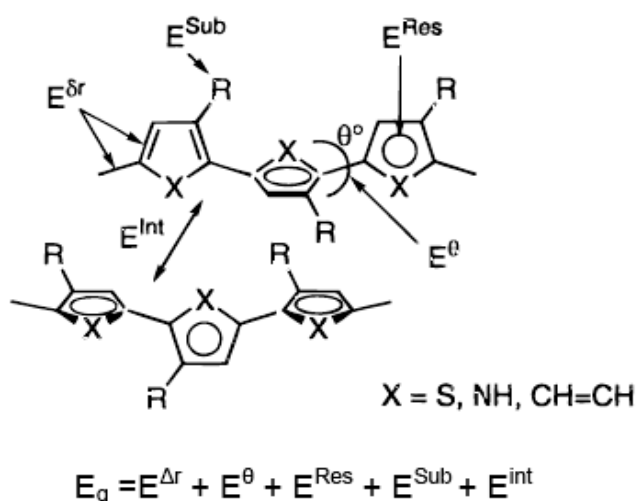


Figure 1.6 Schematic representation of parameters that play a determining role on the band gap [26].

Bond alternation is defined as the maximum difference between the length of a C-C bond inclined relative to the chain axis and a C-C bond parallel to the chain axis [27]. Poly(aromatics) such as polythiophene have non degenerate ground states, i.e. aromatic and quinoid structures are energetically not equivalent. Up to a certain extent, the band gap is known to decrease as the contribution of the aromatic geometry decreases. The classical example of aromaticity control in conjugated polyheterocycles is polyisothianaphthene (PITN), a polythiophene with a benzene ring fused at the 3- and 4-positions along the polymer backbone [28]. Single bonds between the aromatic cycles cause interannular rotations in conjugated polymers. The overlap of the orbitals varies with this twist angle, which causes the departure from co-planarity. The decline in the extent of overlap results in an increase of E_g by a quantity of E_Q . Introduction of flexible side chains causes steric interactions of sulfur groups of neighboring monomeric units which in return increases the rotational distortions for polythiophenes [29]. Regioregular poly(3-alkylthiophene)s have shown much lower band gaps and better electrochemical properties due to the ordering of the polymer films. Especially, head-to-head regiochemical defects are found to cause large twist around the bonds, leading to lowering of π electron configuration. Aromaticity in poly(aromatics) results in a competition between π -electron confinement within the rings and delocalization along the chain. It was shown that the band gap of conjugated polymer generally decreases with a decrease in the resonance energy per electron [28]. The introduction of electron-donating substituents onto a conjugated chain is a commonly used approach to decrease the polymer's oxidation potential by raising the energy of the valence band electrons ("HOMO" of the conjugated chain) and thereby band gap decreases by E_{Sub} . Electron releasing or withdrawing substituents are known to increase the HOMO and lower the LUMO respectively. Among the electrochromic materials, conducting polymers especially polythiophene derivatives, gained special interest owing to their facile switching properties, processibility, ease of color tuneability and their comparatively low cost [30]. Polythiophene thin films are blue ($\lambda_{max} \sim 800$ nm) in their doped (oxidized) state and red ($\lambda_{max} = 490$ nm) in their "undoped" form. Tuning of color is

possible by suitable choice of thiophene monomer, and this represents a major advantage of using conducting polymers for electrochromic applications.

In principle, di-substitution at the β positions should provide the synthetic basis to perfectly stereoregular polymers since di-substitution eliminates the possibility of β coupling and reduces the likelihood of cross-linking. However, this approach is severely limited by the steric interactions between substituents which lead to a decrease in polymer conjugation length. In fact, poly(3,4-dialkylthiophenes) have higher oxidation potentials, higher optical band gaps, and lower conductivities than poly(3-alkylthiophenes). This problem was solved by fusing the ring onto the heterocycle, effective pinning of the substituents back from the main chain, as in the case of poly(3,4-ethylenedioxythiophene). Cyclization between the 3 and 4 positions relieves steric hindrance in thiophenes.

In literature there are series of studies that acknowledge the combination of heterocycles, phenylenes and/ or vinylenes in extended conjugation monomers. Several polymers containing both EDOT and arylene moieties were synthesized.

Indeed a series of electron rich, low oxidation potential bis(EDOT) arylenes, including benzene [30] and carbazole [31] have been reported. Also use of vinylene group in similar approach resulted in polymers with even lower band gaps [31]. These are basically donor-acceptor or the so called push-pull substituted polymers. By this approach both electron donating and withdrawing groups are combined in a 1:1 ratio across the polymer backbone. The resultant polymer has the valence band of the donor and the conduction band of the acceptor groups.

1.7 Polarons, Bipolarons and π -Dimers

The first example of the conducting polymers is polyacetylene (PA). PA has a degenerate ground state, where two structures composed of alternating carbon-carbon double bonds have the exact same total energy. PA chains with an odd number of carbon atoms have an unpaired electron (a neutral soliton). Upon oxidation or reduction, a radical cation or anion is generated which is mobile along the polymer chain as shown in Figure 1.7 A.

Charge has the properties of a solitary wave, and does not dissipate as it traverses the chain. Solitons have a width because the spin density (for a neutral soliton) or the charge density (cationic or anionic solitons) is not localized on one carbon but rather spread over several [32].

As stated all CPs other than poly(acetylene) have non-degenerate ground states. In poly(heterocycles) there is an aromatic state and a quinoidal state of higher energy (except for PITN). Oxidation of a poly(heterocycle) creates a radical cation called a polaron where the delocalization is over *ca.* 4 to 5 rings.

This radical cation exhibits an EPR signal since there is an unpaired spin that is mobile under the influence of the applied potential along the polymer chain. Further oxidation at higher doping levels in poly(heterocycles) can create either a second polaron or a dication, called a bipolaron. A bipolaron is an EPR silent dication delocalized over 4 to 5 rings.

Even though a considerable debate about the nature of charge carriers in CPs has ensued, certain points are now clear in literature. First, at low doping levels, an EPR active signal is observed which is consistent with polarons. Second, as doping level increases, the EPR signal vanishes revealing a spin paired conducting state. Third, oxidized PTh shows a double peak absorption structure in the UV-Vis that is partially consistent with bipolarons as the charge carriers. The theory of electronic transitions for polarons and bipolarons was originated in the Su-Shrieffer-Heeger (SSH) model which predicted bipolarons as the stable charge carriers [33]. This model was enhanced by a continuum electron-phonon coupled model proposed by Fesser, Bishop and Campbell (FBC).[34] Early calculations have shown that the bipolaron is more stable than two polarons[35] by 0.45 eV (the difference between the bipolaron binding energy (0.69 eV) and the polaron binding energies (2 x 0.12 eV)) [36]. More recent calculations have shown that up to an oligomer with ten monomer units, a bipolaron is the stable charged species. Beyond that point, due to charge repulsion between the two cations, two polarons are the more favorable charged species. [37] The puzzle is that if this two polaron state is indeed favored, it is difficult to explain the EPR data which lacks in spins for highly doped polymers. A proposal that provides a partial solution to this problem is the π -dimer (Figure 1-10

C) as the stable charge carrier in highly doped conducting polymers. This would allow the predicted two polaron state to exist but solves the EPR problem. This has been demonstrated for oligomers of PPV [37] and poly(thiophenes) [38]. In most p-type doped CPs, the anions move in and out of the polymer film upon doping and dedoping and can be exchanged in electrolyte spontaneously, but are immobile in the film when dry after a certain doping level has been reached. Typically, the charge carriers must hop from one anion to the nearest anion along the chain as they move. Hence, there is a pinning potential for separating the polaron from its anion. At low doping levels, the pinning potential is becoming larger than the potential throughout the polymer which results in low conductivity. As the doping level increases, charge carriers have to migrate much shorter distances through the film and the pinning potential is thus smaller [39].

1.8 Polymerization Methods

Electrochemical polymerization is the method of choice for rapid characterization of conjugated polymers. Independent of the method used, (cyclic, potentiostatic, or galvanostatic) electrochemical polymerization allows for the synthesis of desired polymer on an electrode surface which facilitates to study electrochemical and optical properties. As shown in Figure 1.8, EDOT is converted to its radical cation by removal of an electron under an applied electric field. This intermediate is stabilized by the ethylenedioxy pendant group. Two reactions can then occur – attack of the radical cation on a neutral monomer or coupling of two radical cations. Both routes yield an intermediate that is rearomatized upon loss of two protons to give a dimer unit. Repeated coupling results in synthesis of the polymer.

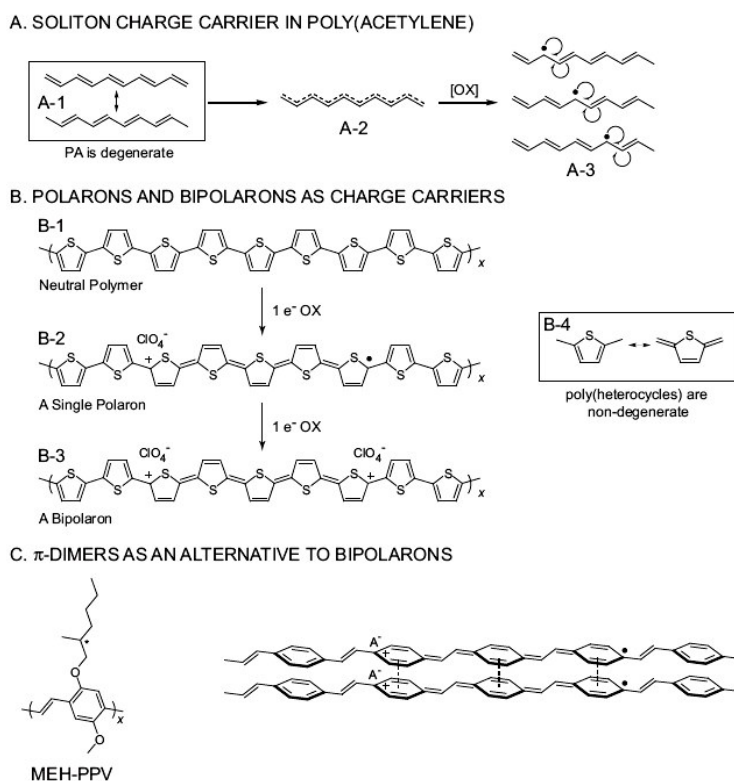


Figure 1.7 Charge carriers in conjugated polymers. (A) Solitons are the primary method of charge transport in doped PA. (B) Polarons and bipolarons are the charge carriers for doped poly(heterocycles) with non-degenerate ground states although π -dimers (C) are proposed as an alternative to polarons, especially in oligomeric materials. [10]

1.9. Donor-Acceptor Theory and Low Band Gap Systems

Minimizing the band gap is an important goal for maximizing the neutral conductivity of CPs. Most of CPs synthesized up to date have band gaps greater than 2 eV and they are characterized as mid- to high band gap polymers. Polymers with band gaps lower than 1.5 eV are considered relatively low band gap materials and few examples are available with band gaps below 0.8 eV [41]. PITN is a notable example of one of the earliest low band gap polymers, since there exists a

competition between aromatic and quinoid geometries in the polymer structure [42]. Band gap determines the conductivity and color of the neutral polymer, moreover the band edges determine ease of doping a polymer and the stability in the doped states compared to the neutral forms. Figure 1.9 describes the four ways most CPs can be classified.

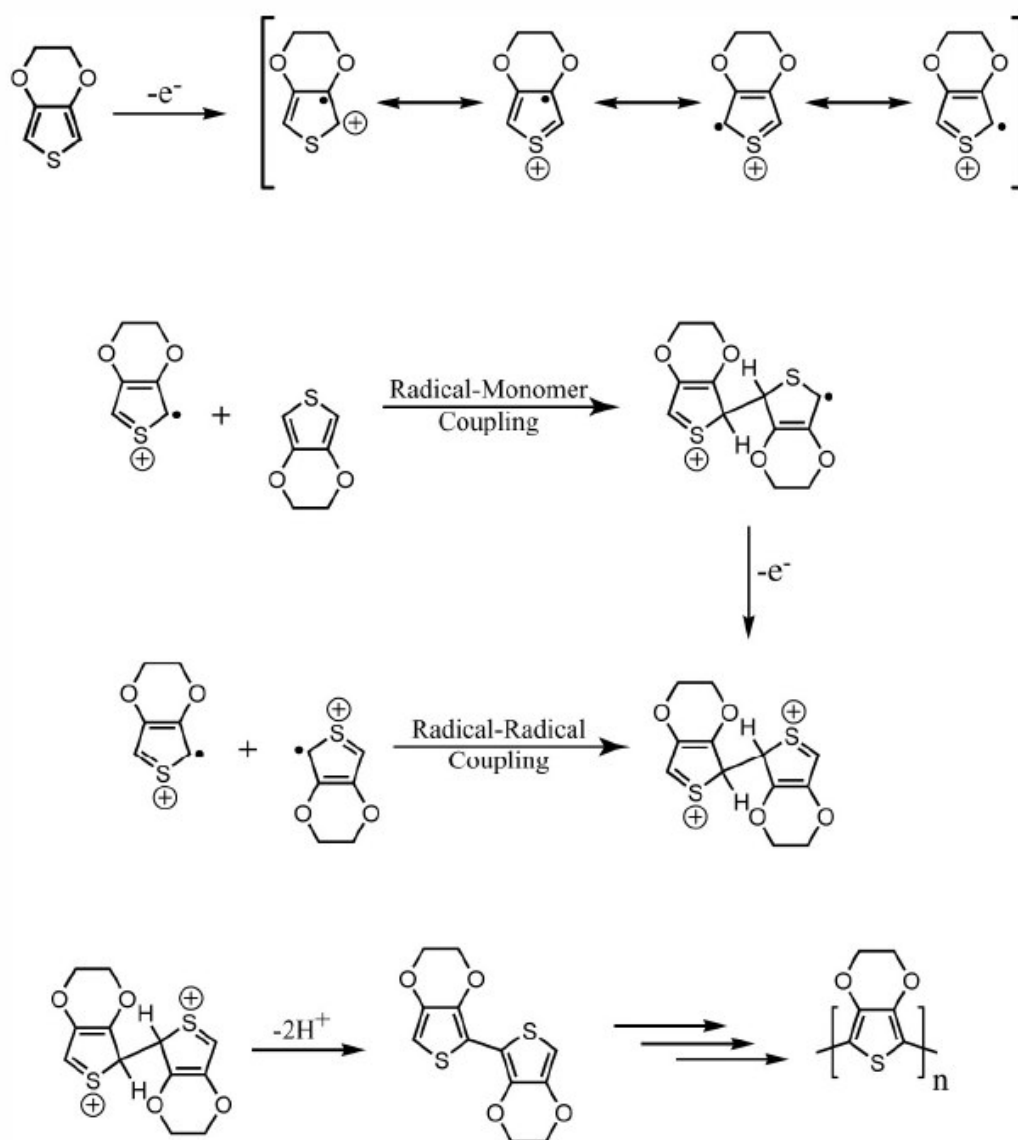


Figure 1.8 Electrochemical polymerization mechanism of EDOT.[40]

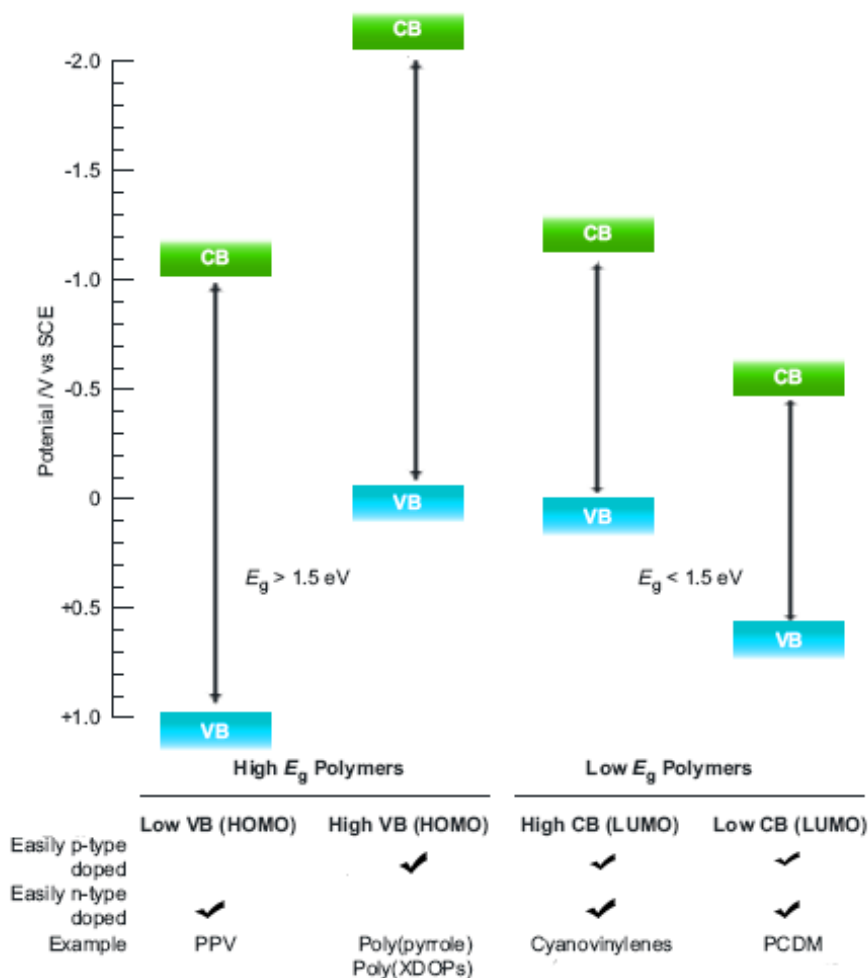
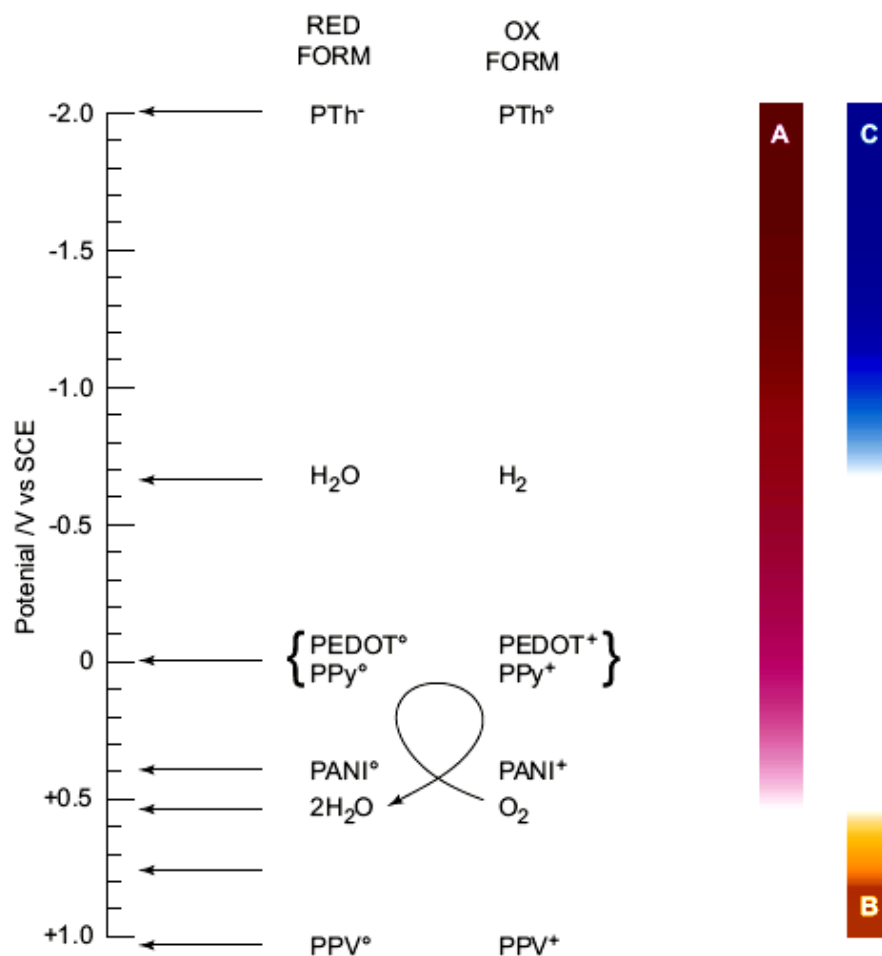


Figure 1.9. Possibilities for positioning of band edges in both high and low band gap polymers.

The common case is a high band gap polymer with a high VB. For many applications, a low band gap polymer with a low CB is desirable and few examples are available. Examples of polymers with these characteristics are PPy, PTh, PEDOT and poly(3,4-alkylenedioxyppyroles) (PXDOPs). These polymers are all prepared by oxidative polymerization routes and are easily p-type doped [43] by virtue of their high lying VB. Due to their high band gap, the CB is generally out of reach for stable electrochemical n-type doping. PTh does exhibit n-type doping at very negative potentials and PEDOT is even more difficult to n-dope compared to PTh. Another

situation is the high gap/low VB polymer such as PPV and its analogues. PPV is not easily doped electrochemically,⁽⁴⁴⁾ but its bands are positioned so that charge carriers of either sign can be injected making this class of polymer useful in light emitting devices where the emission energy is tuned by modifying the band gap.

Low gap polymers are relatively recent topic of research interest and these types of polymers have many interesting applications. Regardless of how the band energies line up, the low band gap often causes these polymers to be transparent in the doped state (p- or n-type). This makes them useful in a variety of devices such as electrodes and smart windows where the transparency can be exploited. As with the high gap polymers, the color of low gap polymers is dictated by the magnitude of the band gap. Since the distance between the edge of the VB and CB is smaller by definition in low gap systems, the CB is generally more accessible to n-type doping even for low gap polymers with relatively high VBs. These classes of materials are significantly important since they are offering the transparency of low gap systems with the ability to be both n-type and p-type doped for the same polymer. Although it is obvious that the VB needs to be relatively low in energy for facile n-type doping, the significant point is how low VB should be in order to have a stable conductive for device applications. The answer to this question is a little complicated and probably lies in the available redox couples that produced are described and illustrated in Figure 1.10.



- A** **p-type** dopable polymers in the neutral state with $E_{1/2}(\text{to } +)$ in this range are oxidized by O_2 (p-doped form stable under ambient conditions).
n-type dopable polymers in the reduced state with $E_{1/2}(\text{to } -)$ in this range are oxidized by O_2 (neutral form stable under ambient conditions).
- B** **p-type** dopable polymers in the neutral state with $E_{1/2}(\text{to } +)$ in this range are stable to O_2 (neutral form stable under ambient conditions).
- C** **n-type** dopable polymers in the reduced state with $E_{1/2}(\text{to } -)$ in this range are oxidized by H_2O (neutral form stable under ambient conditions).

Figure 1.10 Stability of CPs in their oxidized or reduced forms depends on where the formal oxidation potential (E°) lies (a direct consequence of the VB (p-type) or CB (n-type)). A p-type polymer with a low E° is stable in its neutral state. Adapted from [10].

For a p-type polymer, the reaction of interest is the O_2/H_2O couple where oxygen could oxidize the neutral polymer to its p-type doped state. This redox couple is very near the E° (formal redox potential) for several conducting polymers and p-type doped polymers with an E° more anodic to the O_2/H_2O couple are reduced by H_2O and are stable in the neutral form. Polymers with a high enough VB to have an E° cathodic to the O_2/H_2O couple are stable in the p-type, oxidized state. For n-type conducting polymers the reaction of interest is the H_2O/H_2 couple. A polymer with an E° cathodic of this couple (nearly all of the polymers up to date) will be oxidized by H_2O to the neutral form of the polymer. This appears at ca. -0.65 V vs. SCE. With typical overpotentials it is necessary to have a polymer with an E° more anodic to -0.5 V vs. SCE for the polymer to be stable in the presence of water.⁽⁴⁵⁾ This is a far more significant problem than the need to have an E° for p-type doping cathodic to ca. $+0.5$ V vs. SCE (to be stable in the oxidized state), since even moderately electron rich polymers are well cathodic of this value. To have a polymer that is stable against water in its n-type form and stable against oxygen and water in its p-type form, a band gap of less than 1 eV is required.

In designing low band gap systems, there are many methodologies. Five basic approaches have been used to reduce band gap; controlling bond-length alternation (Peierls distortion), creating highly planar systems, inducing order by interchain effects, resonance effects along the polymer backbone, and using donor-acceptor molecules. Bond-length alternation is the difference in the length of single and double bonds along the polymer backbone. The quinoidal form has a much lower band gap than the aromatic state. The classical example of aromaticity control in conjugated polyheterocycles is PITN. Benzene, with energy of aromatization of 1.56 eV, is more aromatic than thiophene (1.26 eV). This, forces PITN to be more energetically stable in the quinoidal state, which provides for a lowered band gap of 1.1 eV compared to polythiophenes.

As shown in Figure 1.11, the higher the torsional angle between adjacent rings the larger the band gap of a system. A number of researchers have utilized many different methods to achieve highly planar low band gap systems. One successful approach has been the ladder-type polymers such as the polyacene family.

Another has been synthesis of polyquinoxalines. However, these systems exhibit extreme cases of bond-length alternation and give much higher energy gaps than expected.

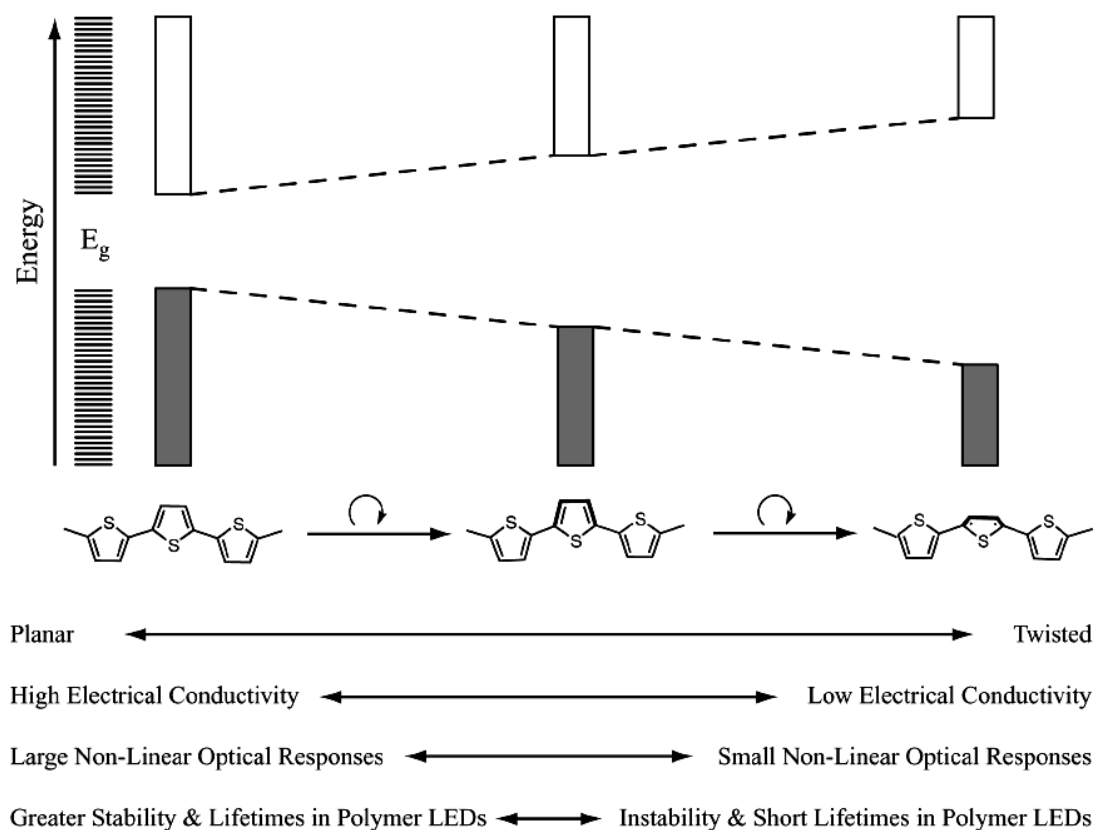


Figure 1.11 Planarity effects on band gap and the electrical and optical properties of conjugated polymers. Adapted from [40].

In the case of PITN, polymerization occurs through 2 and 5 positions of the thiophene ring. This arrangement induces a competition for aromaticity in the monomer repeat since it is impossible for both thiophene and benzene to simultaneously be aromatic. Benzene itself has an energy of aromatization (E_{res}) of 1.56 eV while thiophene is 1.26 eV.[46] These energetics predict that benzene will remain aromatic and force the thiophene to adopt a pseudo-diradical electronic state at the 2 and 5 positions. When polymerized, this effect forces thiophene units to be in

the quinoid form, which lowers the band gap of the system by decreasing bond length alternation. While this proves to be an effective method for lowering the polymer band gap, PITN has a band gap of 1.1 eV, about 1 eV lower than that of PTh but these structural effects seem to be limited in scope.

Research over the last decade aimed almost exclusively to manipulate band gap via synthesizing polymers having alternating donor and acceptor moieties. The donor-acceptor route has by far the most useful in terms of diversity in synthetic possibility and additionally avoiding solubility problems. The donor-acceptor approach can be generally classified into two distinct families; polymers with effective aromatic and quinoid forms (acceptor group directly have resonance effect on the polymer backbone) and those which cannot (acceptor group inductively modify the polymer backbone) as shown in figure 1.12.

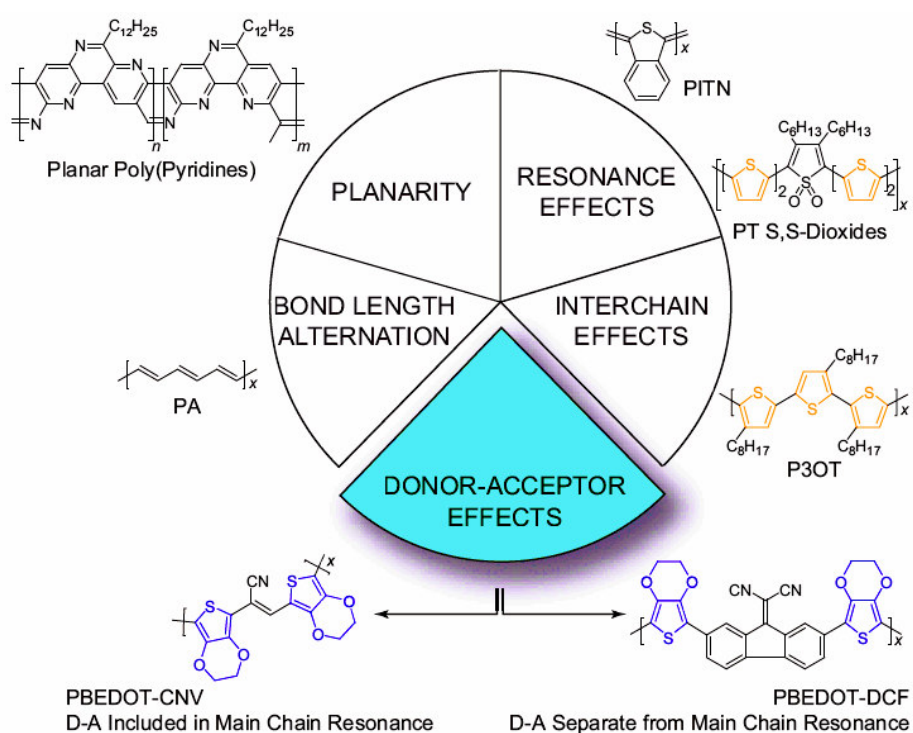


Figure 1.12 Overview of methods for the modification of band gap. [10]

The logic behind the donor-acceptor approach (D-A) is having a high HOMO of the donor and a low level of the LUMO moieties incorporated into the monomer. [47] Figure 1.13 illustrates this concept for PEDOT,[48] poly(cyanoacetylene) (PCA)[49] and PBEDOT-CNV.(anticipated).

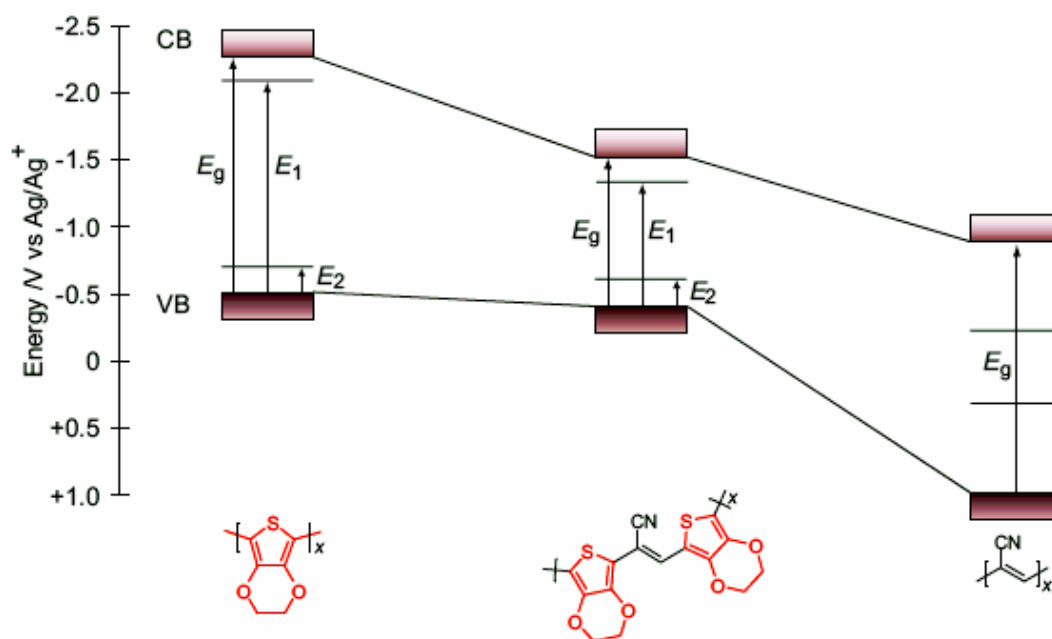


Figure 1.13 The Donor-Acceptor approach, alternating donor and acceptor moieties results in a polymer that has the combined optical properties of the parent donor or acceptor monomers. [10]

In this example, the band gaps are established through the onset of the π to π^* transition in the spectroelectrochemical series and the energies are estimated from the potentials for the electrochemical doping/undoping redox couples. Specifically, the HOMO for PEDOT was obtained by cyclic voltammetry, the band gap by spectroelectrochemistry, and the LUMO level was deduced by subtraction of the band gap from the HOMO level (n-type doping of PEDOT been demonstrated buy even under controlled atmospheric conditions its stability is highly low) [50]. PCA possess a similar set of problems as there is no observable oxidation. LUMO level of

PCA was calculated from cyclic voltammetry and the band gap by spectroelectrochemistry. LUMO energy and band gap value was used to calculate the low lying HOMO energy. As seen from the figure 1.13 the band gap of the resulting D-A type polymer was drastically decreased.

1.10 Pendant Group Effects

Pendant groups on conducting polymers are generally defined as the constituents that do not directly contribute to the electronic structure of the polymer backbone through resonance or induction. Nevertheless, the pendant group structure has an enormous effect on the polymer structure by modification of the secondary structures or bulk morphologies [51-55].

1.11 Alkyl Solubilizing Groups

One significant discovery was that PTh could be made soluble in common organic solvents while maintaining its high conductivity by introduction of an alkyl chain onto the polymer repeat unit [56-61]. It has also been demonstrated that the variation of the chemical functionality of pendant groups has tremendous effects on many properties, such as inducing water solubility, H-bonding, and polymer chain aggregation [62]. The EDOT [63] and ProDOT [64-66] have also been great success since it was found that alkyl substitution can drastically increase the solubility of these polymers.

1.12 Donor-Acceptor Approach for the Synthesis of n-Dopable Conjugated Systems

One of the greatest challenges to the field of conjugated polymers is the ability to generate an ambient stable n-type doped state. Up to date, there are no examples of n-type doped systems stable to ambient conditions due to the high

reactivity of the anion charge carriers with oxygen and water. By controlling both the electron donating and electron accepting abilities of the monomer, it is expected that the corresponding polymers will have accessible oxidation and reduction potentials and lowered band gaps. In recent years, researchers on low band gap polymers demonstrated that introduction of nitrogen within the polymer repeat unit stabilizes the n-type doped state by lowering the LUMO.

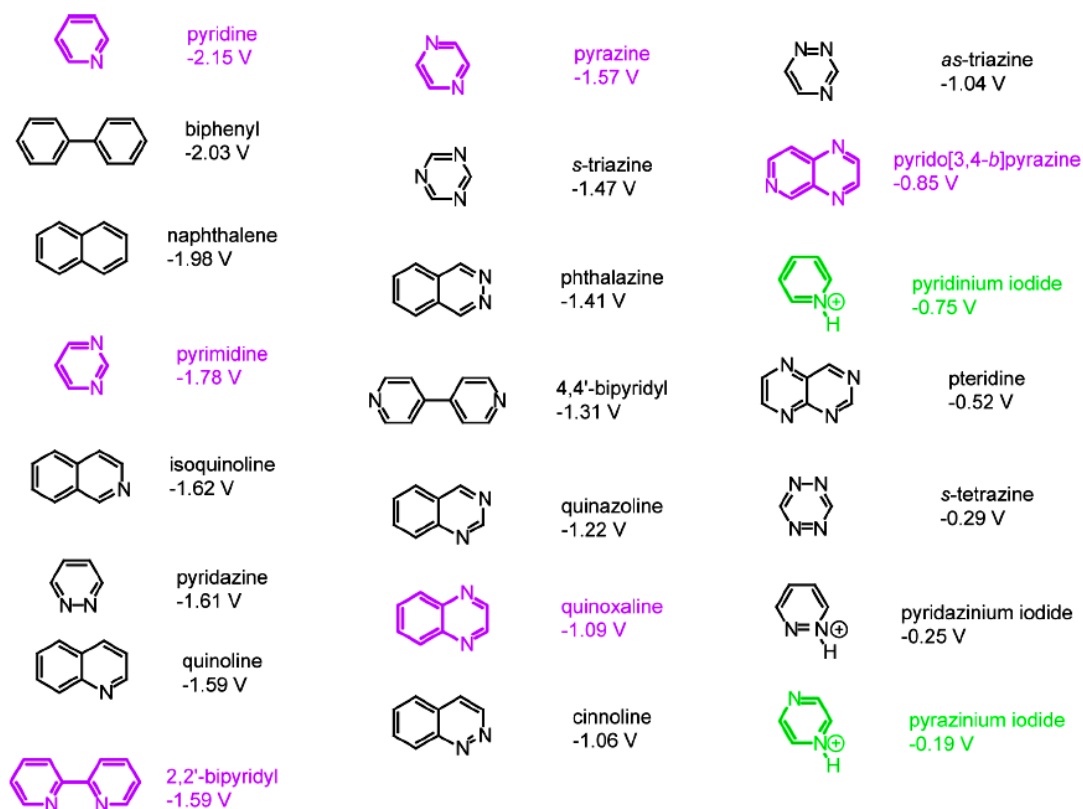


Figure 1.14. Reduction potentials (vs SCE) of common nitrogen containing heterocyclics. Structures highlighted in purple are either commercially available or their dihalo derivatives can easily be synthesized. Structures highlighted in green have easily protonated sites. [40]

As illustrated in Figure 1.14, the incorporation of single nitrogen for example pyridine, allows for reduction (2.15 V vs SCE) equivalent to biphenyl which is a

more extended aromatic system. Heterocyclics containing multiple nitrogens have potentials even more positive than pyridine. The relative placement of the nitrogen atoms is also an important factor. Incorporation of a second nitrogen shifts the reduction potential 300 mV more positive for pyrimidine and 500 mV for pyrazine. Quinoxaline has a reduction potential of -1.09 V, while pyrido[3,4-*b*]pyrazine gets reduced at -0.85 V. This “nitrogen-effect” is due to the lower molecular orbital energy of nitrogen in compare to carbon for these systems [67]. Of the systems shown in Figure 1.14, only the compounds highlighted in purple have dihalo derivatives, which is a significant requirement for metal-catalyzed coupling reactions that are crucial for synthesizing donor-acceptor type monomers.

A second important factor for lowering conduction band levels for nitrogen containing heterocycles is the ability to be protonated easily. This effect is shown in the reduction potential of both pyridinium and pyrazinium as 1.4 V more positive than pyridine and pyrazine, respectively. Several groups have used this effect to reversibly lower the conduction band level, where it significantly alters the electrochemical and optical properties of these systems [68,69].

PEDOT has one of the highest change in transmittance upon doping among the electrochromic polymers [70]. To probe the electron acceptor strength effects in the conduction band energy levels, thieno[3,4-*b*]pyrazine and quinoxaline derivatives were incorporated within the EDOT donor structures to yield donor-acceptor systems with compressed band gaps. This allows both oxidation and reduction to be readily accessible within the desired electrochemical window. The transmissivity for these polymers is expected since donor-acceptor systems yield lower band gaps [71].

1.13 Importance of Neutral State Green Polymeric Materials

In the history of polymeric electrochromic materials, the discovery of a neutral state green polymer was definitely one of the most important achievements for the commercialization of these materials. Most of the polymers studied so far mainly absorb/reflect blue and red colors. The main reason for this is; these materials have

one dominant wavelength. To obtain a green color there should be at least two simultaneous absorption bands in the red and blue regions of the visible spectrum.

In 2004 Gursel et. al. reported electrochemical and optical properties of the first neutral, green colored conjugated polymer[72]. Although this material revealed an extreme stability (stable even after 10000 double potential steps), the residual brown color of the polymer in the oxidized state obstruct the potential use of this material as the missing third leg of additive primary color space. It is important to state that structural modification of a conjugated polymer system can lead to many differently colored polymers [73,74]. Using different polymers in their neutral, intermediate, p-doped and n-doped states can produce a variety of colors [74]. On the other hand, by keeping color mixing theory in mind, it would be possible to obtain all visible spectrum by having materials that have additive or subtractive primary colors in their neutral state. Theoretically, if two color stimuli are mixed, the resulting color stimulus will lie somewhere along the straight line connecting the two points on the chromaticity diagram. For use in displays, polymers should switch between one of the three primary colors and their transmissive states. As stated above most of the polymers studied so far mainly absorb/reflect blue and red colors in their neutral states. On the contrary, to have a green color, there should exist at least two simultaneous absorption bands in the red and blue regions of the visible spectrum. Additionally the difficulty in controlling both absorption bands with the same applied potential must be overcome. These phenomena have been fulfilled with ground breaking work of Sonmez et al [72].

Although the neutral state color is of great importance, the transmittance in the oxidized state is crucial too. The materials having one of the three primary colors should also possess highly transmissive oxidized states in order to be used in commercial electrochromic device applications. Hence, the major prerequisite in the field for producing green polymeric materials with transmissive oxidized states is to have two absorption maxima and disappearance of these absorption bands in the visible region upon successive oxidation.

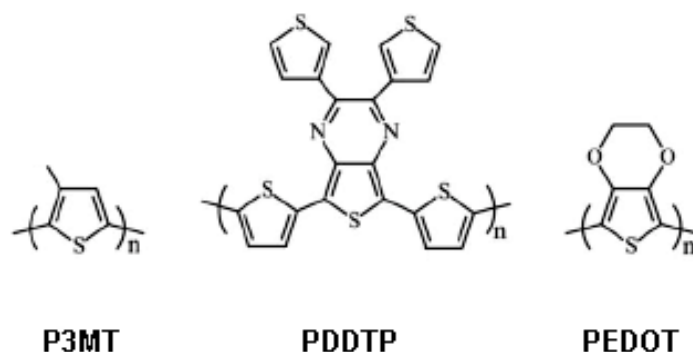


Figure 1.15. Poly(3-methylthiophene) (P3MT), poly(2,3-di(thien-2-yl)thieno[3,4-b]pyrazine) (PDDTP) and poly(3,4-ethylenedioxythiophene) (PEDOT) were the red, green and blue colored polymers respectively. Adapted from [72].

Here, polymers P3HT and PEDOT have absorption maxima in the visible region at 500 and 615 nm, reflecting red and blue colors, in their colored states. Besides, PDDTP absorbs in the regions below and above 550 nm with a valley (absorption minimum) at this wavelength and maxima at 380 and 760 nm, reflecting a very saturated green color. (Figure 16)

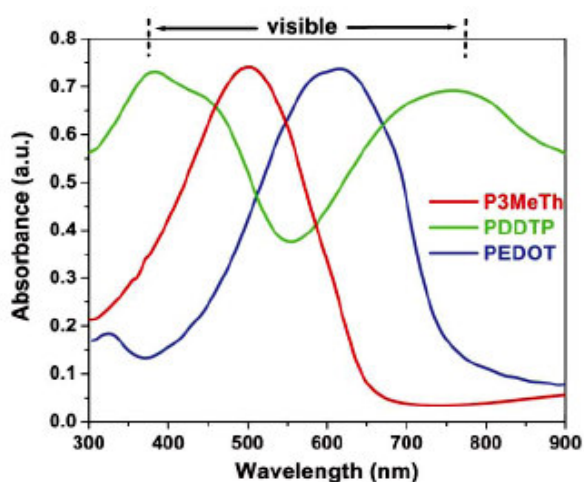


Figure 1.16. Combined spectroelectrochemistry of P3MT, PDDTP and PEDOT in the neutral state. Adapted from [72].

These two absorption bands are controlled together with the same applied potential. A combination of these three spectra covers the entire visible region without reflecting any light that produces a black color. Colors vanish as RGB colored polymers are oxidized, thereby producing a pale blue color for the polymers P3MT and PEDOT and a transmissive brown color for PDDTP (Figure 17).

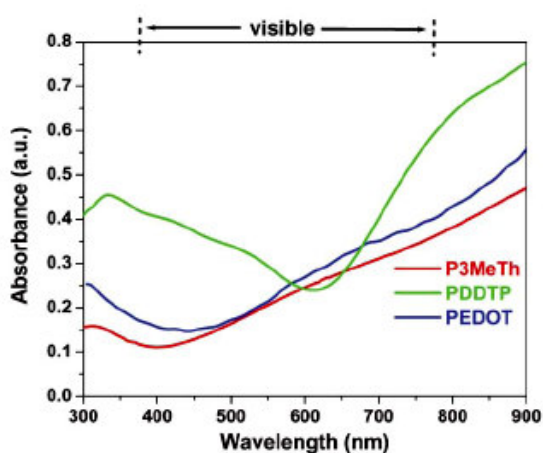


Figure 1.17. Combined spectroelectrochemistry of P3MT, PDDTP and PEDOT in the oxidized state. Adapted from [72]

It should be noted that, although the polymers, P3HT, PDDTP and PEDOT, have highly saturated RGB colors in their neutral forms, the residual pale brown color of PDDTP in the oxidized form is still was a major problem in applications. The red and blue colored polymers have very similar spectrum in their oxidized states. If the green polymer can also produce a similar spectrum to the red and the blue colored polymers in its oxidized state, then it will be convenient to use a color filter to bring all the RGB colors to the white point (W) in the CIE (Commission Internationale de l'Eclairage International Commission on Illumination) color space. The optical contrasts ($\% \Delta T$) of the red (P3HT) and blue (PEDOT) colored polymers, were calculated as 53% and 55% at their dominant wavelengths in the visible region.

The green polymeric electrochromic (PDDTP) shows relatively low optical contrasts at its absorption maxima in the visible region compared to those of the red and the blue colored polymers. It has 23% and 12% transmittance changes ($\% \Delta T$) 370 and 725 nm, respectively. These drawbacks of the first green polymeric material were eliminated by Toppare group with donor-acceptor type polymer bearing benzothiadiazole and EDOT units as the acceptor and donor units respectively. [75]

1.14 Donor-Acceptor Methods towards Green Polymeric Materials

Although the neutral state color is of great importance, the transmittance in the oxidized state is crucial too. The materials having one of the three primary colors should also possess highly transmissive oxidized states in order to be used in commercial electrochromic device applications. Hence, the major prerequisite in the field for producing green polymeric materials with transmissive oxidized states is to have two absorption maxima and disappearance of these absorption bands in the visible region upon successive oxidation. This can be only achieved by the means of donor-acceptor approach [76]. Donor-acceptor systems lead to narrower band gap due to resonances that enable a stronger double bond character between the donor and acceptor units [77]. The low band gaps as low as 0.45 eV [78] have been reported. This is attributed to hybridization between the energy levels, especially the HOMO of the donor and the LUMO of the acceptor [79].

As discussed in detail (Section 1.9.) the main idea behind this approach is the regular alternation of conjugated donor and acceptor moieties in a conjugated chain which leads to broadening of valence and conduction bands to induce a small band gap [80]. In literature there are examples [81] where the resultant polymer revealed two distinct π - π^* transitions due to the transitions from the thiophene based valence band 1) to its antibonding counterpart and 2) to the substituent localized and narrow conduction band [82]. Although two absorption bands is a necessity, the maximum absorption wavelengths are the decisive values to possess neutral state green polymers. Hence the match between donor and acceptor moieties is crucial.

1.15 Aim of this Work

Several donor acceptor type polymers were synthesized and shown to be neutral state green polymeric materials with transmissive oxidized states. EDOT was chosen as the donor group and many acceptor groups including 2,3-diphenyl quinoxaline, diphenylthieno[3,4,b]pyrazine, 2,3-bis(4-tert-butylphenyl)quinoxaline and 2,3-bis(3,4-bis(decyloxy)phenyl)quinoxaline were utilized to realize donor-acceptor type polymers. Additionally, benzo[1,2,5] thiadiazole, quinoxaline, 2,3-di(thiophene-2yl)quinoxaline were also used as the acceptor groups for neutral state green polymeric materials though not included in the scope of this thesis. The polymer synthesized with 2,3-bis(3,4-bis(decyloxy)phenyl)quinoxaline as the acceptor unit was shown to be the first processable neutral state green polymer with a transmissive oxidized state reported up to date.

CHAPTER II

EXPERIMENTAL

2.1. Materials

All chemicals were purchased from Aldrich except for anhydrous tetrahydrofuran (THF) and 3,4 diaminothiophene which were purchased from Across and University of Ulm, Germany [83] respectively. 4,7-Dibromobenzo[1,2,5]thiadiazole [84], 3,6-dibromo-1,2-phenylenediamine [85], benzoin [86], benzyl [86], 1,2-bis(4-tert-butylphenyl)-2-hydroxyethanone [87], 1,2-bis(4-tert-butylphenyl)ethane-1,2-dione [87] , tributyl(2,3-dihydrothieno[3,4-b][1,4]dioxin-5-yl)stannane [88], 5,8-dibromo-2,3-diphenylquinoxaline [89] , 1,2-bis(decyloxy)benzene [90], 1,2-bis(3,4-bis(decyloxy)phenyl)ethane-1,2-dione [90] , 2,3-Diphenylthieno[3,4,b]pyrazine [91], 5,7-dibromo-2,3-diphenylthieno[3,4-b]pyrazine [92] were synthesized according previously reported methods. Acetonitrile (ACN) was dried and distilled over calcium hydride under nitrogen. N-bromosuccinimide was recrystallized from hot water. Tetrahydrofuran (THF) was distilled over Na/benzophenone prior to use. Dimethyl formamide (DMF) was distilled under vacuum over CaH₂.

2.2. Equipments

The cyclic voltammograms were recorded using a system consisting of a potentiostat (Wenking POS 73), an X-Y recorder and a CV cell containing Pt foil working and counter electrodes, and a Ag/Ag⁺ reference electrode. Measurements were carried out at room temperature under nitrogen atmosphere.

Spectroelectrochemical studies were carried out on a HP8453A UV-Vis Spectrophotometer. Colorimetry measurements were obtained by a Coloreye XTH Spectrophotometer (GretagMacbeth). NMR spectra of the monomers were recorded on a Bruker-Instrument-NMR Spectrometer (DPX-400) with CDCl₃ as the solvent and chemical shifts (δ / ppm) were given relative to tetramethylsilane as the internal standard. The IR spectrum was recorded on a VARIAN 1000 FTIR spectrometer. Electron Spin Resonance studies were performed on a Bruker ELEXSYS E580. High Resolution Mass Spectroscopy (HRMS) was performed with a JMS-700 MStation (JEOL) at the Chemistry Department, University of Massachusetts at Amherst. Molecular weights of the polymers were determined on Polymer Laboratories PL-GPC 200. Mass analysis was performed on TOF Bruker Mass Spectrometer with an electron impact ionization source.

2.3. Monomer Syntheses:

2.3.1 2,3-Diphenyl-5,7-bis(3,4-ethylenedioxy-2-thienyl)thieno[3,4-b]pyrazine (GS)

A mixture of 5,7-dibromo-2,3-diphenylthieno[3,4-b]pyrazine (100 mg, 0.202 mmol), tributyl(2,3-dihydrothieno[3,4-b][1,4]dioxin-5-yl)stannane (384 mg, 0.89 mmol), PdCl₂(PPh₃)₂ (100 mg, 0.14 mmol), and DMF (15 mL) were heated at 100 °C for 4 h under argon atmosphere. The solvent was evaporated and extracted with ethyl acetate-brine several times. The organic phases are combined and dried over MgSO₄. The crude product was purified by flash chromatography and a previously reported work-up procedure to remove the Bu₃SnBr was applied to give the title compound as a blue solid (78 mg, 68 % yield).

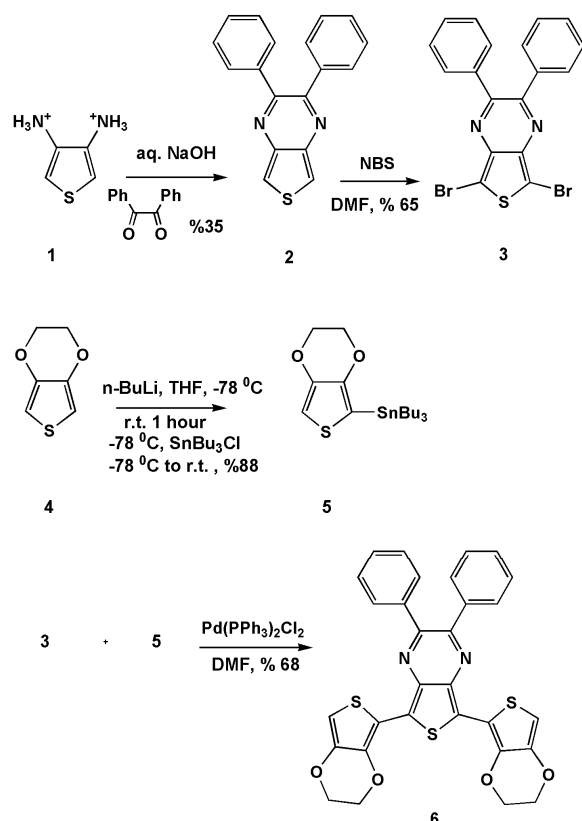


Figure 2.1 Synthetic route to monomer GS.

2.3.2. 2,3-Bis(4-tert-butylphenyl)-5,8-(2,3-dihydrothieno[3,4-b][1,4]dioxin-7-yl)quinoxaline (TBPEQ)

2.3.2.1 2,3-Bis(4-tert-butylphenyl)-5,8-dibromoquinoxaline

A solution of 3,6-dibromo-1,2-phenylenediamine (1.0 g, 3.8 mmol) and 1,2-bis(4-tert-butylphenyl)ethane-1,2-dione (1.223 g, 3.8 mmol) in EtOH (40 ml) was refluxed overnight by with a catalytic amount of PTSA. The mixture was cooled to 0 °C. The precipitate was isolated by filtration and washed with EtOH several times to afford the desired compound. (1.5 g, 72%).

2.3.2.2 3-Bis(4-tert-butylphenyl)-5,8-(2,3-dihydrothieno[3,4 b][1,4]dioxin-7-yl)quinoxaline (TBPEQ)

2,3-Bis(4-tert-butylphenyl)-5,8-dibromo quinoxaline (400 mg, 0.8 mmol) and tributyl (2,3-dihydrothieno[3,4-b][1,4]dioxin-5-yl)stannane (1724 mg, 4 mmol) were dissolved in dry THF (90 ml), the solution was purged with argon for 30 min. and PdCl₂(PPh₃)₂ (120 mg, 0.171 mmol) was added at room temperature under argon atmosphere. The mixture was stirred at 100 °C under argon atmosphere for 15 hours, cooled and concentrated on the rotary evaporator. The residue was subjected to column chromatography (DCM-Hexane 3:1) to afford an orange solid (285 mg, % 58).

2.3.3 2,3-Diphenyl-5,8-(2,3-dihydrothieno[3,4-b][1,4]dioxin-7-yl) quinoxaline (DPEQ)

2,3-Diphenyl-5,8-dibromoquinoxaline (400 mg, 0.9 mmol) and tributyl(2,3-dihydrothieno[3,4-b][1,4]dioxin-5-yl)stannane (1724 mg, 4 mmol) were dissolved in dry THF (90 ml), the solution was purged with argon for 30 min. and PdCl₂(PPh₃)₂ (120 mg, 0.171 mmol) was added at room temperature under argon atmosphere. The mixture was stirred at 100 °C under argon atmosphere for 15 hours, cooled and concentrated on the rotary evaporator. The residue subjected to column chromatography (DCM-Hexane 3:1) to afford an orange solid (264 mg, % 53).

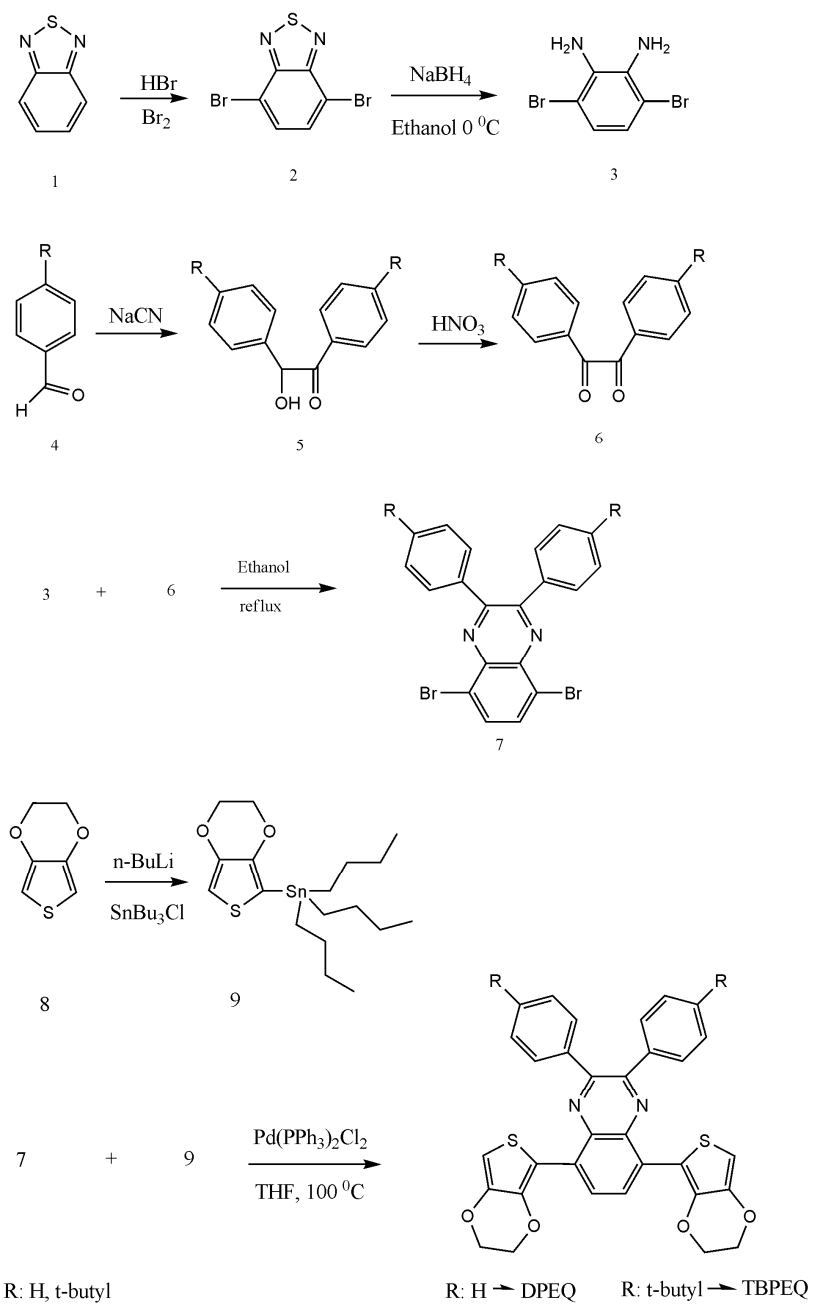


Figure 2.2 Synthetic route to monomers DPEQ and TBPEQ.

2.3.4 2,3-Bis(3,4-bis(decyloxy)phenyl)-5,8-bis(2,3-dihydrothieno[3,4-b][1,4]dioxin-5yl)quinoxaline (DOPEQ)

2.3.4.1 2,3-Bis(3,4-bis(decyloxy)phenyl)-5,8-dibromoquinoxaline

A solution of 3,6-dibromo-1,2-phenylenediamine (1.0 g, 3.8 mmol) and 1,2-bis(3,4-bis(decyloxy)phenyl)ethane-1,2-dione (3.173 g, 3.8 mmol) in ethanol (40 ml) was refluxed overnight by with a catalytic amount of PTSA. The mixture was cooled to 0 °C. The precipitate was isolated by filtration and washed with EtOH several times to afford the desired compound. (3.2 g, 79 %).

2.3.4.1 2,3-Bis(3,4-bis(decyloxy)phenyl)-5,8-bis(2,3-dihydrothieno[3,4b][1,4]dioxin-5yl)quinoxaline (DOPEQ)

2,3-Bis(3,4-bis(decyloxy)phenyl)-5,8-dibromoquinoxaline (200 mg, 0.188 mmol) and tributyl (2,3-dihydrothieno[3,4-b][1,4]dioxin-5-yl)stannane (405 mg , 0.939 mmol) were dissolved in dry THF (100 ml), the solution was purged with argon for 30 min. and PdCl₂(PPh₃)₂ (35 mg, 0.05 mmol) was added at room temperature under argon atmosphere. The mixture was stirred at 100 °C under argon atmosphere for 15 hours, cooled and concentrated on the rotary evaporator. The residue was subjected to column chromatography to afford an orange solid (145 mg, % 65).

2.4. Polymer Syntheses

2.4.1. Homopolymerization of GS

The corresponding polymer of GS (PGS) was potentiodynamically prepared via electrochemical polymerization on a Pt electrode. Compound 6 (10 mM) was polymerized in 0.1 M tetrabutylammonium hexafluorophosphate (TBAPF₆)/acetonitrile (ACN) with repeated scanning between -0.5 and 1.0 V. The free standing

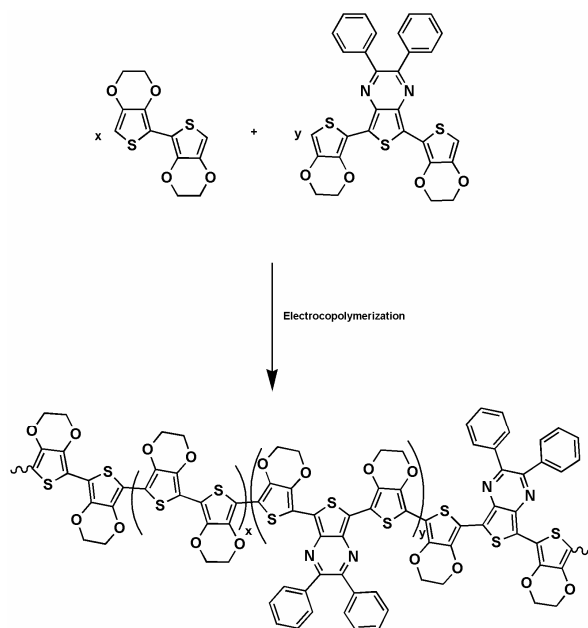


Figure 2.4. Schematic representation of copolymerization of BiEDOT and GS.

2.4.3. Polymerization of TBPEQ and DPEQ

Anodic electropolymerization of both monomers were performed in dichloromethane (DCM) with 0.1 M TBAPF₆ as the supporting electrolyte. The irreversible oxidation peak for TBPEQ emerges apparently on the first cycle at a potential of 0.9 V versus Ag wire reference electrode. DPEQ gets oxidized at a higher potential, 1.0 V. The free standing homopolymers were washed with ACN in order to remove excess TBAPF₆ and unreacted monomer after the electrolysis.

2.4.4. Polymerization of DOPEQ

A solution of DOPEQ (10^{-2} M) was prepared in a mixture of dichloromethane (DCM) and acetonitrile (ACN) (5/95, v/v) due to the high solubility of the polymer in DCM. Repeated scan electropolymerization of DOPEQ was achieved from 0.1 M TBAPF₆ solution of the mixture described above. The free standing homopolymers

were washed with the monomer-free mixture in order to remove excess TBAPF₆ and unreacted monomer after electropolymerization.

2.4.5. Chemical Polymerization of DOPEQ

Oxidative polymerization of DOPEQ was achieved with 4×10^{-2} M FeCl₃ in a 50 ml mixture of nitromethane and chloroform (90/10, v/v) containing 10^{-2} M monomer. The mixture was stirred for 6 hours at room temperature. The solution immediately turned to a dark yellow solution after the addition of FeCl₃. The polymer was precipitated with excess methanol and filtered. It was washed with methanol for several times, dissolved in a mixture of THF and 50 % aqueous solutions of hydrazine and stirred at room temperature for overnight to achieve the dedoping process. A deep green solution was obtained and the solvent was evaporated under reduced pressure. Chloroform was added to residue and the organic phase was extracted several times with water. Combined organic phases were evaporated and the residue was washed with acetone several times to remove the unreacted monomer. Polymer was then dried under vacuum to give the title compound in high yields (90-95 %).

2.5. Characterization of Polymer Films:

2.5.1. Cyclic Voltammetry

Cyclic voltammetry employs a saw-tooth waveform to vary potential linearly over time. Current is measured and a plot of current density as a function of potential is obtained. Conjugated polymers can be p- or n-type doped either by applying an oxidizing or reducing potential, respectively. When the polymer is in insulating state, no current is passed between the working and counter electrodes. Upon doping, substantial amount of current reveals a peak. Cyclic voltammetry is a key technique for the study of conjugated polymers due to its ability to measure peak current (ip), peak current density (jp), and peak potential (Ep). The characteristic peaks in the CV

are caused by the presence of the diffusion layer near the electrode surface. The peak current for a reversible couple is given by Randles & Sevcik equation:

$$i_p = (2.69 \times 10^5) n^{3/2} A D^{1/2} C v^{1/2}$$

where n is the number of electrons, A is the electrode area (in cm^2), C is the concentration (in mol cm^{-3}), D is the diffusion coefficient (in $\text{cm}^2 \text{s}^{-1}$), and v is the scan rate (in Vs^{-1}). Accordingly, the current is directly proportional to concentration and increases with the square root of the scan rate. For these processes, it was assumed that the reactants and products are soluble in solution and the surface processes (adsorption of reactants and products) can be neglected.

In case of the electroactive polymer electrochemistry, the process is somewhat different. Polymerization of electroactive monomer is an irreversible process, where the monomer is irreversibly oxidized and a film of electroactive polymer is formed. Thus, in this situation there are two electroactive species in the system, one of which being the monomer and the other is polymer deposited on the electrode. A typical CV investigation generally starts at low potentials where no redox reactions occur in anodic direction. Anodic current starts to increase in the vicinity of the potential where the electrode has reached sufficient potentials at which the monomer starts to get oxidized to radical cation. The anodic current increases rapidly until the concentration of the monomer at the electrode surface approaches zero, which is signified by the formation of a peak. The intensity of the current starts to decay since the solution in the vicinity of the electrode has almost zero monomer concentration. Monomer oxidation is immediately followed by chemical coupling which results in the formation of dimers and hence the oligomers. However, in some cases like pyrrole, the oxidation peak of monomer could not be observed due to immediate formation of dimers and oligomers all of which are highly electroactive. This results in an infinitely high concentration of electroactive species at the electrode surface which prevents the observation of the monomer peak. Indeed, only a dramatic increase in the cathodic current could be observed. Once these oligomers reach a certain length, they precipitate onto the electrode surface where the chains

can continue to grow in length. In the cathodic run the reduction of the deposited polymer is observed. Upon consecutive cycling, a new oxidation peak appears due to the polymer. It should be noted that as the number of cycles increases there is an increase in the intensity of the current. This is due to increase in the active area of the working electrode owing to coating of an electroactive polymer metal electrode (Figure 2.5)

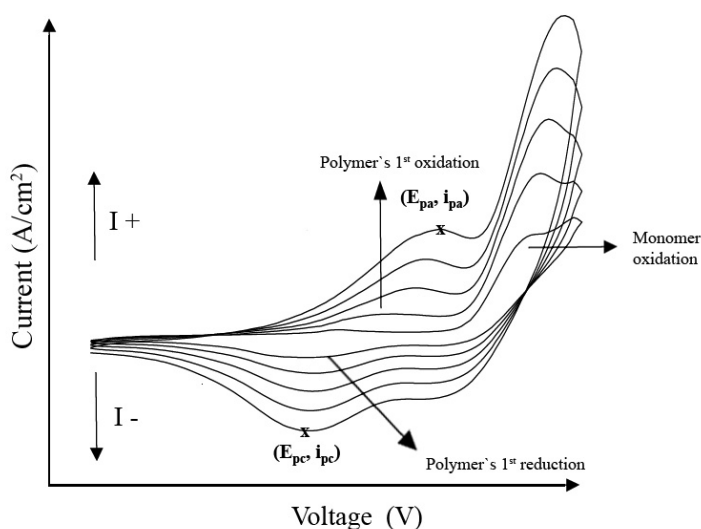


Figure 2.5 Cyclic Voltammogram of a representative type of electroactive monomer. [22].

To study electrochemistry of polymers, a monomer free system should be used. The polymer redox process is quasi-reversible and since the polymer is immobilized at the electrode surface, the redox process is not diffusion controlled. Thus, under these circumstances Randles & Sevcik equation is no longer valid. Instead, according to the theory of immobilized redox centers, the peak current is given by ;

$$i_p = n^2 F^2 \Gamma v / 4RT$$

where Γ is the total amount of reactant present at the electrode surface. According to this equation the current peak linearly depends on scan rate. Thus, investigation of peak current intensity with respect to scan rate will indicate the nature of

electrochemical process like diffusion controlled where the polymer is well adhered to the electrode surface.

2.5.2 Spectroelectrochemistry

In all studies a three electrode cell was employed either with an ITO or a Pt for working electrode. Polymer films were deposited potentiostatically with 25 mC/cm²(ca. 300 nm thickness). UV-Vis spectral data were collected while stepping the potential either with 50 or 100 mV increments.

The redox switching of conjugated polymers is accompanied by changes in electronic transitions. These absorption changes make conjugated polymers useful in electrochromic applications such as smart windows, mirrors, etc. The electronic transitions of conjugated polymers have been the subject of many articles. These electronic transitions can be probed with the use of UV-Vis spectroscopy. Spectra are recorded while the polymer is oxidized by increasing the potential stepwise. This experiment is commonly referred as spectroelectrochemistry, and can be easily accomplished by constructing a three electrode cell inside a UV cuvette for conducting polymers. Spectroelectrochemistry experiments reveal key properties of conjugated polymers such as band gap (E_g), λ_{max} , the intergap states that appear upon doping and the evolution of polaron and bipolaron bands.

2.5.3. Switching Properties

For electrochromic applications the ability of a polymer to switch rapidly and exhibit a striking color change is crucial. Electrochromic switching studies are known to be the easiest and most efficient way to observe these properties. A square wave potential step method coupled with optical spectroscopy was used to probe switching times and optical contrasts for these polymers. In this double potential step

experiment the potential was set at an initial value for a set period of time and was then stepped to a second potential for a set period of time before being switched back to the initial potential.

2.5.4 Colorimetry

Colorimetry provides a precise way to define color. Rather than measuring the absorption bands, colorimetry measures the human eye's sensitivity to light across the visible region and gives a mathematical function to describe the color. This technique measures three values in relation to color: the hue (dominant wavelength), which is the wavelength where maximum contrast occurs, saturation (purity), which is the color's intensity, and brightness (luminance).

A commonly used scale that numerically defines colors has been established in 1931 by The Commission Internationale de l'Eclairage (CIE system) with $L^*a^*b^*$, CIE color spaces (Figure 2.6). Color measurements were performed via Coloreye XTH Spectrophotometer.

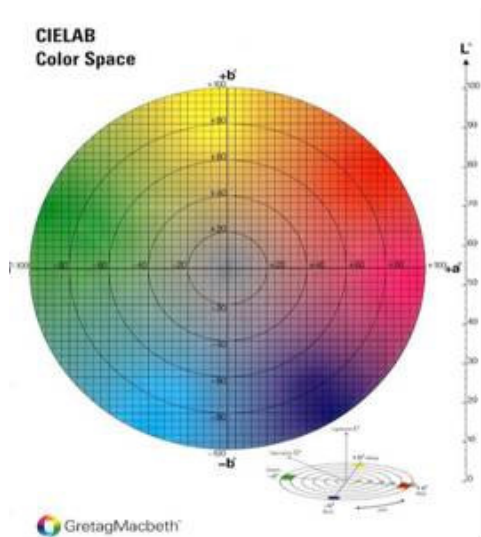


Figure 2.6 CIE LAB color space.

CHAPTER III

RESULTS AND DISCUSSION

3.1. Characterization of the D-A-D Molecules.

$^1\text{H-NMR}$, $^{13}\text{C-NMR}$ spectra of monomers were investigated in CDCl_3 and d_6 -DMSO and chemical shifts (δ) were given relative to tetramethylsilane as the internal standard. Mass analyses were also performed for the characterization of monomers.

3.1.1. 2,3-Diphenyl-5,7-bis(3,4-ethylenedioxy-2-thienyl)thieno[3,4-b]pyrazine

$^1\text{H-NMR}$ (400 MHz, CDCl_3): δ 4.24 (d, $J=2.35$ Hz, 4 H) , 4.41 (t, $J= 1.95$ Hz, 4H), 6.37 (s, 2 H) , 7.24-7.30 (m, 6 H) , 7.55 (d, $J = 7.56$ Hz , 4 H) ; $^{13}\text{C-NMR}$ (100 MHz, CDCl_3): δ 63.7, 64.5, 100.1, 110.6, 112.7, 114.9, 116.7, 121.7, 127.0, 127.8, 129.1, 135.7, 137.1, 138.3, 140.3, 150.6 : HRMS calcd. for $\text{C}_{30}\text{H}_{20}\text{N}_2\text{O}_4\text{S}_3$ (m/z) 568.0585, found 568.0576.

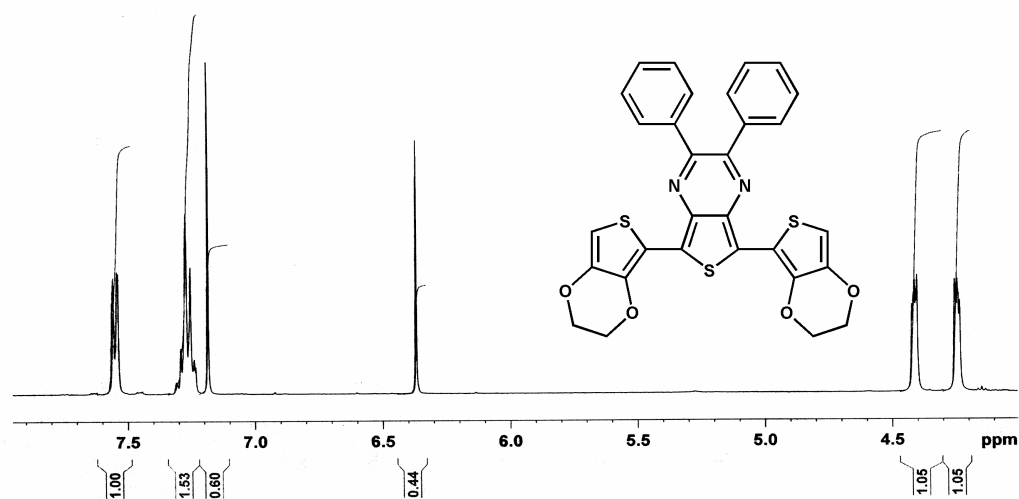


Figure 3.1 $^1\text{H-NMR}$ spectrum of GS.

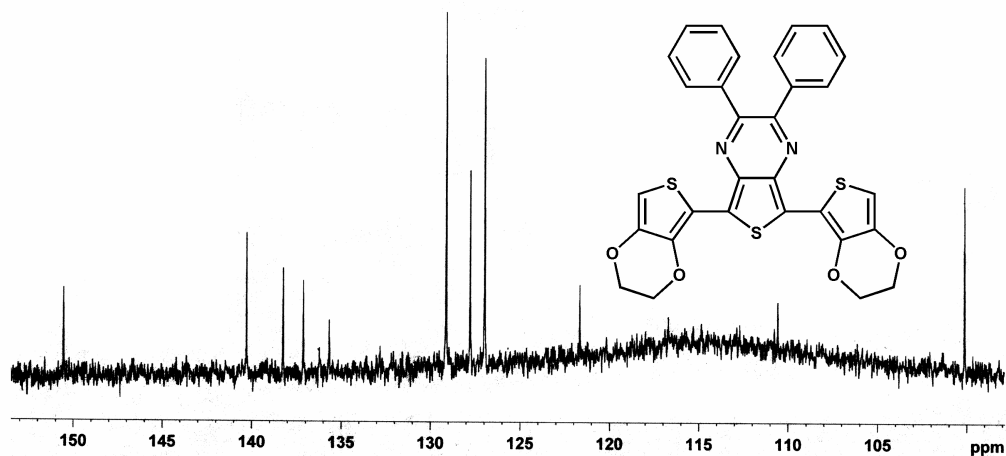


Figure 3.2 ^{13}C -NMR spectrum of GS.

3.1.2. 2,3-bis(4-tert-butylphenyl)-5,8-(2,3-dihydrothieno[3,4-b][1,4dioxin-7-yl)quinoxaline (TBPEQ)

3.1.2.1 2,3-bis(4-tert-butylphenyl)-5,8-dibromoquinoxaline (TBPB)

^1H -NMR (400 MHz, CDCl_3): δ 1.22 (s, 18 H), 7.27 (d, 4 H, $J = 8.26$ Hz), 7.54 (d, 4 H, $J = 8.30$ Hz), 7.72 (s, 2 H). ^{13}C -NMR (100 MHz, CDCl_3): δ 31.30, 34.81, 123.65, 125.31, 129.98, 130.13, 132.76, 135.25, 139.21, 152.90, 154.10, MS: m/e 552 (M^+)

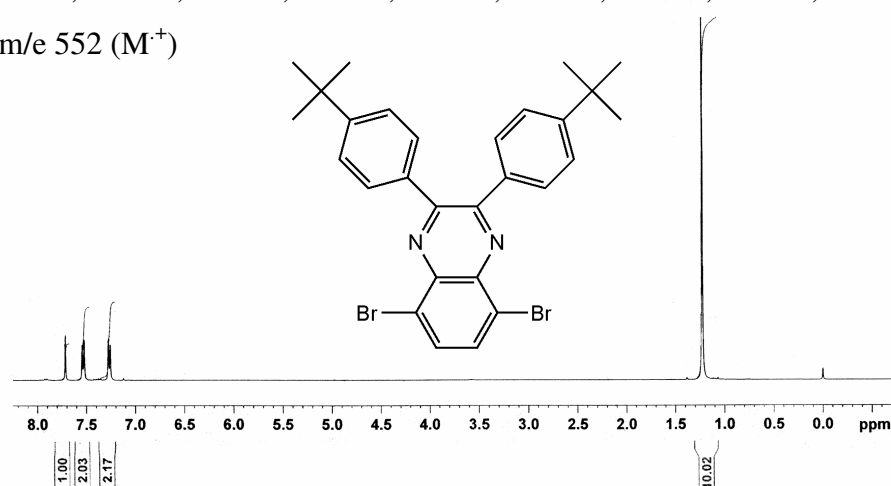


Figure 3.3 ^1H -NMR spectrum of TBPB.

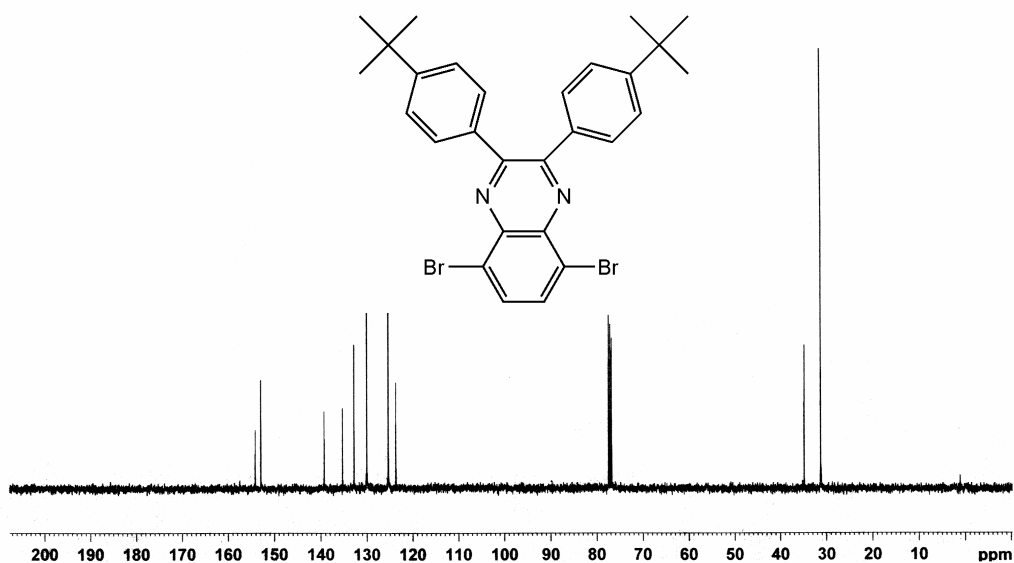


Figure 3.4 ^{13}C -NMR spectrum of TBPB.

3.1.2.2. 2,3-bis(4-tert-butylphenyl)-5,8-(2,3-dihydrothieno[3,4-b][1,4]dioxin-7-yl)quinoxaline (TBPEQ)

^1H -NMR (400 MHz, CDCl_3): δ 1.22 (s, 18 H), 4.30 (m, 4 H), 4.23 (m, 4 H), 6.49 (s, 2 H) 7.30 (d, 4 H, $J = 8.24$ Hz), 7.64 (d, 4 H, $J = 8.22$ Hz), 8.51 (s, 2 H). ^{13}C -NMR (100 MHz, CDCl_3): δ 30.29, 33.71, 63.36, 63.94, 101.97, 112.53, 124.01, 126.81, 127.64, 129.23, 134.86, 135.97, 139.19, 149.74, 150.93, MS: m/e 674 (M^+)

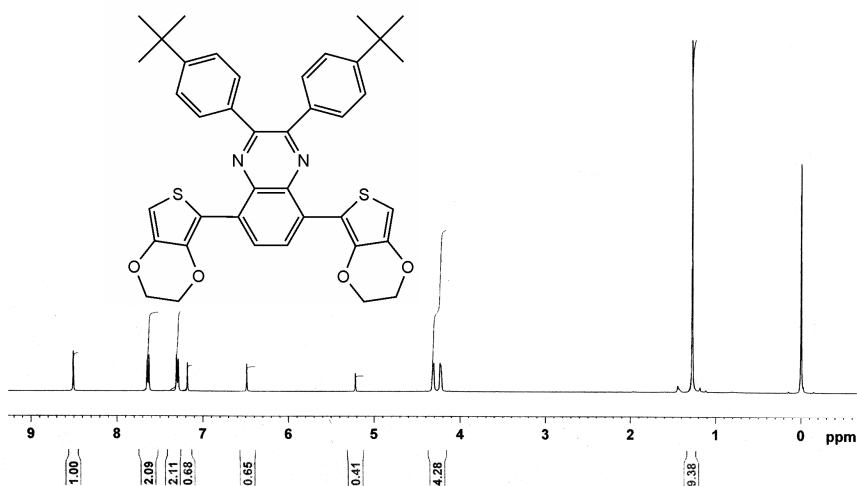


Figure 3.5 ^1H -NMR spectrum of TBPEQ.

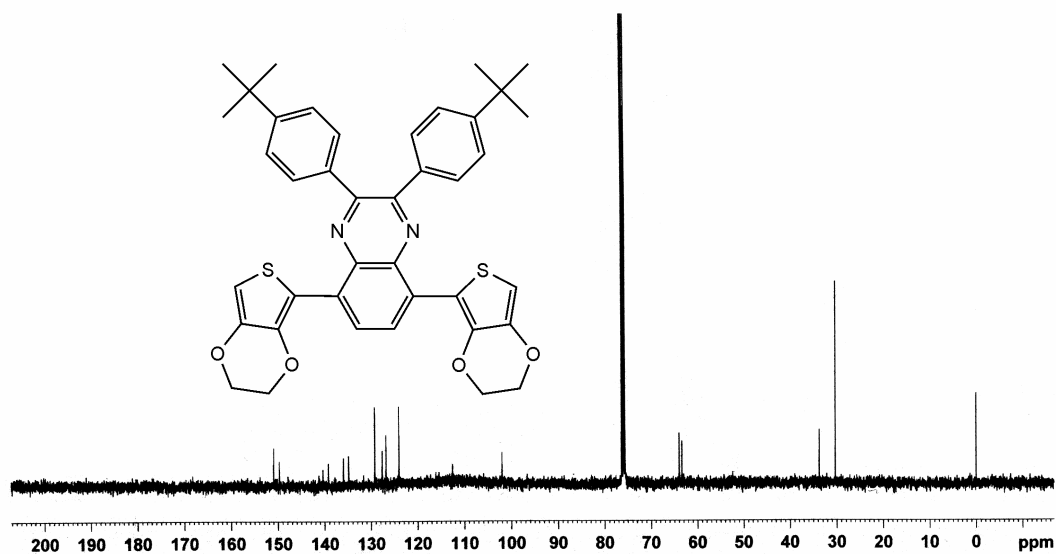


Figure 3.6 ^{13}C -NMR spectrum of TBPEQ.

3.1.3. 2,3-diphenyl-5,8-(2,3-dihydrothieno[3,4-b][1,4]dioxin-7-yl)quinoxaline (DPEQ)

^1H -NMR (400 MHz, d_6 -DMSO): δ 4.32 (m, 4 H), 4.44 (m, 4 H), 6.83 (s, 2 H) 7.44 (m, 4 H), 7.67 (m, 6 H), 8.66 (s, 2 H). MS: m/e 562 (M^+)

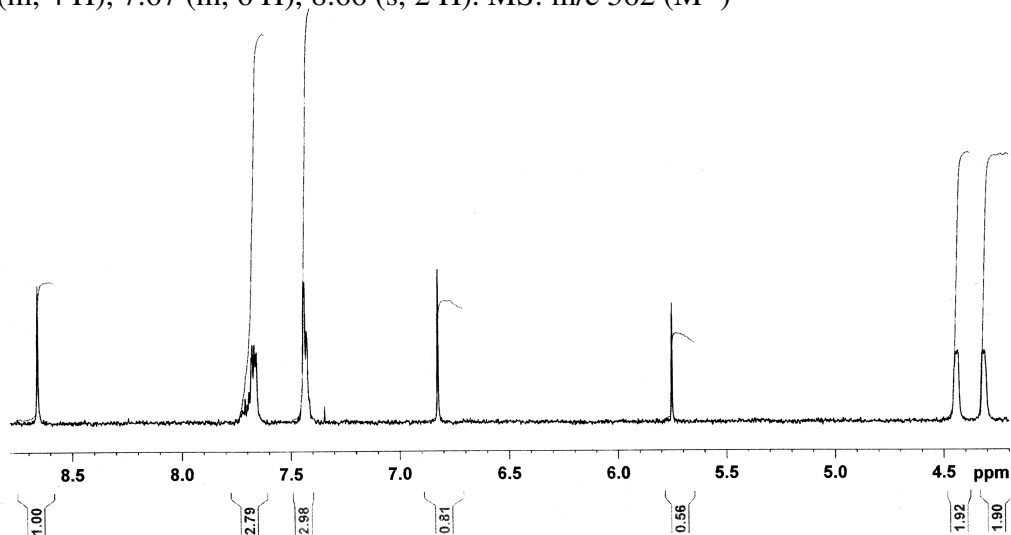


Figure 3.7 ^1H -NMR spectrum of DPEQ.

3.1.4. 2,3-bis(3,4-bis(decyloxy)phenyl)-5,8-bis(2,3-dihydrothieno[3,4-b][1,4]dioxin-5yl)quinoxaline(DOPEQ)

$^1\text{H-NMR}$ (400 MHz, CDCl_3): δ (ppm) 0.80 (t, $J = 3.3$ Hz, 12 H), 1.1-1.4 (m, 56 H), 1.6-1.8 (m, 8 H), 3.85 (t, $J = 6.5$ Hz, 4 H), 3.93 (t, $J = 6.5$ Hz, 4 H), 4.19 (m, 4 H), 4.28 (m, 4 H), 6.41 (s, 2 H), 6.74 (d, 2 H, $J = 8.4$ Hz), 7.19 (d, 2 H, $J = 8.4$ Hz), 7.39 (s, 2 H), 8.49 (s, 2 H). $^{13}\text{C-NMR}$ (100 MHz, CDCl_3): δ (ppm) 13.08, 21.67, 25.06, 25.09, 28.21, 28.23, 28.34, 28.38, 28.45, 28.58, 28.61, 28.63, 28.70, 30.91, 63.33, 63.93, 68.13, 68.22, 101.67, 111.83, 112.46, 115.08, 122.58, 126.60, 127.39, 130.40, 135.73, 139.24, 140.42, 147.66, 148.92, 149.24, MS: m/e 1088 (M^+ -H).

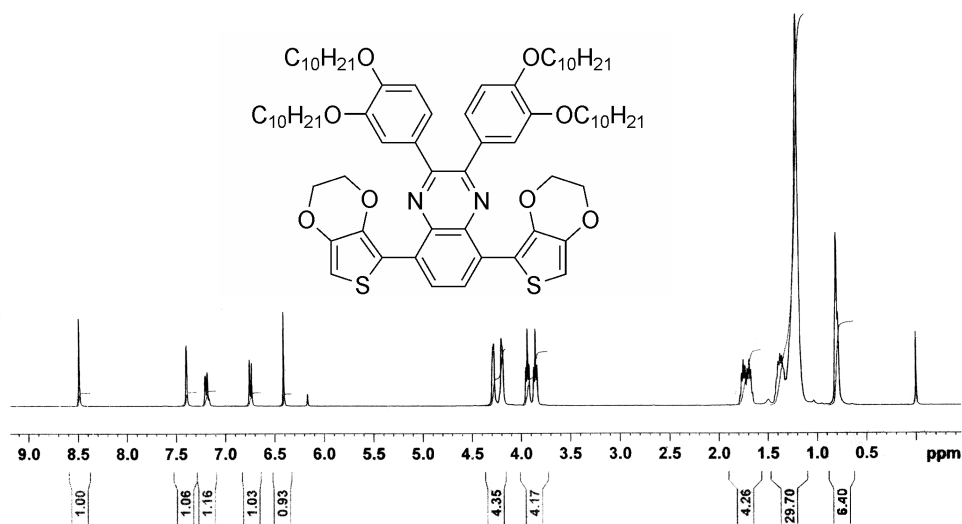


Figure 3.8 $^1\text{H-NMR}$ spectrum of DOPEQ.

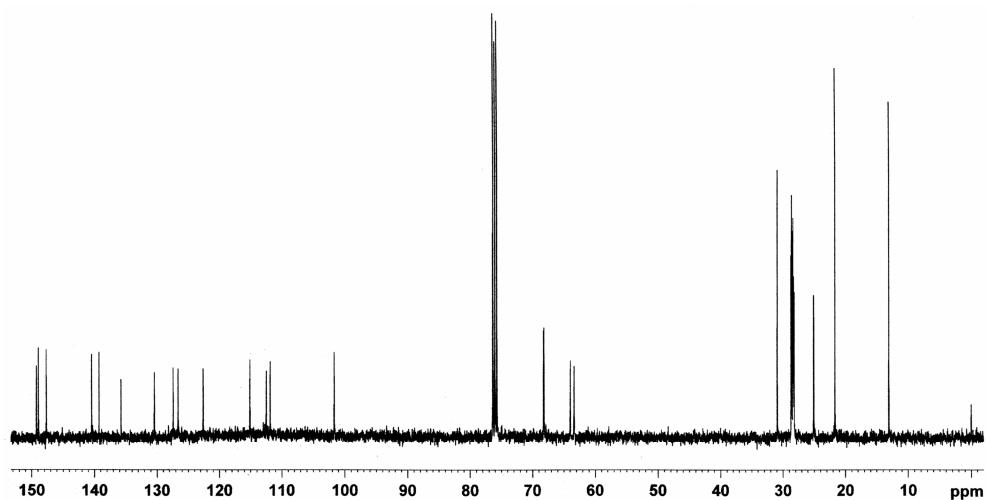


Figure 3.9 $^{13}\text{C-NMR}$ spectrum of DOPEQ.

3.2. Electrochemical and Electrochromic Properties of Donor-Acceptor-Donor Type Polymers

3.2.1 Electrochemical and Electrochromic Properties of Poly(2,3-Diphenyl-5,7-bis(3,4-ethylenedioxy-2-thienyl)thieno[3,4-b]pyrazine) (PGS)

3.2.1.1. Electrochemistry of 2,3-Diphenyl-5,7-bis(3,4-ethylenedioxy-2-thienyl)thieno[3,4-b]pyrazine (GS)

The corresponding polymer of GS (PGS) was prepared via electrochemical polymerization on Pt electrode potentiodynamically. Compound GS (10 mM) was polymerized in 0.1 M tetrabutylammonium hexafluorophosphate (TBAPF₆)/acetonitrile (ACN) with repeated scanning between -0.5 and 1.0 volts. The representative electrochemical growth revealing the electroactivity of the monomer and polymer was given in Figure 3.10.

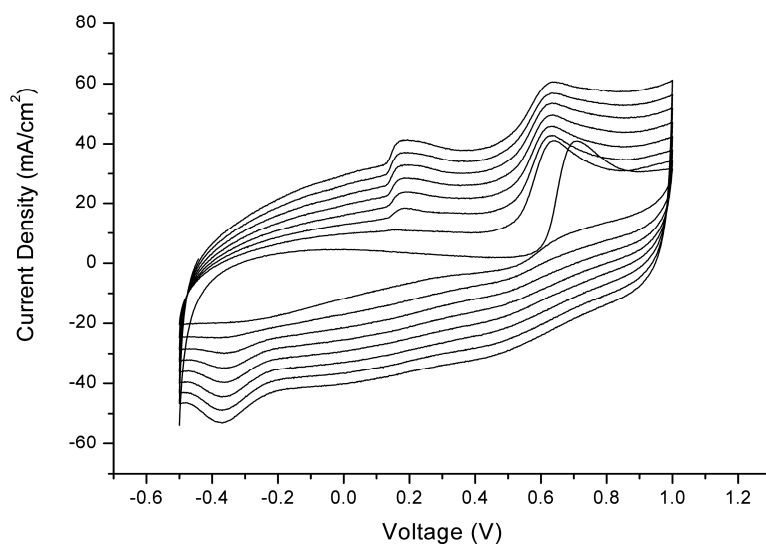


Figure 3.10. Repeated potential scan electropolymerization of GS at 100 mV/s in 0.1 M TBAPF₆/Dichloromethane (DCM).

Compound GS was irreversibly oxidized at 0.7 V vs Ag/Ag⁺ irreversibly resulting in the formation of EDOT radical cations whereafter rapid coupling reactives ($\tau < 10^{-5}$ s) lead to a polymeric structure [93, 94]. With repeated scanning a reversible redox process (+ 0.17 and – 0.37 V) develops signifying the formation of an electroactive polymer.

In compare to 5,7-bis(2-thienyl) thieno[3,4-b]pyrazine ($E_p=1.22$ vs Ag/Ag⁺ [95] analog, the oxidation potential of the monomer is remarkably cathodically shifted. This observation could be attributed to the superior donor capacity of EDOT substituent which leads to a more effective D-A match and an extended conjugation [96]. In addition, a small shift (0.1 V) in the oxidation potential of GS with respect to EDOT – disubstituted thieno[3,4-b]pyrazine was observed, which could be related to the partial overlap of the pyrazine ring π -system with the phenyl substituents [97]. At cathodic potentials PGS was reduced reversibly with a reduction potential of -0.77 V. According to the previously reported electrochemical study of the 2,3-dimethylthieno[3,4-b]pyrazine, this redox couple corresponds to one-electron reduction of the pyrazine ring [98].

In order to investigate the n-doping properties of the polymer, cathodic potentials were applied in TBAPF₆/ACN. A redox couple with an oxidation potential of –1.0 V and a reduction potential of -1.36 V were observed which are important indications for the n-dopable character of the film[99]. Further supporting data on n-doping properties of the polymer is provided in the spectroelectrochemistry section. The scan rate dependence of the polymer films were also investigated as seen from Figure 3.11.

A linear relationship was found between the peak current and the scan rate both for p and n-doping, indicating that the electroactive polymer films were well adhered and the redox processes were non-diffusion limited [100].

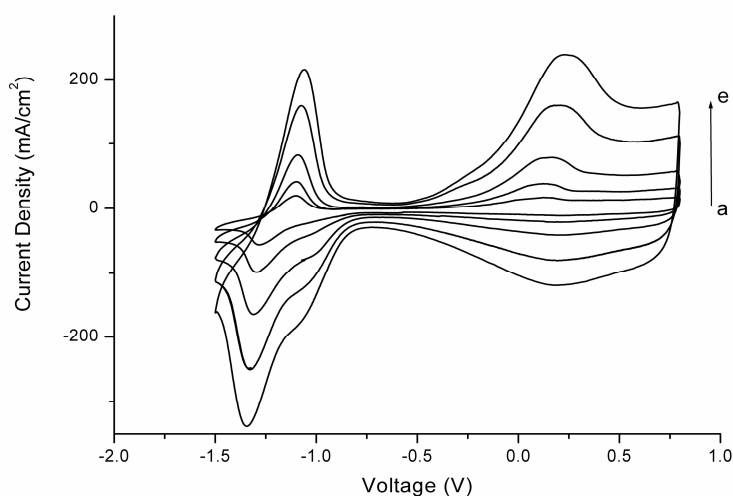


Figure 3.11. Scan rate dependence of PGS in TBAPF₆/ACN (a) 25, (b) 50, (c) 100, (d) 200, (e) 300 mV/s.

3.2.1.2 Optoelectrochemistry and electrochromic switching of 2,3-Diphenyl-5,7-bis(3,4-ethylenedioxy-2-thienyl)thieno[3,4-b]pyrazine (GS)

Spectroelectrochemistry experiments are performed to investigate the optical changes upon doping process.

The spectral behavior of the PGS was investigated by UV-Vis-NIR spectrophotometer in a monomer free electrolyte system while incrementally increasing the applied potential from -1.0V to +0.8V. In neutral form the polymer shows two distinct absorptions centered at 522 nm and 1062 nm which is not common for an optical spectra of a homopolymer (Figure 3.12. A).

Stepwise oxidation of the polymer results in a gradual decline in the intensity of the absorbance located in the visible region. Simultaneously, the intensity of the second transition at 1062 nm decreases up to an applied potential of 0.3 V and later on it is overwhelmed by the broad absorption due to charge carrier band formation upon oxidation.

A great deal of discussion has been made over whether this transition corresponds to a polaron charge carrier (trapped charges with in the film due to lack of electrochemical reduction) or if it corresponds to a second π - π^* transition. In

literature, there have been few examples of such materials [101] which are considered as the polymers having two distinctive π - π^* transitions. However, these claims are not supported by the ancillary techniques like ESR. This technique has been widely used in conducting polymers to study the nature of the charged defects formed upon doping. It is known that polymers like polythiophene and its derivatives give rise to spin-1/2 polarons upon light doping and develop into spinless bipolarons upon heavy doping [102].

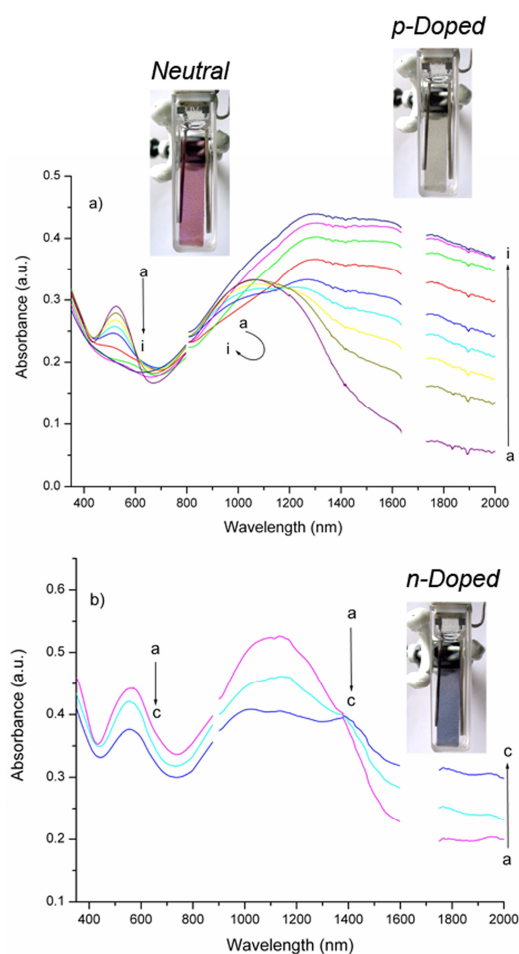


Figure 3.12 Spectroelectrochemistry of PGS film on an ITO coated glass slide in monomer-free 0.1 M TBAPF₆/ACN electrolyte solution. A) p-type doping at applied potentials; (a) -0.8, (b) -0.6, (c) -0.5, (d) -0.4, (e) -0.3, (f) -0.1 (g) +0.2, (h) +0.5, (i) +0.8. vs Ag/Ag⁺. B) n-type doping at applied potentials (a) -1.7, (b) -2.0, (c) -2.2 V vs Ag/Ag⁺.

Figure 3.13 shows ESR and UV-VIS-NIR spectra of PGS at selected oxidation states. As is evident from the figure, the relative intensities of ESR signals and UV-VIS spectral behavior of the polymer change remarkably upon varying the degree of oxidation. In order to monitor the various oxidation states PGS film, the polymer film was first oxidized at 1.2 V vs Ag wire in a monomer free electrolytic solution and then its ESR spectrum was recorded in DCM (Figure 3.13 a).

As seen from Figure 3.13 a, the reduced ESR signal (singlet with $g = 2.00175$) identifies a lower concentration of polarons compared to figure 3.13 c. This is also supported by UV-VIS spectrum of PGS on ITO recorded at 1.2 V; the spectrum consists of a broad band in the region 1000-2000 nm (Figure 5 b). Upon successive addition of hydrazine as the chemical reducing agent, the signal intensity gradually enhanced indicating the formation of polarons due to the reduction of bipolarons (see Figure 3.13 c).

Figure 3.13 c reveals a sharp singlet with $g = 2.00205$ and Figure 3.13 d consist of two bands at 522 nm and 1062 nm due to π - π^* transition. The increase in signal intensity continued up to a certain limit with hydrazine addition, which is then followed by a gradual decrease in the signal intensity. Figure 3.13 e depicts the ESR spectrum of PGS in pure hydrazine within which polymer film is in its completely neutral state. At this state the ESR signal is rather small. To eliminate the possible effect of trapped charges, the film was also electrochemically neutralized via application of -1.0V to achieve a fully de-doped state and its ESR spectrum was recorded. However, there was no considerable change in the rather small signal intensity. Thus, the small signal in the ESR spectra of reduced film could be due to structural defects [103]. Although, ESR spectrum of PGS recorded in pure hydrazine and also after the application of -1.0 V exhibit a weak singlet due to structural defects, UV-VIS spectrum of PGS recorded under these conditions exhibits two strong bands at 522 nm and 1062 nm (Figure 3.13 f). Hence, this behavior is regarded as the significant indication of a conjugated system having two distinctive π - π^* transitions with electronic band gaps of 1.7eV and 0.77 eV for the transitions at 522 and 1062 nm respectively.

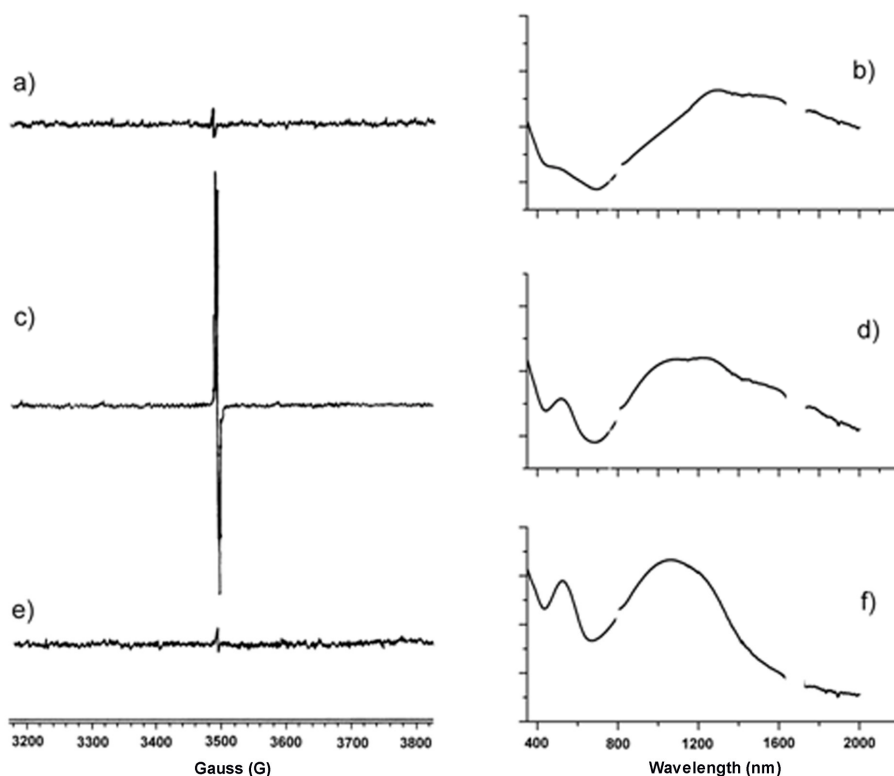


Figure 3.13 ESR and UV-Vis Spectra of PGS film at various oxidation states on Pt and ITO electrodes respectively. a-b) after oxidation at +1.2 V (fully oxidized state), c-d) after addition of certain amount of hydrazine (polaronic state), e-f) in pure hydrazine (neutral state).

These results revealed that we achieved an effective match of alternating donor and acceptor units in the backbone of the conjugated system leading to one of the lowest band-gaps reported to date [96]. Upon increase of applied potential, the color of the polymer changes from a red-purple absorbing state (Y:28, x:0.337, y:0.318) to a highly transmissive oxidized state (Y:55, x:0.308, y:0.334).

The reduction of a polymer is not necessarily an n-doping process. To state that the process is n-type doping, there should be considerable structural,

conductivity and optical differences after the introduction of charge carriers to conjugated system. Thus, to be able to demonstrate the presence of n-type doping, both the electrochemistry of the reduced state and the spectral changes that occurs upon reduction should be examined. Similar to p-doping studies, spectroelectrochemistry was performed in order to probe the optical changes that occur during the n-doping of the polymer. This property was hardly investigated in literature with an exception of few studies [104]. The optoelectrochemical spectral series was monitored while the polymer was sequentially stepped between its neutral and fully reduced forms (n-doped state). Neutral polymer exhibits two π - π^* transitions with absorption maxima of 522 nm and 1062 nm where the polymer film is in red-absorbing state. As the potential was sequentially decreased the intensity of the peaks were reduced with the concomitant growth of broad low energy absorption beyond 1500 nm. The overall absorbance was slightly lower in intensity and red shifted relative to the neutral state for both transitions leading to a blue color (Y:32, x:0.286, y:0.310). Further applied negative potentials led to a decrease in the absorption since the film degrades as a result of over-reduction. Significantly, the increase in absorbance at long wavelength region (Figure 3.12 B) during reduction designates the formation of charge carriers and true n-type doping process [104].

The % transmittance (%T) values at different wavelengths including the λ_{\max} of the polymer were measured by UV-Vis-NIR spectrophotometry while the polymer was switched between -1.0 V and $+1.0$ V with a residence time of 5 s. The optical contrast of the homopolymer, which was measured as the difference between %T in the neutral and oxidized states, was calculated as 17 % and 44 % at the 522 and 1750 nm respectively (Figure 3.14).

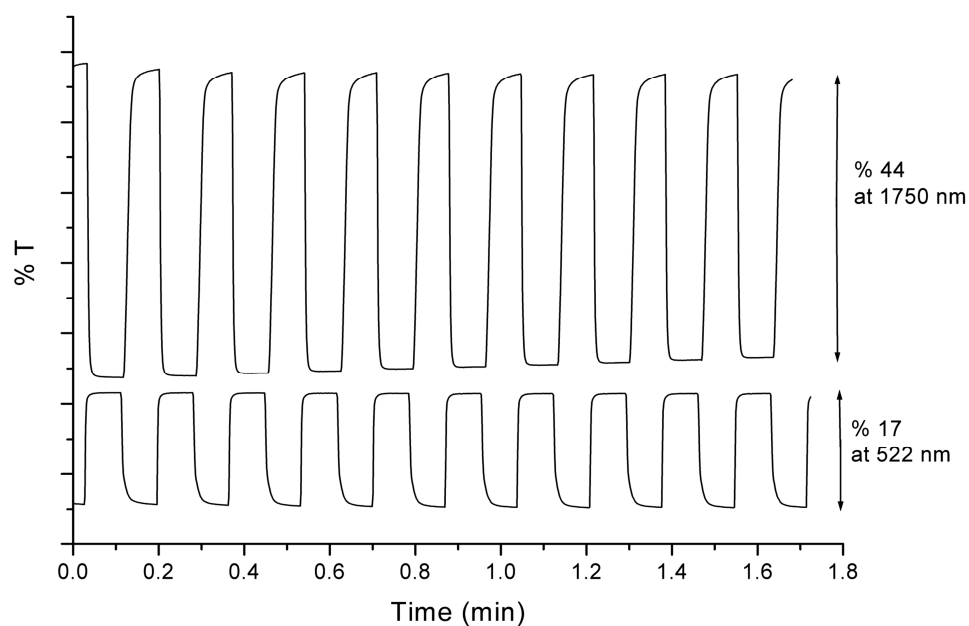


Figure 3.14 Electrochromic switching, optical absorbance change of PGS deposited on ITO electrode monitored at 522 and 1750 nm in 0.1 M TBAPF₆/ACN

Especially, the high optical contrast (44%) within the NIR region makes this material a good candidate for NIR device applications. In addition, kinetic studies have also confirmed the exclusive switching ability of the homopolymer which displays a switching time less than 0.5 s. To the best of our knowledge this value is one of the fastest switching times reported to date [96, 105].

3.2.2. Electrochemical and Electrochromic Properties of Poly(2,3-Diphenyl-5,7-bis(3,4-ethylenedioxy-2-thienyl)thieno[3,4-b]pyrazine-co-bi-etylenedioxy thiophene) P(GS-co-Biedot)

3.2.2.1. Electrochemistry of Poly(2,3-Diphenyl-5,7-bis(3,4-ethylenedioxy-2-thienyl)thieno[3,4-b]pyrazine-co-bi-etylenedioxythiophene) P(GS-co-BiEDOT)

Copolymerization is a facile method to observe interesting combinations of the properties observed in the corresponding homopolymers [106]. In order to achieve an effective copolymerization reaction electrochemically, oxidation potentials of the two monomers should be close to each other. BiEDOT was chosen due to its oxidation potential ($E_{a, \text{BiEDOT}} = \sim +0.6 \text{ V}$, $E_{a, \text{GS}} = +0.71 \text{ V}$ vs Ag wire) and superior optical and mechanical properties [107]. BiEDOT was synthesized according to previously reported method and the oxidative electrochemical copolymerization was achieved by repeated potential cycling of a solution containing BiEDOT and GS (w/w, 50:50) with 0.1 M TBAPF₆ in acetonitrile.

A structural representation of the reaction taking place during electrochemical copolymerization was shown in Figure 2.4.

Since BiEDOT and GS are oxidized at the same potential range, radical cations of both monomers are formed concurrently at the working electrode where they can react with each other. Formation of a random copolymer is anticipated since both monomers have EDOT radical cations. Hence, no preference is expected between the active species [108]. Similar to homopolymer, the copolymer represented both n- and p-type doping behavior.

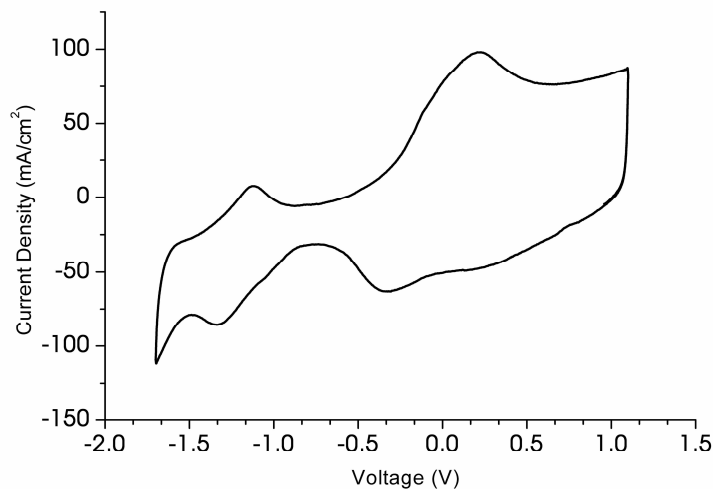


Figure 3.15. Cyclic voltammetry of the copolymer in 0.1M TBAPF₆/ACN at scan rate of 100 mV/s.

During copolymerization, as the BiEDOT units join the polymer backbone, the relative percentage of 2,3-diphenylthieno[3,4-b]pyrazine units decreases per chain. Hence, the negative charge carrier capacity of the resultant polymer decreased which was indicated by relative difference in charge density between the p-doped and the n-doped states as shown in Figure 3.15.

3.2.2.2. Optoelectrochemistry and electrochromic switching of Poly(2,3-Diphenyl-5,7-bis(3,4-ethylenedioxy-2-thienyl)thieno[3,4-b]pyrazine-co-bi-ethylene dioxythiophene) P(GS-co-BiEDOT)

Copolymerization of distinct monomers can lead to an interesting combination of the properties observed in the corresponding homopolymers and it is a logical approach for the fine-tuning of the color for electrochromic applications. One of the most persuasive proofs for electrochemical copolymerization is the spectroelectrochemical studies which provide information on the electronic structure of the resultant material [109]. During optoelectrochemistry study of the copolymer

similar procedure was applied. In neutral state the copolymer displays two distinctive π - π^* transitions at 538 nm and 999 nm (Figure 3.16).

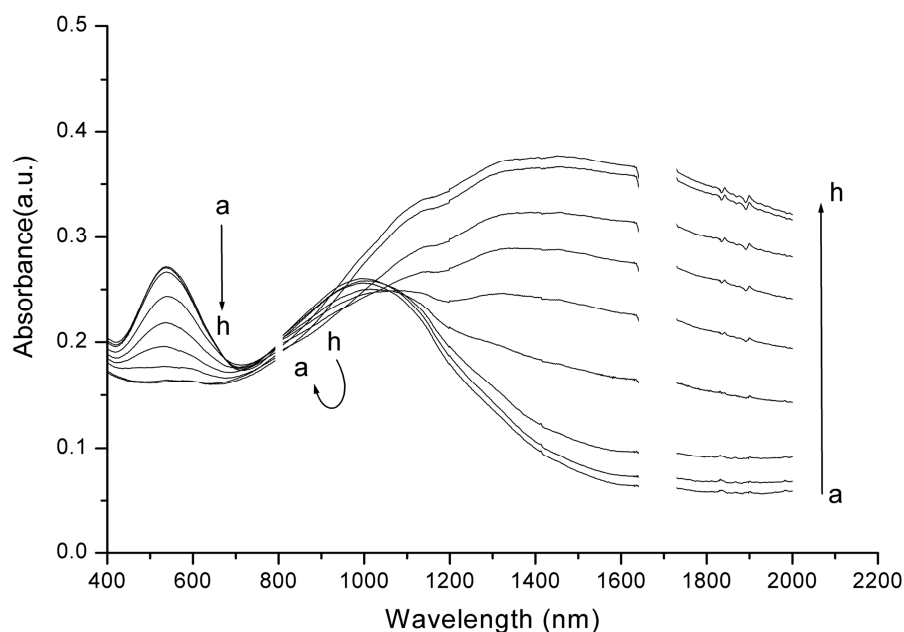


Figure 3.16 Spectroelectrochemistry of copolymer as a function of applied potential between -1 and 0.6 V in 0.1 M TBAPF₆/ACN: (a) -1.0, (b) -0.8, (c) -0.6, (d) -0.4, (e) -0.2, (f) 0.0, (g) +0.4, (h) 0.6 V vs Ag wire.

The electronic band gap defined as the onset energy for the π - π^* transition is calculated as 0.88 eV. The red shift in the high energy transition is attributed to the increase in BiEDOT content (absorption maximum of PBiEDOT is 587 nm which is located between the absorption bands of the homopolymer). This leads to a change in color of the polymer to purple. The relative intensity of the lower energy transition with respect to the higher energy transition is remarkably declined in compare to that of homopolymer in the neutral state. This could originate from the lessening of the relative presence of the TP units and consequently the donor-acceptor match in the material. Upon stepwise oxidation evolution of a new absorption band beyond 1200 nm was observed due to charge carriers which was accompanied by a gradual

decrease in the intensity of the bands related to π - π^* transitions. At 0.6 V the fully oxidized state was achieved where the color of the copolymer was light blue with an intensified absorption at around 1450 nm (Figure. 3.16).

Effect of copolymerization on optical contrast and switching time was also investigated with kinetic studies where the results are illustrated in Figure 3.17.

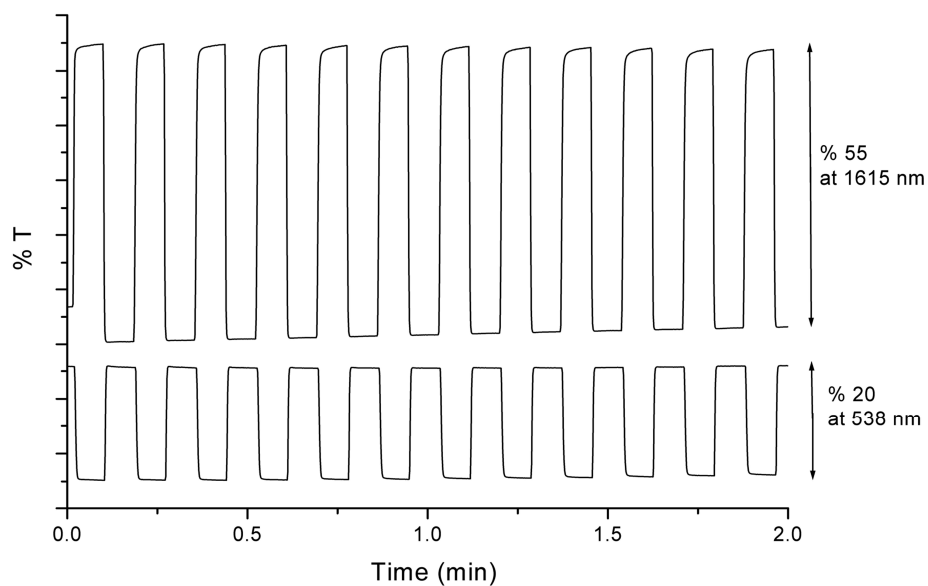


Figure 3.17. Electrochromic switching, optical absorbance change monitored at 538 nm and 1750 nm for copolymer in 0.1 M TBAPF₆/ACN.

Poly(GS-co-BiEDOT) has optical contrasts of 20 % and 55 % at 538 nm and 1615 nm respectively. The switching times are calculated as less than 0.4 s at 538 nm and 0.5 s at 1615 nm which are again much faster than the typical switching times 1-2 s for an electrochromic polymer [110-114].

3.2.3. Electrochemical and Electrochromic Properties of 2,3-bis(4-tert-butylphenyl)-5,8-(2,3-dihydrothieno[3,4-b][1,4]dioxin-7-yl)quinoxaline (TBPEQ) and 2,3-diphenyl-5,8-(2,3-dihydrothieno[3,4-b][1,4]dioxin-7-yl)quinoxaline (DPEQ).

3.2.3.1. Electrochemistry of 2,3-bis(4-tert-butylphenyl)-5,8-(2,3-dihydrothieno[3,4-b][1,4]dioxin-7-yl)quinoxaline (TBPEQ) and 2,3-diphenyl-5,8-(2,3-dihydrothieno[3,4-b][1,4]dioxin-7-yl)quinoxaline (DPEQ).

Anodic electropolymerizations of both monomers were performed in dichloromethane (DCM) with 0.1 M TBAPF₆ as the supporting electrolyte. The irreversible oxidation of TBPEQ emerges on the first cycle at a potential of 0.9 V versus Ag wire reference electrode. Figure 3.18 reveals the cyclic voltammogram of the anodic electropolymerization of TBPEQ at 100 mV/s on Indium tin oxide (ITO) coated glass slides. A well-defined redox couple quickly grows to form an electroactive polymer film (TBPEQ) with an E_{pa} of -0.01 V and E_{pc} of -0.24 V versus same reference electrode. DPEQ oxidizes at a higher potential, 1.0 V.

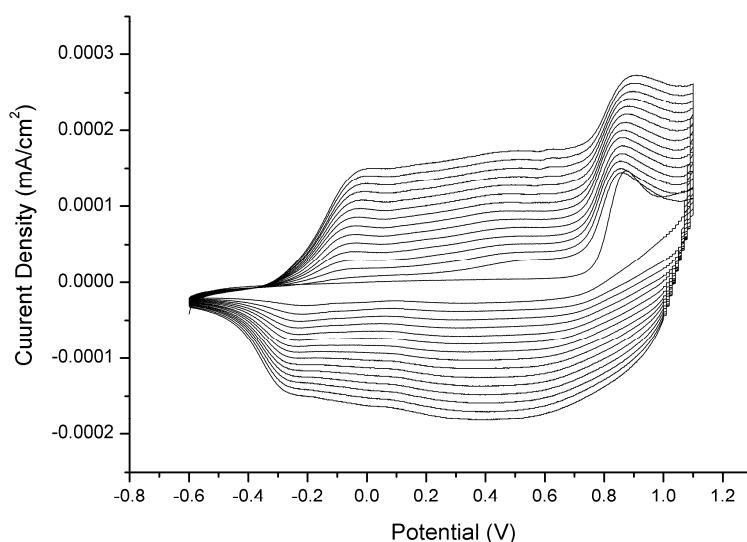


Figure 3.18 Repeated potential scan electropolymerization of TBPEQ at 100 mV/s in 0.1 M TBAPF₆/DCM on ITO electrode.

Polymers' redox couple also develops at higher potentials with an E_{pa} of 0.27 V and E_{pc} of 0.08 V (Figure 3.19). It is surprising to note that, the lower donor capacity t-butyl groups on pendant phenyl rings greatly affect both the monomer oxidation and the polymer redox couple potentials.

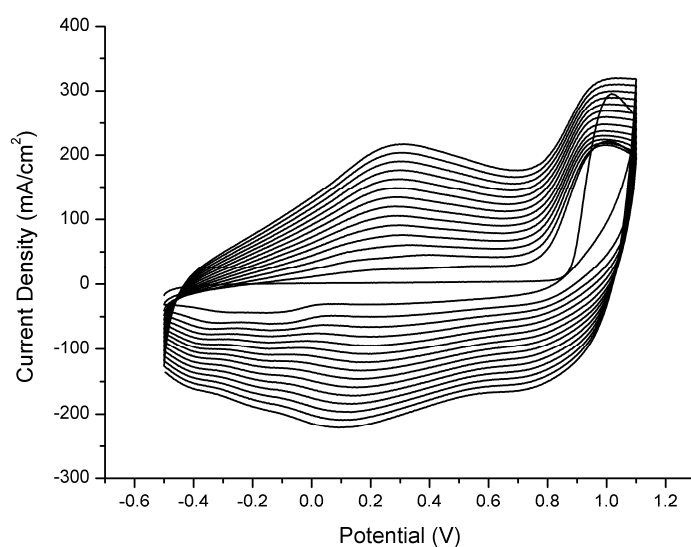


Figure 3.19 Repeated potential scan electropolymerization of PDPEQ at 100 mV/s in 0.1 M TBAPF₆/DCM on ITO electrode.

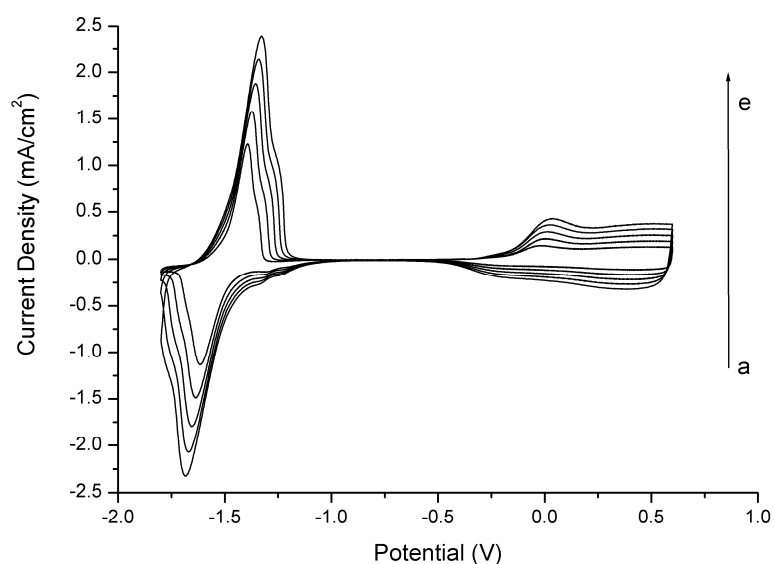


Figure 3.20 Scan rate dependence of PTBPEQ film in TBAPF₆/ACN (a) 100, (b) 150, (c) 200, (d) 250, (e) 300 mV/s.

A direct relation between current response and scan rate was observed for both polymers which proves that the films were well-adhered and electroactive (Figure 3.20 and Figure 3.21).

The DPEQ and TBPEQ films were coated on Pt wire potentiodynamically over 30 cycles from a 0.01 M monomer and 0.1M TBAPF₆ DCM solution. Anodic and cathodic peak currents revealed a linear relationship as a function of scan rate for both polymers, indicating that electrochemical processes are not diffusion limited and quasi-reversible even at high scan rates [115].

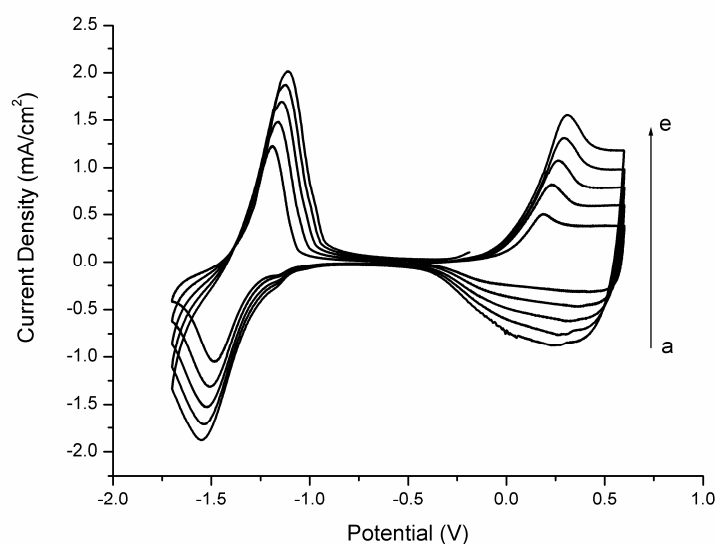


Figure 3.21 Repeated potential scan electropolymerization of PDPEQ at 100 mV/s in 0.1 M TBAPF₆/DCM on ITO electrode.

The long-term switching stability is a severe requirement for electrochromic polymers due to their potential use in numerous commercial applications, especially smart windows [116]. Both monomers were deposited on Pt wire via cyclic voltammetry (CV) from a monomer solution of 0.01 M in 0.1 M TBAPF₆/DCM electrolyte. Polymer films were cycled between their fully neutral (-0.6 V) and oxidized states (0.8 V) in lithium perchlorate / propylene carbonate (PC) electrolyte/solvent couple. Once electrochemical equilibrations were reached (1000

cycles) DPEQ and TBPEQ revealed outstanding redox stabilities upon cycling, where less than 8 % decrease in total charge was observed even after 5000 cycles. PTBPEQ showed a difference of less than 5 % for the anodic peak current and a decrease of less than 4 % for the cathodic one which designate the robustness of the polymers upon switching between the neutral and oxidized states.

3.2.3.2. Optoelectrochemistry and electrochromic switching of 2,3-bis(4-tert-butylphenyl)-5,8-(2,3-dihydrothieno[3,4-b][1,4]dioxin-7-yl)quinoxaline(TBPEQ) and 2,3-diphenyl-5,8-(2,3-dihydrothieno[3,4-b][1,4]dioxin-7-yl)quinoxaline (DPEQ).

Spectroelectrochemistry experiments were performed to probe the optical changes upon doping. Polymer films were deposited on ITO glass slides as described previously and spectral changes were investigated by UV-Vis-NIR spectrophotometer in a monomer free 0.1 M TBAPF₆, ACN solution while increasing the applied potential from – 1.0 V to 0.8 V.

Both polymers have two distinct absorption bands which are essential for having neutral state green conducting polymers. Although two absorption bands is a necessity, the maximum absorption wavelengths are the decisive values to possess neutral state green polymers. The absorption maxima of PTBPEQ were centered at 452 nm and 711 nm whereas PDPEQ has these at 448 nm and 732 nm. The t-butyl groups affect not only the monomer oxidation and the polymer redox couple potentials but also the maximum absorption wavelengths of the corresponding transitions. This behavior is attributed to the different electronic structures of the polymers, and to the different acceptor capacities of the quinoxaline derivatives which lead to unique donor-acceptor matches with EDOT moieties. A minimum absorption was observed at around 530 nm for PTBPEQ and the differences in transmittance of the peaks at 452 nm and 711 nm were calculated with respect to this point (Figure 3.22). The values were found to be 47 % and 58 %, which are the highest values reported up to date for a neutral state green polymer [72,117]. These values are excellent to produce a highly saturated green color. PTPEQ also have a

minimum absorption at around 530 nm and corresponding differences in transmittance were calculated as 41 % and 46 % with respect to this point. The electronic band-gap of the polymers were calculated as 1.18 eV for PTBPEQ and 1.01 eV for PDPEQ, keeping in mind that polymers with donor-acceptor units exhibit band-gaps between 0.9 eV to 1.3 eV in general [72,96]. Upon oxidation of PTBPEQ, the intensities of both absorption bands decreased gradually leaving tiny absorptions in the visible region.

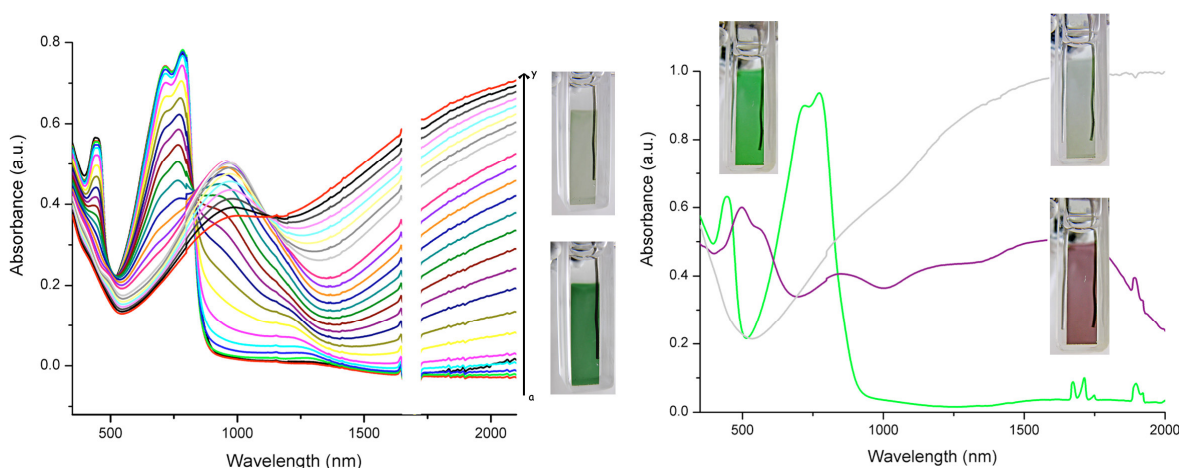


Figure 3.22. a. p-doping. Spectroelectrochemistry of PTBPEQ film on an ITO coated glass slide in monomer-free, 0.1 M TBAPF₆/ACN electrolyte-solvent couple at applied potentials(V); (a) -1.0, (b) -0.8, (c) -0.6, (d) -0.4, (e) -0.3, (f) -0.2 (g) -0.1, (h) -0.05, (i) 0, (j) 0.05, (k) 0.1, (l) 0.15, (m) 0.2, (n) 0.25, (o) 0.3, (p) 0.35, (q) 0.4, (r) 0.45, (s) 0.5, (t) 0.55, (u) 0.6, (v) 0.65, (w) 0.7, (x) 0.75, (y) 0.8 b. n-doping Spectroelectrochemistry of PTBPEQ at 0.8, -1.0 and -1.7 V.

This resulted in an extremely transmissive colorless oxidized state which is essential for the realization of polymer electrochromic based display devices. The polymer is unique in literature with its highly saturated green color in the neutral and exceptional transparency (most transparent reported up to date) in the oxidized state. The intensities of the absorption bands also vanished upon successive oxidation of

PDPEQ films (Figure 3.23.) It reveals a highly transparent light green color in the oxidized state. Electron-dominated transport (n-type doping) appears to be limited in literature due to extreme reactivity of carbanions to water and oxygen [104].

Conducting polymers with stable negatively doped states are of high interest, since more complicated device structures can be attained with these materials. As previously stated by Reynolds et. al., a simple electrochemical reduction cannot be a direct evidence for n-type doping process. In addition an evidence for charge carrier formation upon reduction should be studied via spectroelectrochemistry or in-situ conductivity measurements. The strong increase in the near-infrared absorption region upon reduction is a clear evidence of true n-type doping process [118].

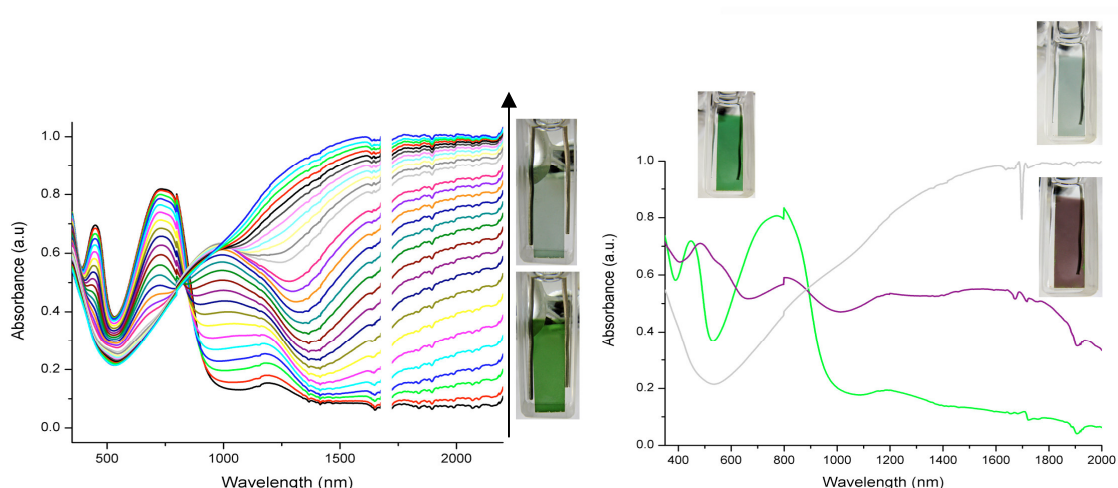


Figure 3.23 a. p-doping. Spectroelectrochemistry of PDPEQ film on an ITO coated glass slide in monomer-free, 0.1 M TBAPF₆/ACN electrolyte-solvent couple at applied potentials between -1.0 to 1.0 V **b.** n-doping Spectroelectrochemistry of PDPEQ at 0.8, -1.0 and -1.7 V.

The PDPEQ and PTBPEQ films were coated on a Pt wire potentiodynamically over 20 cycles from a 0.01 M monomer and 0.1M TBAPF₆ acetonitrile solution since n-type doping process was achieved with thinner films. At an applied negative potential of -1.8 V drastic changes in the visible and serious

increases in the NIR regions were observed in the absorption spectra of both polymers. Hence, having strong absorption changes in NIR region and the CV waves at negative potentials, it is clear that both PDPEQ and PTBPEQ are revealing true n-type doping processes.

The stabilities, optical contrasts and response times upon electrochromic switching of the polymer films between their neutral and oxidized states were monitored both in the visible and NIR regions. Figure 3.24 reveals the electrochromic switching properties of PTBPEQ.

The corresponding data for PDPEQ was shown in Figure 3.25. The polymer films were switched between their neutral and oxidized states with a time interval of five seconds. The optical contrasts of PTBPEQ in the visible region are 33 % at 452 nm and 43 % at 711 nm. These optical contrasts are the highest reported up to date for a green polymeric material. [72,96] PDPEQ revealed satisfactory optical contrasts in visible region as well with 29 % at 732 nm and 35 % at 448 nm. Moreover, PDPEQ has an outstanding optical contrast of 77 % at 1800 nm which is a very significant property for many NIR applications.

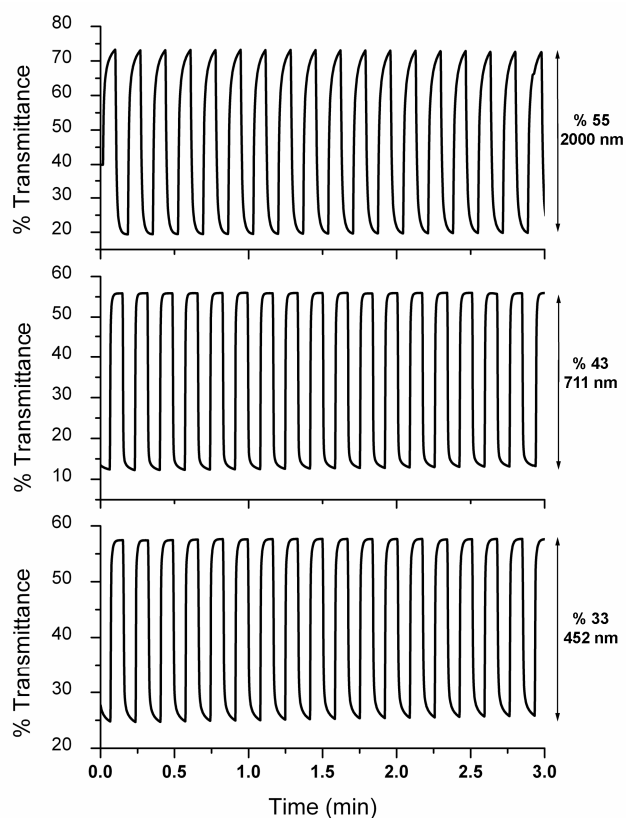


Figure 3.24 Electrochromic switching, optical absorbance change monitored at 452 and 711 nm and 2000 nm for PTBPEQ in 0.1 M TBAPF₆/ACN.

Both polymers switch very rapidly between neutral and oxidized states and achieve 95 % of their excellent optical contrasts in the visible region in less than 1 s. PTBPEQ has excellent switching times of 1 s and 0.8 s at 452 nm and 711 nm respectively. PDPEQ has similar switching times of 1.2 s at 448 nm and 0.72 s at 732 nm. The polymer achieves an outstanding optical contrast of 77 % in NIR region only in 2 s.

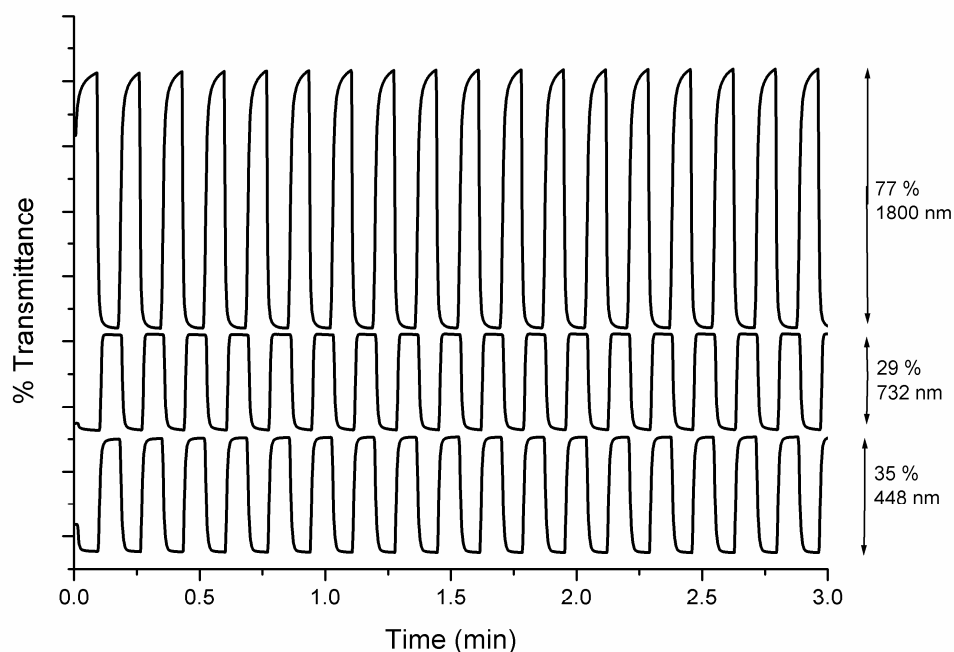


Figure 3.25 Electrochromic switching, optical absorbance change monitored at 448 and 732 nm and 1800 nm for PDPEQ in 0.1 M TBAPF₆/ACN.

3.2.4 Electrochemical and Electrochromic Properties of 2,3-bis(3,4-bis(decyloxy)phenyl)-5,8-bis(2,3-dihydrothieno[3,4-b][1,4]dioxin-5yl)quinoxaline (DOPEQ):

3.2.4.1 Electrochemistry of 2,3-bis(3,4-bis(decyloxy)phenyl)-5,8-bis(2,3-dihydrothieno[3,4-b][1,4]dioxin-5yl)quinoxaline(DOPEQ):

The polymerization via both electrochemical and chemical methods gave neutral state green polymer. A solution of DOPEQ (10^{-2} M) was prepared in a mixture of dichloromethane (DCM) and acetonitrile (ACN) (5/95, v/v) due to the high solubility of the polymer in DCM. Repeated scan electropolymerization of DOPEQ was illustrated in figure 3.26. Following the monomer oxidation at 0.8 V, an

electroactive polymer film quickly grows on the indium tin oxide (ITO) coated glass slides revealing an oxidation potential of 0.5 V and a reduction potential of 0.07 V.

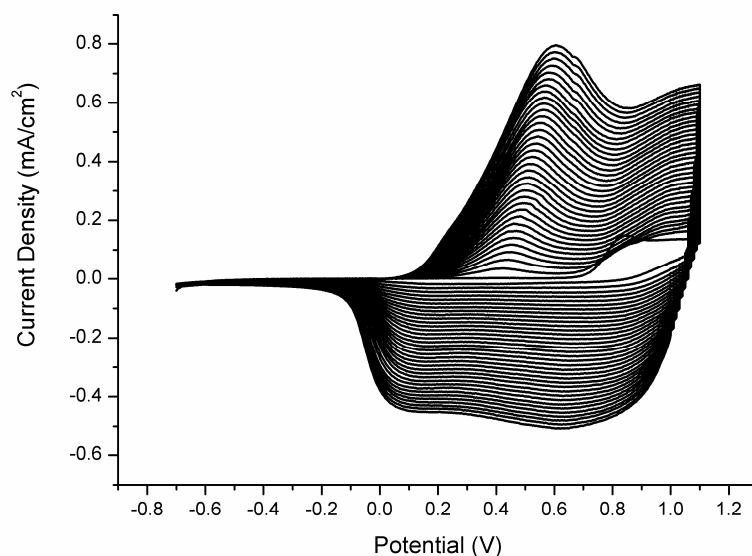


Figure 3.26. Repeated potential scan electropolymerization of DOPEQ at 100 mV/s in 0.1 M TBAPF₆/DCM/ACN on ITO electrode

The chemically produced polymer was dissolved in chloroform and spray-coated on ITO glass slides to investigate its electrochemical and electrochromic properties. Cyclic voltammetry studies revealed that the polymer was oxidized and reduced at the same potentials with that of the electrochemically produced polymer (Figure 3.27).

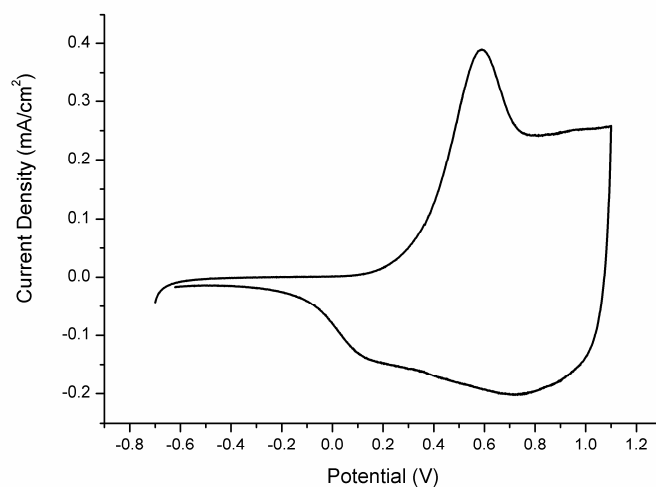


Figure 3.27. Single scan cyclic voltammetry of chemically synthesized PDOPEQ at 100 mV/s in 0.1 M TBAPF₆/ACN on ITO electrode.

A direct relation between the current response and scan rate was perceived for both electrochemically and chemically produced PDOPEQ which directly proves that the films were well-adhered; the electrochemical processes are not diffusion limited and quasi-reversible even at high scan rates (Figures 3.28 and 3.29)[115] .

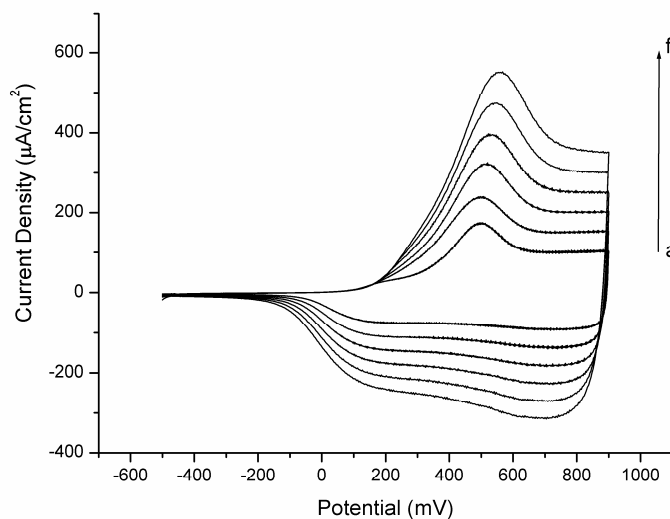


Figure 3.28. Scan rate dependence of PDOPEQ (electrochemically synthesized) film in TBAPF₆/ACN (a) 100, (b) 150, (c) 200, (d) 250, (e) 300 mV/s.

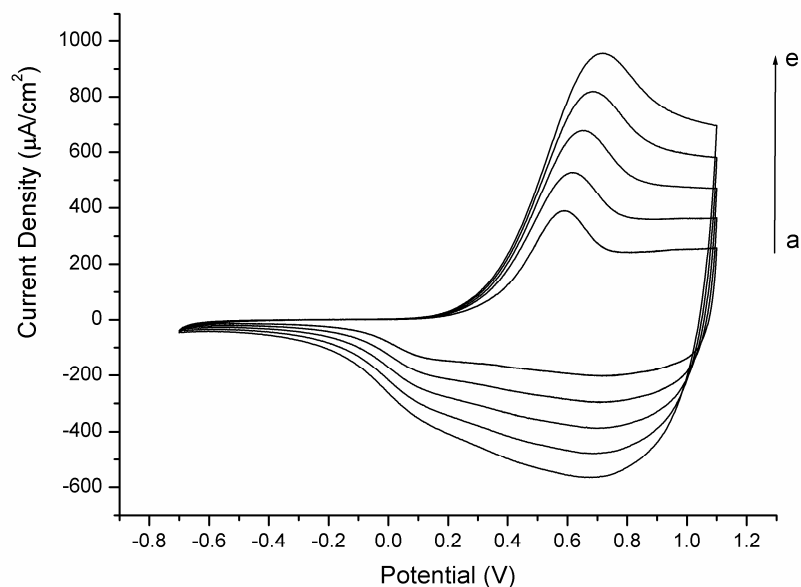


Figure 3.29. Scan rate dependence of PDOPEQ (chemically synthesized) film, spray-coated on ITO, in TBAPF₆/ACN (a) 100, (b) 150, (c) 200, (d) 250, (e) 300 mV/s.

The polymer film was coated potentiodynamically on ITO as described previously and cycled for 5000 cycles in propylene carbonate / LiClO₄ to investigate the robustness of the polymer against redox cycling. The polymer revealed tremendous stability since 90 % of the electroactivity remains intact even after 5000 cycles.

3.2.4.2. Optoelectrochemistry and Electrochromic Switching of 2,3-bis(3,4-bis(decyloxy)phenyl)-5,8-bis(2,3-dihydrothieno[3,4-b][1,4]dioxin-5yl) quinoxaline (DOPEQ):

Spectroelectrochemistry studies were achieved to probe the optical changes upon doping and dedoping processes. Figure 3.30 reveals spectroelectrochemistry

and the corresponding colors of electrochemically prepared PDOPEQ at the reduced state and upon doping.

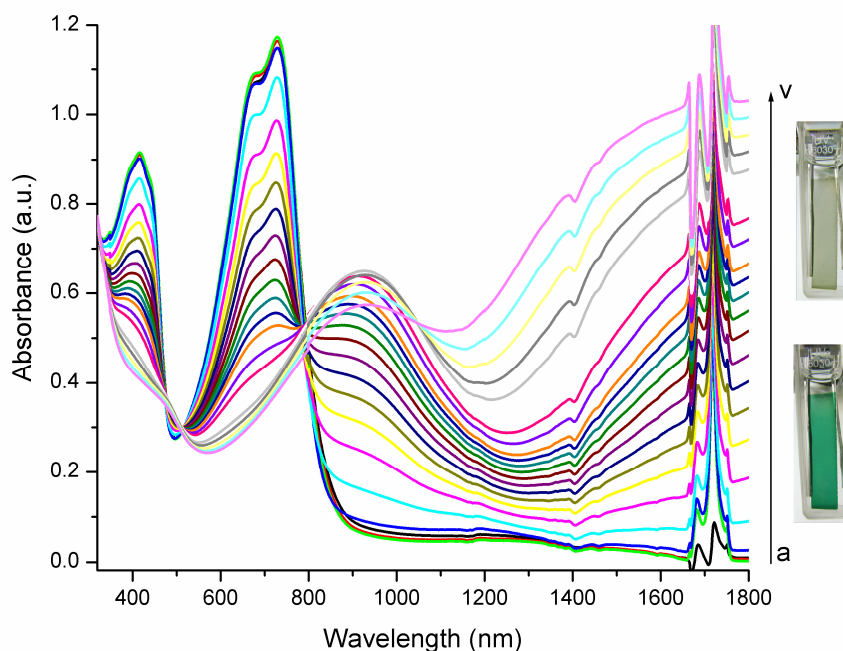


Figure 3.30. Colors of PDOPEQ film on an ITO coated glass slide at neutral and oxidized states and spectroelectrochemistry of PDOPEQ film on an ITO coated glass slide in monomer-free, 0.1 M TBAPF₆ /ACN electrolyte-solvent couple at applied potentials; (a) -0.6, (b) -0.15, (c) 0 (d) 0.05, (e) 0.075, (f) 0.1 (g) 0.15, (h) 0.175, (i) 0.2, (j) 0.225, (k) 0.25, (l) 0.275, (m) 0.3, (n) 0.35, (o) 0.4, (p) 0.45, (q)0.5, (r) 0.55, (s) 0.6, (t) 0.65, (u) 0.7, (v) 0.8 V

PDOPEQ films revealed two absorption bands, as expected from a donor-acceptor type polymer, centered at 415 nm and 690 nm. Although two absorption bands are necessary to obtain a green color, maximum absorption points are also crucial. Absorptions around 400 nm and 700 nm are the excellent absorption maxima to yield a saturated green color in the reduced state. Besides, 41 % and 46 % transmittance differences were calculated with respect to a valley obtained at 500 nm which are the highest ones reported up to date for a processable green electrochromic

polymer. Upon doping nearly all absorptions in the visible region deplete leaving a tail around 380 nm where a highly transparent oxidized state was obtained.

Spectroelectrochemistry study was also performed for the chemically produced and spray coated polymer films as seen in figure 3.31.

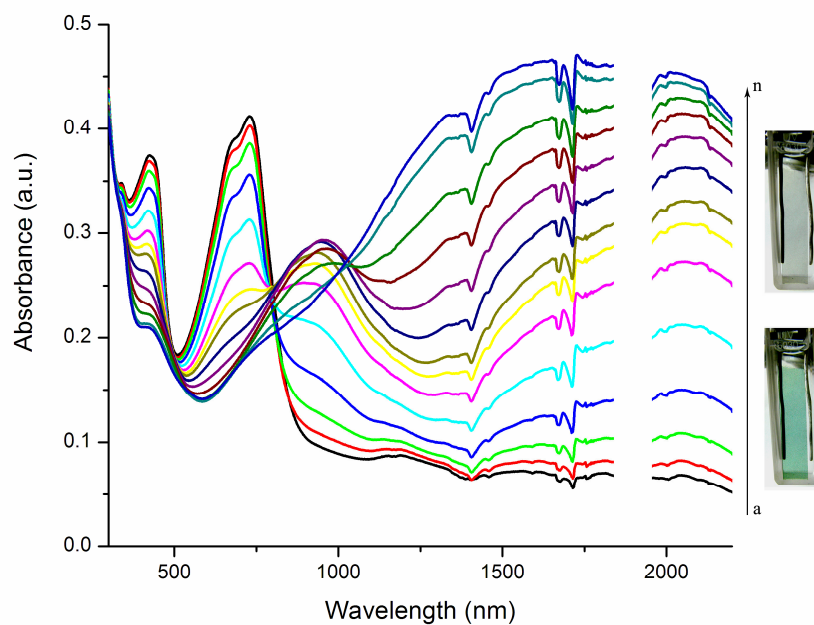


Figure 3.31 Colors of chemically synthesized PDOPEQ that spray-coated on an ITO coated glass slide at neutral and oxidized states and spectroelectrochemistry of PDOPEQ film on an ITO coated glass slide in monomer-free, 0.1 M TBAPF₆/ACN electrolyte-solvent couple at applied potentials; (a) -0.5, (b) 0.25, (c) 0.3, (d) 0.35, (e) 0.4, (f) 0.45, (g) 0.5, (h) 0.55, (i) 0.65, (j) 0.75, (k) 0.85, (l)0.95, (m) 1.1, (n) 1.2 V

The corresponding spectroelectrochemical series and Y,x,y values are almost identical to those of electrochemically produced polymer. These properties make this material the only processable neutral state green polymer (Y: 443 x: 0.270 y: 0.400) with a transmissive oxidized state (Y: 626 x: 0.314 y: 0.348). This will enable the commercial use of polymer electrochromic based display devices.

The electronic band-gap of the polymer was calculated as 1.45 eV for PDOPEQ, a relatively high band gap keeping in mind that, polymers with donor-acceptor units exhibit band-gaps between 0.9 eV to 1.3 eV in general [72,96] .

Optical contrasts, switching times and the stabilities of the polymer films upon electrochromic switching between the neutral and oxidized states were investigated in both visible and near-IR regions. The optical contrasts of the PDOPEQ films were calculated to be 29 %, 42 % and 90 % at 415 nm, 690 nm and 1800 nm respectively. Polymer achieves 95 % of these optical contrasts in less than 1 second in the visible region (Figure 3.32).

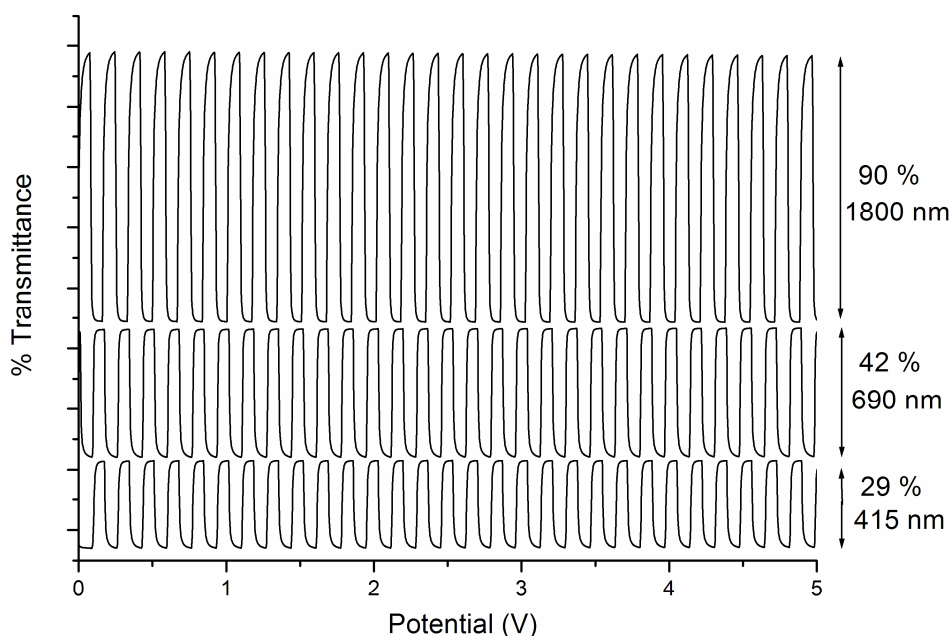


Figure 3.32. Electrochromic switching, optical absorbance change monitored at 415 and 690 nm and 1800 nm for PDOPEQ in 0.1 M TBAPF₆/ACN.

Besides, PDOPEQ realizes an outstanding optical contrast of 90 % in NIR region only in 2 seconds. These results are way better than the first example of the processable green polymeric material [119].

CHAPTER 4

CONCLUSION

The D-A-D type monomers were synthesized via Stille coupling methods and full characterization of the materials were performed by NMR and Mass Analyses. The polymers of the corresponding monomers were synthesized by electrochemical methods except for PDOPEQ which were synthesized by means of both electrochemical and chemical methods. Cyclic voltammetry experiments, spectroelectrochemistry, kinetic studies and long-term switching experiments for all the polymers were performed in order to enlighten the electrochemical and electrochromic properties.

These novel donor-acceptor type polymers were shown to be neutral state green polymeric materials with excellent transmissive oxidized states except for PGS. Green polymeric materials revealed superior optical contrasts in the visible region (highest reported up to date) and have outstanding optical contrasts (even higher than 70 %) in the NIR region. Exceptional long-term stability even after 5000 cycles, ease of electrochemical synthesis and extremely fast switching times of these polymers are also highly promising. Besides these, polymers have shown to n-dopable, as proved by both reduction waves in CV at negative potentials and significant increase in the NIR region upon reduction. Regarding these superior properties, various quinoxaline-EDOT copolymers can be synthesized to produce materials with desired properties. Addition to all excellent electrochromic properties as a green polymer, PDOPEQ was proven to be the first processable green polymer with a highly transmissive oxidized state since it is soluble in all common organic solvents. Putting all these together, these polymers are excellent choices for the commercial realization of RBG based polymer electrochromic device applications without a doubt.

REFERENCES

1. C. K. Chiang, Y. W. Park, A. J. Heeger, H. Shirakawa, E. J. Louis, A. G. MacDiarmid, *Phys. Rev. Lett.* 1977 39 1098
2. a) A. Gandini, M. N. Belgancem, *Prog. Polym. Sci.* 1997 22 1203 [12] (b) A. F. Diaz, K. K. Kanazawa, G. P. Gardini, *J. Chem. Soc., Chem. Commun.* 1979 635 (c) A. F. Diaz, J. I. Castillo, J. A. Logan, W. Lee, *J. Electroanal. Chem.* 1981 129 115 (d) K. Lee, A. J. Heeger, *Synth. Met.* 1997 84 715 110 (e) A.G. Bayer Eur. Patent 339,340, 1988 (b) F. Jonas, L. Schrader, *Synth. Met.* 1991 41 831 (c) G. Heywang, F. Jonas, *Adv. Mater.* 1992 4 116 (f) G. Grem, G. Leditzky, B. Ullrich, G. Leising, *Adv. Mater.* 1992 4 36 (g) J.H. Burroughes, D.D.C. Bradley, A.R. Brown, R.N. Marks, K. MacKay, R.H. Friend, P.L. Burn, A.B. Holmes, *Nature* 1990 347 539 (h) J. Rault-Berthelot, J. Simonet, *J. Electrochem. Soc.* 1985 182 187 (i) A. G. MacDiarmid, A.J. Epstein, *Farad. Discuss. Chem. Soc.* 1989 88 317 (j) A. Desbene-Monvernay, P.-C. Lacaze, J.-E. Dubois, *J. Electroanal. Chem.* 1981 129 229
3. R. G. Mortimer, *Chem. Soc. Rev.* 1997 26 147
4. J. H. Burroughes, D. D. C. Bradley, A. R. Brown, R. N. Marks, K. Mackay, R. H. Friend, P. L. Burns, A. B. Holmes, *Nature* 1990 347 539
5. N. S. Sariciftci, L. Smilowitz, A. J. Heeger, F. Wudl, *Science* 1992 258 1474
6. j. Miasik, A. Hooper B. C. Tofield *J. Chem. Soc. Farad. Trans. Phys. Chem. in Cond. Pha.* 1986 82 1117.
7. H. Koezuka, A. Tsumura, *Synthetic Metals* 1989 28 C753
8. P. K. H. Ho, D. S. Thomas, R. H. Friend, N. Tessler, *Science* 1999, 285, 233. I. Schwendeman, R. Hickman, G. Sonmez, P. Schottland, K. Zong, D.M. Welsh, J. R. Reynolds, *Chem. Mater.* 2002 14 3118
9. J. I. Reddinger, J. R. Reynolds, *Advances in Polymer Science* 1999 45 59
10. trans-PA has a neutral conductivity of 10^{-5} - 10^{-6} S cm⁻¹.

11. J. C. W.Chien, *Polyacetylene Chemistry, Physics and Material Science*; Academic Press, Harcourt Brace Jovanovich: Orlando, 1984; Chapter 5.
12. The bond length alternation has been experimentally determined to be ~ 0.08
A. (a) C. R.Fincher, C. E.Chen, A. J.Heeger, A. G.Macdiarmid, J. B.Hastings, *Phys. Rev. Lett.* 1982 48 100 (b) C. S.Yannoni, T. C.Clarke, *Phys. Rev. Lett.* 1983 51 1191
13. U.Salzner, P. G.Pickup, R. A.Poirier, J. B. J.Lagowski, *Phys. Chem. A* 1998 102 2572
14. J. R. Reynolds, J. B. Schlenoff, J. C. W. Chien, *J. Electrochem. Soc.* 1985 132 1131
15. D. M. de Leeuw, M. M. J. Simenon, A. R. Brown, R. E. F. Einerhand, *Synth. Met.* 1997 87 53.
16. C. J. DuBois, F. Larmat, D. J. Irvin, J. R. Reynolds, *Synth. Met.* 2001 119 321.
17. C. J. DuBois, K. A. Abboud, J. R. Reynolds, *J. Phys. Chem. B* 2004 108 8550
18. C. J. DuBois, J. R. Reynolds, *Adv. Mater.* 2002 14 1844
- 19 D. R. Rosseinsky, R .J. Mortimer, *Adv. Mater.* 2001 13 783
- 20 R.J. Mortimer, *Electrochim. Acta* 1999 44 2971
- 21 M A. De Paoli, W. A. Gazotti, *J. Braz. Chem. Soc.*, 2002 13 410
- 22 G. Sonmez, I. Schwendeman, P. Schottland, K. Zong, J. R. Reynolds *Macromolecules* 2003 36 639
- 23 K. Fesser, A.R. Bishop, D.K. Campbell, *Phys. Rev. B* 1983 27 4804
- 24 B.C. Thompson, P. Schottland, G. Sonmez, J.R. Reynolds, *Synth. Met.*, 2001 119 333
- 25 J. Roncali, *Chem. Rev.* 1997 97 173
- 26 J. L.Bredas, *J. Chem Phys.* 1985 82 3808
- 27 F. Wudl, M. Kobayashi, A. J. Heeger, *J. Org. Chem.* 1984 49 3382
- 28 R.D. McCullough, *Adv. Mater.* 1998 10 93
- 29 G. A. Sotzing, J. L. Reddinger, A. R. Katritzky, J. Soloducho, R. Musgrave, J. R. Reynolds, *Chem. Mater.* 1997 9 1578
- 30 G. A. Soltzing, J. R. Reynolds, *J Chem. Soc. Chem. Commun* 1995 703

- 31 (a) C. Rebbi, *Sci. Am.* 1979 240 92. (b) D. S.Boudreaux, R. R.Chance, J. L.Bredas, R.Silbey, *Phys Rev. B: Condens. Matter.* 1983 28 6927 (c) H.Thomann, L. R.Dalton, Y.Tomkiewicz, N. S.Shiren, T. C.Clarke, *Phys. Rev. Lett.* 1983 50 533
- 32 W. P.Su, J. R.Schrieffer, A. J.Heeger, *Phys. Rev. Lett.* 1979 42 1698
- 33 K.Fesser, A. R.Bishop, D. K.Campbell, *Phys. Rev. B.* 1983 27 4804
- 34 A. J.Heeger, S.Kivelson, J. R.Schrieffer, W.Su, *P. Rev. Mod. Phys.* 1988 60 781
- 35 J. L.Bredas, G. B.Street, *Acc. Chem. Res.* 1985 18 309
- 36 A.Sakamoto, Y.Furukawa, M.Tasumi, *J. Phys. Chem. B* 1997 101 1726
- 37 M.G.Hill, J.-F.Penneau, B.Zinger, K. R.Mann, L. L.Miller, *Chem. Mater.* 1992 4 1106
- 38 J. R.Reynolds, J. B.Schlenoff, J. C. W.Chien, *J. Electrochem. Soc.* 1985 132 1131
- 39 (a) D. A.Vanden Bout, W.-T.Yip, D.Hu, D.-K.Fu, T. M.Swager, P. F.Barbara, *Science* 1997 277 1074 (b) D.Hi, J.Yu, P. F.Barbara, *J. Am. Chem. Soc.* 1999 121 6936
- 40 Some poorly defined materials with extremely low band gaps have been reported but further confirmations are necessary: (a) H .Huang, P. G.Pickup, *Chem. Mater.* 1998 10 2212 (b) H .Huang, P. G.Pickup, *Chem. of Mater.* 1999 11 1541
- 41 F. Wudl, *J. Org. Chem* 1984 49 3382.
- 42 p-type doping is the creation of charge carriers by partial oxidation of a polymer or semiconductor creating a partially vacated VB. Conversely, n-type doping is the creation of charge carriers by partial reduction creating a partially filled CB.
- 43 S.Tanaka, J. R.Reynolds, *J. Macro. Sci., Pure Appl. Chem.* 1995 A32 1049
- 44 D. M.de Leeuw, M. M. J.Simenon, A. R.Brown, R. E. F.Einerhand, *Synth. Met.* 1997 87 53
- 45 J. March, *Advanced Organic Chemistry*; Wiley: New York, 1985.

- 46 (a) H. A. M. van Mullekom, J. A. J. M. Vekemans, E. E. Havinga, E. W. Meijer, (Review not Released Yet). (b) E. W. Havinga, W. ten Hoeve, H. Wynberg, *Synth. Met.* 1993 55 299
- 47 PEDOT data was obtained as described in the experimental section detailing spectroelectrochemistry.
- 48 C. B. Gorman, R. C. West, T. U. Palovich, S. Serron, *Macromolecules* 1999 32 4157
- 49 Only recently has n-type doping of PEDOT been demonstrated. Even under rigorously controlled atmospheric conditions its stability is unremarkable. H. J. Ahonen, J. Lukkari, J. Kankare, *Macromolecules* 2000 33 6787
- 50 L. Groenendaal, G. Zotti, P.-H. Aubert, S. Waybright, J. R. Reynolds, *Adv. Mater.* 2003 15 855
- 51 L. B. Groenendaal, F. Jonas, D. Freitag, H. Pielartzik, J. R. Reynolds, *Adv. Mater.* 2000 12 481
- 52 J. Roncali, *J. Mater. Chem.* 1999 9 1875
- 53 J. Roncali, *Chem. Rev.* 1992 92 711
- 54 J. Roncali, *Chem. Rev.* 1997 1 173
- 55 R. D. McCullough, *Adv. Mater* 1998 10 93
- 56 T.-A. Chen, R. D. Rieke, *J. Am. Chem. Soc.* 1992 114 10087
- 57 R. D. McCullough, R. D. Lowe, *Chem. Commun.* 1992 1 70
- 58 R. D. McCullough, R. D. Lowe, M. Jayaraman, D. L. Anderson, *J. Org. Chem.* 1993 58 904
- 59 R. D. McCullough, S. Tristram Nagle, S. P. Williams, R. D. Lowe, M. Jayaraman, *J. Am. Chem. Soc.* 1993 115 4910
- 60 R. S. Loewe, S. M. Khersonsky, R. D. McCullough, *Adv. Mater.* 1999 11 250
- 61 R. S. Loewe, P. C. Ewbank, L. Z. Jinsong Liu, R. D. McCullough, *Macromolecules* 2001 34 4324
- 62 J. Roncali, *Mater. Chem.* 1999 9 1875
- 63 L. B. Groenendaal, F. Jonas, D. Freitag, H. Pielartzik, J. R. Reynolds, *Adv. Mater.* 2000 12 481

- 64 A. Cirpan, A. A.Argun, C. R. G.Grenier, B. D.Reeves, J. R.Reynolds, *J. Mater. Chem.* 2003 13 2422
- 65 D. M.Welsh, L. J.Kloppner, L.Madrigal, M. R.Pinto, B. C.Thompson, K. S.Schanze, K. A.Abboud, D.Powell, J. R.Reynolds, *Macromolecules* 2002 35 6517
- 66 B. D.Reeves, C. R. G.Grenier, A. A.Argun, A.Cirpan, T. D.McCarley, J. R.Reynolds, *Macromolecules* 2004 37 7559
- 67 (a) I. H.Jenkins, N. G.Rees, P. G.Pickup, *Chem. Mater.* 1997 9 1213 (b) I. H.Jenkins, U.Salzner, P. G.Pickup, *Chem. Mater.* 1996 8 2444 (c) T.Kanbara, Y.Miyazaki, T. J.Yamamoto, *Polym. Sci., Part A: Polym. Chem.* 1995 33 999 (d) B.-L.Lee, T.Yamamoto, *Macromolecules* 1999 32 1375 (e) M. Onada, *J. Appl. Phys.* 1995 78 1327 (f) N.Saito, T.Kanbara, T.Kushida, K.Kubota, T.Yamamoto, *Chem. Lett.* 1993 1775 (g) T. Yamamoto, *J. Polym. Sci., Part A: Polym. Chem.* 1996 34 997 (h) T.Yamamoto, Z.Zhou, T.Kanbara, M.Shimura, K.Kizu, T.Maruyama, Y.Nakamura, T.Fukuda, B.-L.Lee, N.Ooba, S.Tomaru, T.Kurihara, T.Kaino, K.Kubota, S.Sasaki, *J. Am. Chem. Soc.* 1996 118 10389 (i) K. B.Wiberg, T. P.Lewis, *J. Amer. Chem. Soc.* 1970 92 7154
- 68 (a) R. E. Martin, J. A.Wytko, F.Diederich, C.Boudon, J.Gisselbrecht, M.Gross, *Helv. Chim. Acta* 1999 82 1470 (b) H.Wang, R.Helgeson, B.Ma,; F.Wudl, *J. Org. Chem.* 2000 65 5862
- 69 (a) F.Jonas, G.Heywang, W.Schidtberg, Novel polythiophenes, process for their preparation, and their use. German Patent DE 3,813,589, November 2, 1989. (b) F. Jonas, G. Heywang, W. Schidtberg, J. Heinze, M. Dieterich, Polythiophenes, process for their preparation and their use. Eur. Patent App. EP 339,340, September 25, 1990. (c) F. Jonas, G. Heywang, W. Schidtberg, J. Heinze, M. Dieterich, Polythiophenes, process for their preparation and their use. US Patent US 4,959,430, September 25, 1990. (d) G.Heywang, F.Jonas, *Adv. Mater.* 1992 4 116 (e) D. M.Welsh, A.Kumar, E. W.Meijer, J. R.Reynolds, *Adv. Mater.* 1999 11 1379

- 70 A.Kumar, D. M.Welsh, M. C.Morvant, F.Piroux, K. A.Abboud, J. R.Reynolds, *Chem. Mater.* 1998 10 896
- 71 G. A.Sotzing, J. R.Reynolds, P. J.Steel, *Adv. Mater.* 1997 9 795
- 72 G.Sonmez, C. K. F. Shen, Y. Rubin and F. Wudl, *Angew. Chem., Int. Ed.* 2004 43 1498
- 73 S. A. Sapp, G. A. Sotzing and J. R. Reynolds, *Chem. Mater.* 1998 10 2101.
- 74 B. C. Thompson, P. Schottland, K. Zong and J. R. Reynolds, *Chem. Mater.* 2000 12 1563
- 75 G. Sonmez, H. B. Sonmez, C. K. F. Shen and F. Wudl, *Adv. Mater.* 2004 16 1905
- 76 E. E. Havinga, W. Ten Hoeve, H. Wynberg, *Polym. Bull.* 1992 29 119
- 77 P. Nils-Krister, S. Mengtao, K. Par, P. Tonu, I. Olle, *J. Chem. Phys.* 2005 123 204718
- 78 H. A. M. van Mullekom, J. A. J. M. Vekemans, E. E. Havinga, and E. W. Meijer, *Mater. Sci. Eng., R.*, 2001 32 1.
- 79 G. Brocks, A. Tol, *J. Phys. Chem.*, 1996 100 1838
- 80 U. Salzner, *J. Phys. Chem. B.* 2002 106 9214
- 81 A. Berlin, G. Zotti, S. Zecchin, G. Schiavon, B. Vercelli, A. Zanelli *Chem. Mater.* 2004 16 3667
- 82 U. Salzner, M.E. Kose, *J. Phys. Chem. B.* 2002 106 9221
- 83 Private communication with Prof. Bauerle: 10 grams of substance contains 3.5 grams free base.
- 84 P. Audebert, P. Hapiot, *Synth. Met.* 1995 75 95.
- 85 M. Younus, A. Kohler, S. Cron, N. Chawdhury, M. Al-Mandhary, M. S. Khan, J. Lewis, N. J. Long, R. H. Friend, P. R. Raithby, *Angew. Chem. Int. Ed.* 1998 37 3036.
- 86 A. B. Da Silveria Neto, A. Lopes Sant'Ana, G. Ebeling, S. R. Goncalves, E. V. U. Costa, H. F. Quina, J. Dupont, *Tetrahedron* 2005 61 10975.
- 87 Y. Tsubata, T. Suzuki, T. Miyashi, Y. Yamashita, *J. Org. Chem.* 1992 57 6749.

- 88 A. I. Vogel, Vogel's Textbook of Practical Organic Chemistry, 5th Ed. (Eds: B. S. Furniss, A. J. Hannaford, P. W. G. Smith, A. R. Tatchell, Longman Scientific & Technical, England, 1989, Ch. 6.
- 89 G. Y. Han, P. F. Han, J. Perkins, H. C. McBay, *J. Org. Chem.*, 1981 46 4695.
- 90 S. S. Zhu, T. M. Swager, *J. Am. Chem. Soc.*, 1997 119 12568.
- 91 C. Chen, Y. Wei, J. Lin, M. V. R. K. Moturu, W. Chao, Y. Tao, C. Chien, *J. Am. Chem. Soc.*, 2006 128 10992.
- 92 Mohr, V. Enkelmann, and G. Wegner. *J. Org. Chem.* 1994 59 635.
- 93 P. Audebert, P. Hapiot, *Synth Met* 1995 75 95.
- 94 S. Rasmussen, J. C. Pickens, J. E. Hutchison, *Chem. Mater.* 1998 10 1990.
- 95 C. Kitamura, S. Tanaka, Y. Yamashita, *Chem. Mater.* 1996 8 570.
- 96 A. Berlin, G. Zotti, S. Zecchin, G. Schiavon, B. Vercelli, A. Zanelli *Chem. Mater.* 2004 16 3667.
- 97 D. D. Kenning, K. A. Mitchell, T. R. Calhoun, M. R. Funfar, D. J. Sattler, and S. C. Rasmussen *J. Org. Chem.* 2002 67 9073.
- 98 J. Armond, C. Bellec, L. Boulares, P. Chaquin, D. Masure, J. Pinson, *J. Org. Chem.* 1991 56 4840.
- 99 J. Lee, B. Jung, S. Lee, J. Lee, H. Cho, H. Shim *J. Polym. Sci. Part. A: Polym. Chem.* 2005 43 1845.
- 100 A. Kumar, D. M. Welsh, M. C. Morvant, F. Piroux, K. A. Abboud, J. R. Reynolds, *Chem. Mater.* 1998 10 896.
- 101 G. Sonmez, C. K. F. Shen, Y. Rubin and F. Wudl, *Angew. Chem., Int. Ed.* 2004 43 1498
- 102 S. Roth, H. Bleier, *Adv. Phys.* 1987, 36, 385.
- 103 M. Onada, Y. Menda, S. Morita, K. Yoshino, *J. Phys. Soc. Jpn.* 1990 59 213.
- 104 C. J. DuBois, K. A. Abboud, J. R. Reynolds, *J. Phys. Chem. B* 2004 108 8550.
- 105 H. U Yildiz, E. Sahin, I. M. Akhmedov, C. Tanyeli, L. Toppare, *J. Polym. Sci. Part A: Polym. Chem.* 2006 44 2215.
- 106 O. Turkarslan, M. Ak, C. Tanyeli, İ. M. Akhmedov, L. Toppare *J. Polym. Sci. Part A: Polym. Chem.* 2007 45 4496.

- 107 G.A. Sotzing, J. R. Reynolds, P.J. Steel *Adv. Mater.* 1997 9 795.
- 108 C. L. Gaupp, J. R. Reynolds *Macromolecules* 2003 36 6305.
- 109 P. Manisankar, C. Vedhi, G. Selyanathan, *J. Polym. Sci. Part A: Polym. Chem.* 2007 45 2787.
- 110 D. M. DeLongchamp, M. Kastantin, P. T. Hammond, *Chem. Mater.* 2003, 15, 1575.
- 111 D. M. DeLongchamp, P. T. Hammond, *Adv. Mater.* 2001 13 1455.
- 112 D. M. DeLongchamp, P. T. Hammond, *Chem. Mater.* 2004 16 4799.
- 113 C. A. Cutler, M. Bouguettaya, J. R. Reynolds, *Adv. Mater.* 2002 14 684.
- 114 S. Liu, H. Mohwald, D. Volkmer, D. G. Kurth, *Adv. Mater.* 2002 14 225.
- 115 G. Sonmez, H. Meng, Q. Zhang, F. Wudl, *Adv. Funct. Mater.*, 2003 13 726.
- 116 H. W. Heuer, R. Wehrmann, S. Kirchmeyer, *Adv. Funct. Mater.*, 2002 12 89.
- 117A. Durmus, G. E. Gunbas, P. Camurlu, L. Toppare, *Chem. Commun.*, 2007 31 3246.
- 118 B. C. Thompson, Y. Kim, T. D. McCarley, J. R. Reynolds, *J. Am. Soc. Chem.* 2006 128 12714.
- 119 G. Sonmez, H. B. Sonmez, C. K. F. Shen, R. W. Jost, Y. Rubin, F. Wudl, *Macromolecules* 2005 38 669